INVESTIGATION OF THE LIMITATIONS OF VIRAL GENE TRANSFER TO MURINE EMBRYONIC STEM CELLS

A Dissertation
Presented to
The Academic Faculty

By

Jamie M. Chilton

In Partial Fulfillment
of the Requirements for the Degree
Doctor of Philosophy in Biomedical Engineering

Georgia Institute of Technology and Emory University

August 2008

INVESTIGATION OF THE LIMITATIONS OF VIRAL GENE TRANSFER TO MURINE EMBRYONIC STEM CELLS

Approved by:

Joseph Le Doux, Ph.D., Advisor
Department of Biomedical Engineering
Georgia Institute of Technology & Emory University

David Archer, Ph.D
Department of Pediatrics
Emory University

Michelle LaPlaca, Ph.D.
Department of Biomedical Engineering
Georgia Institute of Technology & Emory University

Todd McDevitt, Ph.D.
Department of Biomedical Engineering
Georgia Institute of Technology & Emory University

Anthanassios Sambanis, Ph.D.
School of Chemical & Biomolecular Engineering
Georgia Institute of Technology & Emory University

Steven Stice, Ph.D.
Department of Animal & Dairy Science
University of Georgia

Date Approved: May 16, 2008

To Mama and Dad,
My best friends and biggest fans

ACKNOWLEDGEMENTS

First and foremost I would like to thank my advisor, Joseph Le Doux, for the example he set as the epitome of an ethical scientist and an analytical thinker. He will always be the standard I will strive to emulate in my future career. I would also like to thank Todd McDevitt and David Archer for graciously allowing me to work in their labs and join their lab meetings, as well as offer their support. I am also grateful to Michelle LaPlaca, Athanassios Sambanis, and Steven Stice for their supportive, insightful, and very helpful discussions and suggestions. I would also like to acknowledge the BME department and the IBB staff for their invaluable assistance. And last, but certainly not least, I am grateful for the pleasure of working with four outstanding, dynamic, and unique women – Natalia Landazuri, Delfi Krishna, Cindy Jung, and Nimisha Gupta. I cannot thank them enough for all they have taught me in the lab and about life.

TABLE OF CONTENTS

ACKNOWLEDGEMENTS iv

LIST OF TABLES vii

LIST OF FIGURES viii

SUMMARY x

CHAPTER 1: BACKGROUND AND OBJECTIVES
1.1 Diabetes 1
1.2 Stem Cells 2
1.3 Strategies for creating a transplantable beta cell line from ES cells 4
1.4 Pancreas development 6
1.5 Genetic methods for pancreatic differentiation of ES cells: ectopic expression of master transcription factors to generate beta or insulin-producing cells 9
1.6 Culturing methods for pancreatic differentiation of ES cells 12
1.7 Gene therapy applications for embryonic stem cells 14
1.8 Recombinant retroviruses and lentiviruses as gene transfer vectors 16
1.9 Limitations to retrovirus-mediated gene transfer to embryonic stem cells 22
1.10 Enhancement of gene transfer using virus-polymer complexation 24
1.11 Thesis objectives 25
1.12 Organization of thesis 26
1.13 References 27

CHAPTER 2:
2.1 Introduction 41
2.2 Materials and Methods 42
2.3 Results 48
2.4 Discussion 57
2.5 Acknowledgements 60
2.6 References 60

CHAPTER 3:
3.1 Introduction 64
3.2 Materials and Methods 65
3.3 Results 73
3.4 Discussion 84
3.5 Acknowledgements 88
3.6 References 89

CHAPTER 4:
4.1 Introduction 96
4.2 Materials and Methods 98
4.3 Results 106
4.4 Discussion 120
4.5 Acknowledgements 123
4.6 References 123

CHAPTER 5:
5.1 Introduction 127
5.2 Materials and Methods 128
5.3 Results 132
5.4 Discussion 135
5.5 Acknowledgements 137
5.6 References 137

CHAPTER 6: CONCLUSIONS AND FUTURE DIRECTIONS
6.1 Summary of results 141
6.2 Conclusions 143
6.3 Suggestions for future research 143

APPENDIX A: EXPERIMENTAL PROTOCOLS
A.1 Confocal Microscopy Image Analysis 145

APPENDIX B: ADDITIONAL DATA
B.1 Determination of the starting concentration of active virus (C_{vo}) in virus stocks and active virus particles delivered per cell (A) 147

LIST OF TABLES

TABLE

4.1 R1 mES cells integrate fewer viral transgenes and demonstrate lower transgene expression levels per cell than NIH 3T3 cells.....118

4.2 Fractional efficiencies with which retroviruses and lentiviruses complete major steps in the transduction process in R1 mES cells relative to NIH 3T3 cells....119

5.1 Titers of virus stocks and transgenes delivered.....133

B.1 Numerical values of the integral I for a VSV-G-pseudotyped lentivirus with a half-life of 19 hours.....150

B.2 *RFP-lacZ* retrovirus stocks deliver a higher number of active viruses per cell to NIH 3T3 fibroblasts.....151

LIST OF FIGURES

FIGURE

1.1 Linear model of transcription factors involved in pancreas development. 9

1.2 Basic structure of a retrovirus 17

1.3 Production of recombinant retrovirus stock solutions by producer cell lines 18

1.4 Transduction of target cells by recombinant retroviruses 20

1.5 Procedure for enhancing gene transfer using anionic and cationic polymers 25

2.1 Schematic diagram of the two MSCV retroviral vectors constructed, containing the MSCV long terminal repeat (LTR) promoter followed by a packaging sequence (Ψ^+) 49

2.2 Expression of eGFP can be detected in EFC1 mES cells and NIH 3T3 cells 51

2.3 Transduced eGFP+ HeLa cells stain positive for FTngn3 protein expression 53

2.4 Expression of the Ngn3 transgene is signicantly lower in transduced EFC1 mES cells than in NIH 3T3 cells 54

2.5 Transduction of EFC1 mES cells with MSCV-FTngn3-eGFP leads to increased expression of Ngn3 and its downstream factors 56

2.6 Following embryoid body (EB) formation, expression of Ngn3 is sigficantly lower than 2 days post transduction of EFC1 mES cells 57

3.1 Schematic diagram of the bicistronic MSCV-eGFP retroviral vector containing the MSCV long terminal repeat (LTR) promoter followed by a packaging sequence (Ψ^+), a multiple cloning site (MCS), the enhanced green fluorescent protein (eGFP), and an internal ribosome entry site (IRES) 74

3.2 Retroviruses, when used to transduce D3 and R1 murine embryonic stem cells (mES), have significantly higher titers when they are pseudotyped with ecotropic or VSV-G envelope proteins than when they are pseudotyped with amphotropic or 10A1 envelope proteins 75

3.3 D3, R1, and NIH 3T3 cells express similar levels of mRNA for the ecotropic (MCAT-1) and amphotropic (Pit-2) retrovirus receptors 76

3.4 High doses of Polybrene (PB) and chondroitin sulfate C (CSC) reduces the growth rate, but not the pluripotency, of D3 and R1 mES cells 79

3.5 The number of transduced cells increases when ecotropic retrovirus is concentrated by complexation with Polybrene and chondroitin sulfate C 81

3.6 Delivery of ecotropic virus, concentrated up to 40-fold by complexation with PB and CSC, increases transgene expression in NIH 3T3 cells, but not in D3 or R1 mES cells 82

3.7 Ecotropic retrovirus transfers fewer genes to mES cells than to NIH 3T3 cells .. 83

4.1 The half-lives of ecotropic and VSV-G pseudotyped lentivirus are similar 108

4.2 Fewer retroviruses bind to R1 mES cells than to NIH 3T3 cells as determined by virus capsid ELISA 110

4.3 Fewer lentiviruses bind to R1 mES cells than to NIH 3T3 cells as determined by virus capsid ELISA 112

4.4 Fewer retroviruses and lentiviruses bind to R1 mES cells than to NIH 3T3 cells as determined by immunofluorescence microscopy..... 114

5.1 Transduction of D3 mES cells with SIV-eGFP lentivirus and HIV-1-eGFP lentivirus shows higher transgene expression per individual cell than with MSCV-eGFP retrovirus 134

5.2 Triple null F6 mES cells have 2-fold fewer eGFP+ cells than wild-type F4 mES cells when transduced with all three virus stocks 135

SUMMARY

By definition, gene therapy is the delivery of genetic material to produce a therapeutic effect. Interest has increased in using embryonic stem (ES) cells as targets for gene therapy. Their properties of self-renewal, clonogenicity, and pluripotentiality give ES cells the potential to be an unlimited source of cells for cell replacement therapy particularly suitable for genetic modification. Recombinant retroviruses are common vehicles for genetic modification, as they accurately and stably integrate the gene of interest into the target cell genome and theoretically offer long-term therapy.

To respond to the nation's desperate need to solve its critical shortage of donated pancreata for transplantation, the long-term goal of current tissue engineering research is to generate physiologically functional insulin-producing cells for alleviation of the complications of type 1 diabetes. However, these efforts have been limited by the inability to generate large numbers of cells suitable for transplantation. The original objective of this proposal was to address this cell source limitation by investigating the genetic modification of murine embryonic stem (mES) cells. We hypothesized that sustained ectopic expression of proendocrine transcription factor neurogenin 3 (ngn3) in mES cells would be an efficient trigger to enhance the differentiation and beta cell functionality of ES cells.

However, genetically modifying ES cells to generate insulin-producing cells and to elucidate the mystery of the endocrine pancreas lineage has proven difficult due to the mechanisms ES cells employ to silence retrovirus gene expression. We found that expression of ngn3 and the enhanced green fluorescent protein (eGFP) reporter gene were both significantly silenced in genetically modified mES cells. Therefore, the objectives of this thesis were redirected to overcome this obstacle and enhance the

efficiency of transduction in ES cells and to identify any additional restrictions in gene transfer to ES cells.

We first investigated whether delivering more transgenes would improve retroviral gene transfer to murine embryonic stem (mES) cells. We formed polymer complexes with MSCV-derived ecotropic retroviruses, concentrated them up to 40-fold, and transduced two different murine embryonic stem cell lines, and a mouse fibroblast cell line as a control. The number of integrated transgenes increased more than 50-fold in the embryonic stem cell lines, yet, surprisingly, transgene expression did not increase. Interestingly, the embryonic stem cells had significantly fewer integrated transgenes than the mouse fibroblasts, even though transduction conditions were identical, which suggests that embryonic stem cells may be restricted in more than one step of retrovirus transduction.

We next investigated which steps of the virus lifecycle restrict efficient transduction of ES cells. Using recombinant MMuLV-derived retrovirus and recombinant HIV-1-derived lentivirus, we compared three major steps in the transduction of R1 mES and NIH 3T3 cells: 1) the number of active virus particles that adsorb to cells in a given absorption time; 2) the number of integrated transgenes; and 3) the corresponding level of gene expression. We found that retroviruses and lentiviruses similarly bind 3 or 4-fold less efficiently to R1 mES cells than to NIH 3T3 cells. R1 mES cells integrated 3-fold fewer retrovirus transgenes than NIH 3T3 cells and showed 11-fold lower retrovirus transgene expression levels. In comparison, R1 mES cells integrated 10-fold fewer lentivirus transgenes than NIH 3T3 cells and showed 8-fold lower lentivirus transgene expression levels. Although silencing remains the biggest obstacle to retroviral gene transfer, these results indicate virus binding and integration in the transduction process are also limiting in ES cells.

We also investigated whether depletion of linker histone 1 in ES cells would alleviate silencing of retrovirus transgenes and improve gene transfer. To study the role of H1 in retroviral gene transfer, we transduced histone H1c, H1d, H1e triple null mouse embryonic stem cells with three different recombinant vectors – murine embryonic stem cell retrovirus (MSCV), and SIV and HIV-1 derived lentiviruses. We found that transduction of mES cells depleted of histone H1 did not improve viral gene transfer, and triple null mES cells had about a 2-fold reduction in the number of eGFP+ cells for all three viruses in comparison to wild-type mES cells.

In summary, we applied methods to overcome the major obstacle of retrovirus gene silencing and identified additional restrictions in retroviral gene transfer. This research is significant for improving protocols for gene transfer to ES cells and facilitating the use of modified ES cells in regenerative medicine.

CHAPTER 1

BACKGROUND AND OBJECTIVES

1.1 Diabetes

Diabetes, affecting over 125 million people worldwide and 16 million in the US, is a disease where the patient exhibits relative or absolute insulin deficiency, resulting in many pathological manifestations including renal failure, retinopathy, neuropathy, and extremity amputation [1-6]. Complete autoimmune destruction of pancreatic beta cells characterizes type I diabetes, also known as insulin-dependent diabetes mellitus (IDDM) [5]. The patient's pancreatic beta cells can no longer produce insulin in response to high blood glucose levels following meals [5]. The major clinical problems of type I diabetes are due to the long-term effects of chronic hyperglycemia [4]. Patients with diabetes suffer from hyperglycemia because no therapy to date can maintain blood glucose within the relatively narrow range typical of a normally functioning pancreas [4].

Unfortunately, patients with diabetes mellitus must currently manage their disease through three to four insulin injections per day. These injections do not replace the normal physiological ability to couple the sensing of blood glucose levels with the rapid release of appropriate amounts of insulin [7]. As a result, diabetes patients live with an increased risk of life-threatening episodes of hypoglycemia. In addition, the extreme shortage of pancreas donors prevents pancreas tissue transplants from becoming a pragmatic solution to diabetes mellitus [7]. Thus, researchers now look to tissue engineering solutions to repair the loss of pancreatic physiological function and to hopefully alleviate the complications of diabetes.

1.2 Stem cells

Cellular therapy offers a promising new approach for treating disease. A major obstacle, however, in the clinical application of cellular therapy to date is the tremendous shortage of needed cells and tissues required for effective human transplantation, especially cells that are compatible with the immune system of the patient. As a result, interest has grown in pursuing three major sources of cells – embryonic stem cells, adult stem cells, and immortal primary cell lines – as a solution to this shortage in cell supply [1, 8-10]. In particular, the isolation of embryonic stem (ES) cells has generated great enthusiasm over the potential of producing an unlimited source of transplantable cells, due to their capacity to differentiate, as well as their ability to proliferate well in culture.

Stem cells have the awesome capacity to develop into any adult tissue or to continue to undergo self-renewal [11]. The choice between such prolonged self-renewal and differentiation is highly regulated by intrinsic signals and the external microenvironment. Stem cells are characterized as either “totipotent,” “pluripotent,” or “multipotent” during development. For the first few divisions, the cells of a fertilized egg are ‘totipotent’; that is, they are capable of differentiating into all cell types necessary to support the development of the organism including both the embryo proper and all extra-embryonic material. A few days later, stem cells from the inner cell mass of the blastocyst are “pluripotent,” having a more restricted developmental potential and are limited to differentiating into all cell types necessary for development of the embryo. This developmental potential of stem cells becomes even more restricted later in development and throughout the life span of the organism, with adults having a limited number of “multipotent” stem cells only capable of differentiating into cells of the organ in which they reside, or cell types of a common embryonic origin, a feature referred to as plasticity. Stem cells have been identified in almost all organs within the past 10-20 years, with hematopoietic stem cells (HSC) the most extensively characterized [12].

Embryonic stem cell research is largely focused on stem cells of human and mouse origin, with primate stem cells also receiving ample attention over the last decade. Mouse embryonic stem (mES) cells were first isolated in 1981 by two different groups only months apart [13, 14], while isolation of non-human primate embryonic stem cells and human embryonic stem (hES) cells occurred more than a decade later. In 1995, Jamie Thomson's group at WiCell Institute in Madison, Wisconsin isolated the first primate ES cell line [15]. Just three years later in 1998, Thomson's group isolated the first hES cell line [16].

To date, there are several common features that these ES cells share. In addition to being pluripotent and self-renewing, ES cells express the transcription factor Oct-4, which is believed to be an important marker for regulating pluripotency and self-renewal [17]. Nanog is another transcription factor that is also believed to essential for the maintenance of pluripotency and self-renewal [18]. Studies show that these markers are expressed exclusively in cells of the ICM, and decreases in expression of either of these two key factors correlate with the loss of pluripotency and self-renewal and establish the onset of differentiation [19, 20].

Despite these common features of ES cells, there also exist some key differences between human and mouse ES cells. The most significant difference is in the dependence of mES cells on the cytokine Leukemia Inhibitory Factor (LIF) for maintenance of pluripotency in *in vitro* culture systems [21]. Human ES cells do not show this dependency and appear to not need LIF of either mouse or human origin for maintenance of pluripotency [21]. Another key difference between mES cells and hES cells is the difference in surface marker expression used for classification of ES cells. Mouse ES cells express the surface protein Stage Specific Embryonic Antigen 1 (SSEA-1) while hES cells are negative for SSEA-1. Likewise, mES cells are negative for SSEA-3, SSEA-4, and Tumor Rejection Antigens (Tra) Tra-1-60 and Tra-1-81, while hES cells

are positive for all [22]. The expression of these markers is important for classification of ES cells and as a measure of pluripotency, as hES cells will loose the expression of SSEA-3, SSEA-4, Tra-1-60 and Tra1-81, as well as Oct-4 and Nanog, while gaining the expression of SSEA-1, upon differentiation. Mouse ES cells will also lose expression of Oct-4 and Nanog, but will also lose SSEA-1, and have been shown to gain expression of SSEA-3 and SSEA-4 upon differentiation [22].

Stem cells of the inner cell mass (ICM) of an unmanipulated blastocyst-stage embryo will promptly differentiate into primitive ectoderm [23]. This primitive ectoderm will ultimately become the three embryonic germ (EG) layers during gastrulation [23]. Pluripotent mES cell lines are derived from the ICM of a 3.5 day blastocyst [13, 14], while hES cells are from a 5-7 day blastocyst [16]. ES cells are isolated from embryos grown to the blastocyst stage, and after removal of the trophectoderm, the ICM is disaggregated and plated, and outgrowths are selected and expanded [23]. Even when removed from their normal embryonic environment, ICM-derived ES cells can proliferate and replace themselves indefinitely [23]. If cultured properly in an undifferentiated state, ES cells will maintain the developmental potential to form derivatives of all three EG layers [23].

In light of these stem cell properties, ES cells in theory offer a potentially unlimited supply of needed cell types and could be engineered into any tissue [2].

1.3 Strategies for creating a transplantable beta cell line from ES cells

Despite efforts, the generation of functional beta cells from an ES cell source has been, for the most part, unsuccessful. The differences in research geared at deriving pancreatic beta cells from mES cells or hES cells has largely been due to ES cell availability rather than technical challenges that are unique to one species verses another. The technological hurdles for generating ES cell derived beta cells are similar

across both mouse and human ES cells [24]. However, due to the increased knowledge and interest in hES cells in the last decade, many research efforts are shifting from mouse to human ES cells, and thus it can be expected that the majority of future breakthrough's will undoubtedly occur in hES cell focused research.

Research with mES cells derived cell types does have a certain advantage over studies with their human counterparts. Mouse ES cells that are of the same lineage as a great variety of mouse disease models are readily available [25], which allow the study of large populations of subjects of virtually any disease. In particular, a large variety of mouse models is available for various diabetes phenotypes [26-28]. Such availability of target disease models makes transplantation studies of engineered mouse cell types to evaluate the effectiveness of cellular based therapies for disease less complicated than xeno-transplantation studies between mouse models and human cell types. Due to the differences in species, xeno-transplantation treatments pose special concerns such as immunorejection that allograft studies do not. Transplantation of hES cell derived cell types into human patients is still years away from clinical investigation, thus these types of studies with mouse models provide powerful "proof of principle" data that demonstrate the therapeutic potential of ES cell derived cell types, a necessary step to facilitate interest in proceeding to non-human primate or human studies.

Although in theory, ES cells provide an unlimited cell source for the engineering of transplantable beta cells, enormous gaps still exist in our knowledge of beta cell development from ES cells. Unlike inducing the erythroid, lymphoid, or neural lineage via in vitro differentiation, inducing endoderm-derivatives and insulin-producing cells in particular, has proven to be far more difficult. Thus, efforts to generate functional beta cells from well-defined in vitro differentiation protocols have been met with variable success.

In general, the strategies to induce in vitro pancreatic differentiation of ES cells includes engineering ectopic expression of pancreatic master regulatory genes or altering the extracellular environment by 1) changing the geometry of the culture environment – embryoid body (EB) formation or monolayer culture; 2) providing extracellular signals – growth and other factors; 3) nutrient (glucose, amino acids, oxygen) restriction or serum reduction; and 4) utilizing extracellular matrix components and adhesion molecules (laminins, integrins) [2, 5, 29, 30]. Before tissue engineering efforts can differentiate ES cells into pancreatic beta cells *in vitro* however, the processes that regulate pancreas development *in vivo* must first be understood.

1.4 Pancreas development

At around embryonic day 9.5 (E9.5) in the mouse, an evagination on the dorsal side of the primitive gut endoderm initiates pancreas development [7, 31-33]. A ventral protrusion quickly follows. Both epithelial buds rapidly grow to form a branched network surrounded by mesenchymal tissue [7]. Within the next 10 days, the endocrine, ductal, and acinar cells of the pancreas develop [7]. Around E14.5 the definitive pancreas forms as the dorsal and ventral lobes fuse together. From E14 to E18 endocrine cells migrate to the mesenchyme from the epithelium to form the islets of Langerhans [7]. These islets are composed of four cell types – β cells, which produce insulin; α cells, which produce glucagon; δ cells, which produces somatostatin; and PP cells, which produce pancreatic polypeptide. It is not until the end of gestation at about E18.5 that the four islet cell types assemble in a specific manner such that β cells form the core surrounded by the other cells types [7]. Islet maturation continues even after birth when the ability to regulate insulin secretion in response to glucose develops [7].

Two phases of transcription factor expression control the development of the pancreas. The first phase plays a prominent role in the growth and differentiation of the dorsal and ventral buds protruding from the gut endoderm. The second phase accompanies the formation of the branching epithelial network and leads to endocrine and exocrine fate commitments [7, 31-33].

Transcription factors: general concepts

Cell differentiation and cell fate determination of stem cells recognizably depend on differential gene expression, which causes the increasing divergence of protein content in the various cell types formed during development. Differential gene transcription is the greatest contributor to this divergence in cell protein content, and achieving it depends significantly on the combination of transcription factors (TFs) the cell possesses [8]. Synthesis of TFs and exchange of signals between cells dominate the nuclear activity of early embryos, with over half of all genes activated at the onset of animal development encoding TFs [3]. Consequently, activation of an increasingly complex range of genes ensues to define an organism's various cell and tissue types [3].

Currently known transcription factor cascade in endocrine pancreas development

Transcription factors HNF3, HB9, p48, Brn4, NeuroD1/Beta2, PDX-1, Pax 4, Pax 6, Isl-1, Nkx2.2, and Nkx6.1, and ngn3 have all been implicated in playing an important role in endocrine pancreatic determination and differentiation [3, 34-36]. Among all the proendocrine transcription factors, ngn3 and PDX-1 are considered the master regulators, whose expression and functions in the developing pancreas have been more extensively characterized.

Ngn3 (neurogenin 3) is a basic helix-loop-helix (bHLH) factor whose expression ensues in the second phase of transcription factor cascades in pancreatic development.

Ngn3 has a central role in determining the endocrine lineage in the pancreas, defining which cells are islet progenitor cells. Homozygous ngn3 null mutations in mice lead to the development of diabetes and their death 1-3 days after birth. In the ngn3-deficient mice, no islets of Langerhans can be found, nor any of the four islet cell types and endocrine precursor cells at any stage of development [37-42].

PDX-1 (pancreatic duodenal homeobox 1) plays an essential role in early development during the first phase of transcription factor expression for development of the entire pancreas and later on in the second phase for normal beta cell function. PDX-1 defines the specific compartment of the endodermal foregut to become the dorsal and ventral pancreas, and its absence will result in the arrest of pancreatic morphogenesis and differentiation completely. Later on, PDX-1 is necessary in adult animals to maintain beta cell phenotype and to activate the expression of the beta-specific insulin, islet amyloid polypeptide (IAPP), GLUT2, and glucokinase (GK) genes [41, 43-49].

The current model demonstrating the role of the various transcription factors in endocrine pancreas differentiation depicts a very simplistic linear cascade for the proposed position of each factor (see Figure 1B). Such delineation, however, does not elucidate on their exact mechanism for driving differentiation. These factors can act at several steps or in conjunction with one another. In this simplified model, many details are left out on the specific interaction of transcription factors. For instance, both NeuroD1/Beta2 and Pax4 are direct downstream targets of ngn3, as ngn3 binds to and activates their promoters. In the absence of ngn3, expression of both NeuroD1/Beta2 and Pax4 is lost. Further downstream NeuroD1/Beta2 has been shown to interact with the E Box regulatory regions of the insulin promoter, while PDX-1 binds to the A Box regions [50, 51]. Acting cooperatively, they promote insulin transcription. Without NeuroD1/Beta2 or PDX-1 expression, insulin transcription is severely compromised. In addition, NeuroD1/Beta2 has been shown to form a heterodimer with ubiquitous factor

E47 to interact with the E Box domains on the PDX-1 promoter, which are identical to the insulin promoter, to upregulate PDX-1 in beta cells [43, 52]. A lack of NeuroD1/Beta2 expression correlates to a huge decrease in the number of beta cells. Expression of PDX-1 consequently leads to maintenance of beta cell functionality, upregulating glucokinase (GK; glycolytic enzyme acting as a glucose sensor for insulin secretion), glucose transporter 2 (GLUT2), and prohormone convertase 2 (PC2; enzyme responsible for cleaving proinsulin to yield mature insulin) [43, 53].

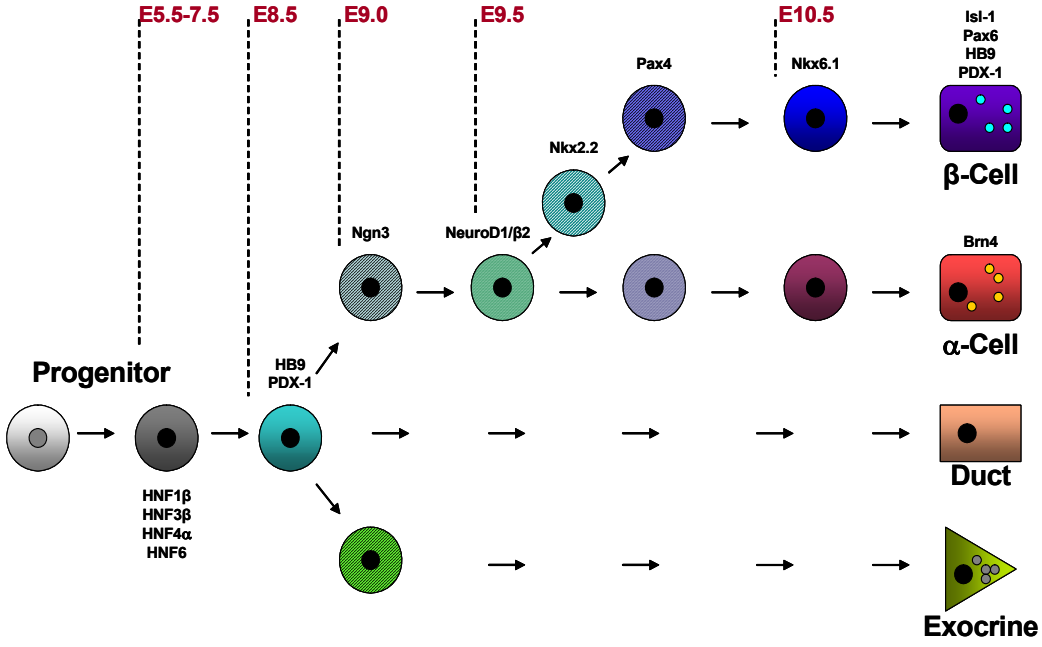

Figure 1.1. Linear model of transcription factors involved in pancreas development [3, 29, 54-56].

1.5 Genetic methods for pancreatic differentiation of ES cells: ectopic expression of master transcription factors to generate beta or insulin-producing cells

Several studies have already manipulated key transcription factors in the endocrine pancreas transcription factor cascade model by overexpressing them in

various cell model systems. Earlier studies have evaluated non stem cell, nonendocrine cell models for their ability to transdifferentiate into suitable insulin-producing cell sources for transplantation upon ectopic expression of transcription factors. Heremans et al. [57] used recombinant adenoviruses to ectopically express ngn3 and NeuroD/β2 in adult human pancreatic duct cells. This ectopic expression resulted in Notch ligand, neuroendocrine, and beta cell marker expression. The number of insulin-positive cells increased 15-fold in modified ductal cells over control. A direct correlation between the ectopic expression of ngn3 and the emergence of endocrine marker expression existed. This study also verified that Pax4 and NeuroD1/Beta2 are downstream targets of ngn3. However, the studies conducted by Heremans et al. failed to generate cells with a glucose-induced insulin release. These cells also possessed very low cellular insulin content.

Yoshida et al. stably transfected an intestinal epithelium-derived cell line, IEC-6, with PDX1. For the infected duct cells, gene expression of NeuroD/B2, Pax4, Nkx2.2, Pax6, and Nkx6.1 were all induced, as well as a 15-fold increase in insulin-positive cells. The transfected IEC-6 cells showed some markers of pancreatic beta cell phenotype and were induced to produce insulin upon treatment with betacellulin. These studies demonstrated that overexpression of key transcription factors only leads to partial expression of the beta cell phenotype and function in nonendocrine cell types, as the cells generated secreted insulin regardless of glucose concentration.

Later studies focused on ectopic expression of transcription factors in stem cell models. Blyszczuk et al. [58] coelectroporated R1 mouse ES cells with vectors incorporating the mouse PDX-1 and Pax4 genes and cultured them under slightly modified Lumelsky et al. differentiation conditions. They found that ectopic expression of Pax4 promoted the differentiation of populations with 60% insulin-producing cells

arranged in clusters which released insulin in response to glucose and normalized blood glucose levels in streptozotocin-induced diabetic mice.

Vetere et al. [59] transiently transfected mouse teratocarcinoma F9 embryonic stem cells, induced to differentiate with retinoic acid, with an ngn3 expression vector and evaluated transcription factor expression in transfected cells. They established the transcription factor sequence Ngn3 $\rightarrow$ NeuroD $\rightarrow$ Pax6 $\rightarrow$ Isl1 by analyzing gene expression via quantitative PCR 24, 48, and 72 hours following transfection.

None of the stem cell studies to date, however, analyze in depth the combinational effects of genetic modification and culturing conditions on pancreatic differentiation nor analyze in depth the pancreatic transcription factor cascade of modified cells. Blyszczuk et al. looked at mRNA levels of shh, PDX-1, Pax6, IAPP, Pax4, isl-1, ngn3, insulin, GLUT2, B-tubulin over 25 days of differentiation, but made no analysis of the hierarchy of transcription factors occurring during differentiation nor any analysis of a definitive expression pattern necessary to derive insulin-producing cells. Even though their cells produced insulin, Blyszczuk et al do not expound upon how the insulin content compares to normal islet cells. Vetere et al. made progressive steps in such hierarchy analysis by focusing on expression levels of ngn3, NeuroD, Pax6, and Isl1 in transfected F9 cells 24, 48, and 72 hours after transfection or in 10day old EBs. However, these findings did not link transcription factor expression to beta physiological function, so this hierarchy may not be representative of cells able to produce insulin at a physiological level. Such findings concerned only retinoic acid differentiated cells, and not stem cells cultured under established methods of pancreatic islet differentiation. Thus room remains for further in depth analysis of the transcription factor hierarchy for stem cells taken through a complete differentiation process.

1.6 Culturing methods for pancreatic differentiation of ES cells

Several major groups have pioneered efforts to differentiate ES cells toward a pancreatic fate utilizing sophisticated culturing methods. Soria et al pioneered efforts to differentiate ES cells into the endoderm cell lineage by transfecting mouse ES cells with the βgeo gene driven by the human insulin promoter to select for insulin-producing cells [30]. Their *in vitro* differentiation method involves growing ES cells in suspension culture (embryoid bodies) in DMEM without LIF and further differentiating the cultures in DMEM supplemented with 10mmol/l nicotinamide [30]. Soria et al. were able to obtain an ES-derived insulin-secreting cell clone with a total insulin content of 16.5 ng/μg protein and insulin secreting dynamics somewhat resembling islets [30]. This amount is about 90% of a normal mouse islet's insulin content [30]. Although Soria et al. measured insulin release in response to glucose incubation, they did not verify the pancreatic lineage of these cells. They were able to transplant $1x10^6$ insulin positive cells into streptozotocin-induced diabetic mice. After transplantation, these mice showed corrected hyperglycemia within 1 week, but their condition was completely reversed after 12 weeks [30].

Assady et al. went on to demonstrate that embryoid body (EB) formation led to the spontaneous differentiation of human ES cells into insulin-producing cells [60]. After embryoid body formation, the hES cells were left unpassaged until confluence, and replated onto gelatinized six-well tissue culture plates without a feeder layer [60]. A growth medium of knockout DMEM supplemented with 20% serum replacement, 1% nonessential amino acids, 0.1mmol/l 2-mercaptoethanol, 1mmol/l glutamine, 4ng/mol human recombinant basic fibroblast growth factor (bFGF) was used [60]. The cells generated by Assady et al. did express some beta cell markers, but they produced insulin at very low levels in response to 2 hour glucose incubations, and no quantification of the amount of insulin-producing cells produced with this method was determined.

A more complex culturing method for generating islet-like cell types came from Lumelsky et al. with their five stage protocol which involved expansion of murine ES cells (stage 1), generation of EBs in absence of LIF (stage 2), selecting for nestin-positive cells in ITSFn medium (stage 3), expanding endocrine progenitors in N2 medium containing B27 supplement and bFGF (stage 4), and differentiation of islet-like clusters by withdrawing bFGF and adding nicotinamide (stage 5) [61] Glucose triggered insulin release from these cells demonstrated mechanisms similar to those *in vivo*, but streptozotocin-induced diabetic mice did not display a sustained correction of hyperglycemia upon transplantation of cultured ES cell derived insulin positive cells. Only 15-31% of cells cultured by this method were insulin-positive, and they contained 50 times less insulin per cell than normal islet cells [61]. Since then, Hori et al. have built on the methods established by Lumelsky et al. by incorporating LY294002, an inhibitor of phosphoinositide 3-kinase (PI3K), into stage 5 of the islet differentiation protocol to increase total endocrine cell number and insulin content [62].

Most recently, Baetge et al. has developed a five stage culture method considerably more complex than Lumelsky et al. that differentiated hES cells to produce insulin positive cells along with glucagon positive cells, but also produced a population of cells that were simultaneously glucagon and insulin positive. Only 7%-12% of the total population was exclusively insulin positive [63]. This same group went on to produce pancreatic endoderm progenitors following a modified four stage culture scheme that produced cells that were PDX-1 positive but were pre-mature to expressing insulin or glucagon. They then transplanted these PDX-1 positive precursor cells into SCID mice. Results showed that these cells went on to develop into mature cells that expressed a variety of pancreatic transcription factors such as PDX-1 and Nkx6.1 as well as endocrine hormones insulin, glucagon, and ghrelin. Despite this success, however,

some transplanted cells also went on to form teratomas, a consequence that would be unacceptable for clinical use in humans [64].

Although these methods generate insulin positive or islet-like structures from both murine and human ES cells by both viral transduction and modified culture methods, they fail to generate them at high enough frequency, with high enough insulin content, or high enough glucose-responsiveness to merit levels appropriate for clinical transplantation. At least 700-900,000 islets with a normal insulin content of 10μg per million cells are needed for transplantation to alleviate type 1 diabetes [61]. The cells described above have low insulin content, far below physiologically functional beta cells. In addition, the cell lineage of these low insulin-producing cells has not been explored in detail to further ascertain their ability to maintain beta cell differentiation long enough to be suitable for cellular therapy. The few studies, such as the ones mentioned above, that have explored transplantation of engineered beta-like or insulin positive cell types typically show some response to regulating glucose levels *in vivo* initially, but fail to correct the diabetic condition over the long term. There also remains the serious concern over the stability of grafted cells to maintain their beta-like form in a stable state without the risk of tumor formation. Enrichment strategies to increase the yield of sustainable beta-functional cells thus need to be greatly improved.

1.7 Gene therapy applications for embryonic stem cells

By definition, gene therapy is the delivery of genetic material to produce a therapeutic effect. Methods to deliver therapeutic genetic material fall into two broad categories: non-viral and viral vectors [65]. Non-viral vectors include liposomes (cationic lipids mixed with nucleic acids), nanoparticles, naked DNA delivered by injection or electroporation, nanoparticles, or other means [66, 67]. Non-viral vectors still suffer from inefficient gene transfer and their expression tends to be transient, preventing their use

in many disease applications requiring sustained, high-level expression of the transgene [66]. Viral vectors, on the other hand, are derived from viruses with either RNA or DNA genomes. Viral vectors can be either integrating or nonintegrating vectors. As integrating vectors, viral vectors offer the potential for stable, long-term expression of the therapeutic gene due to their integration within the target cell genome [66]. In target cells where they are maintained as episomes, nonintegrating viral vectors can also offer efficient gene transfer [66].

Whether by nonviral or viral means, interest has increased in using embryonic stem (ES) cells as targets for gene therapy. Their properties of self-renewal, clonogenicity, and pluripotentiality give ES cells the potential to be an unlimited source of cells for cell replacement therapy particularly suitable for genetic modification [68, 69]. Applications of genetically modified ES cells include: 1) studying gene function in stem cell biology and development; 2) directing differentiation into specific tissue types; 3) selecting and isolating cultures of appropriately differentiating cells for transplantation; 4) eliminating contaminating cells *in vivo*; and 5) developing immunotolerance of transplanted cells [68, 69].

While clinical application has yet to become a reality, several studies have already shown the potential of genetically modified ES cells. Zandstra et al [70] were able to achieve enrichment of cardiomyocytes following genetic modification of mES cells with a vector encoding a fusion gene consisting of the alpha-cardiac myosin heavy chain (MHC) promoter driving the aminoglycoside phosphotransferase (neomycin resistance) gene. Following the differentiation culture period, treatment with G418 resulted in cultures composed of more than 70% cardiomyocytes, as verified through gene expression, immunohistological and electron microscopic analysis. In another study, Blyszczuk et al. [58] coelectroporated R1 mES cells with vectors incorporating the mouse proendocrine *PDX-1* and *Pax4* transcription factor genes and cultured them

under pancreatic differentiation conditions. They found that ectopic expression of Pax4 promoted the differentiation of populations with 60% insulin-producing cells arranged in clusters, which released insulin in response to glucose. When the genetically modified, insulin-producing mES cells were transplanted into streptozotocin-induced diabetic mice, blood glucose levels normalized. In a novel approach, Schuldiner et al [71] devised a system to remove transplanted, undifferentiated hES cells forming teratomas in mice *in vivo*. The hES cells were genetically modified prior to transplantation with a vector encoding the herpes simplex thymidine kinase (*HSV-tk*) gene, which is sensitive to the FDA-approved drug ganciclovir. Tumors formed by the transplanted hES cells were ablated in mice following administration of ganciclovir, offering an insight to developing a safety strategy to eliminate contaminating cells in the host recipient.

1.8 Recombinant retroviruses and lentiviruses as gene transfer vectors

In order to express ectopic genes in a target cell, recombinant retroviruses are common vehicles for gene transfer, as they accurately and stably integrate the gene of interest into the target cell genome and theoretically offer long-term therapy [72, 73]. Control of long-term expression from retroviral vectors can also be implemented through inducible or tissue-specific promoters being included in the vector design [66]. Frequently used retroviruses for gene transfer are derived from the Moloney murine leukemia virus (MLV) or from the human immunodeficiency virus type 1 (HIV-1), a member of a more complex subgroup of retroviruses called lentiviruses.

Recombinant retroviruses are replication-incompetent derivatives of wild-type retroviruses. Wild-type retrovirus particles (Figure 1.2) consist of two identical copies of RNA genome surrounded by structural core proteins and encapsidated by a lipid bilayer membrane. From this membrane protrudes multiple knobs of surface envelope proteins. The viral RNA consists of three essential genes, *gag*, *pol*, and *env*, which are flanked by

long terminal repeats (LTR). Core structural proteins such as the capsid, matrix and nucleocapsid are encoded by the *gag* gene and are generated by the proteolytic cleavage of the *gag* precursor protein. Viral enzymes protease, reverse transcriptase, and integrase are encoded by the *pol* gene and are derived from the *gag-pol* precursor. The *env* gene encodes for the envelope glycoproteins to mediate virus fusion.

To infect a cell (Figure 1.3), retroviruses attach first to the cell surface through nonspecific interactions between surface proteins on the cell and on the virus [74, 75]. Now at the cell surface, retroviruses bind specifically to their receptor if available to enter the cell through membrane fusion. Following fusion, virus proteins and the virus genome are released into the cell. The viral enzyme reverse transcriptase converts the viral RNA into double-stranded proviral DNA. With its accompanying viral proteins, the proviral DNA forms a preintegration complex and translocates to the cell nucleus. Once inside the nucleus, the viral enzyme integrase mediates integration of the provirus into the host cell genome, where host cell transcription factors initiate transcription from the LTR.

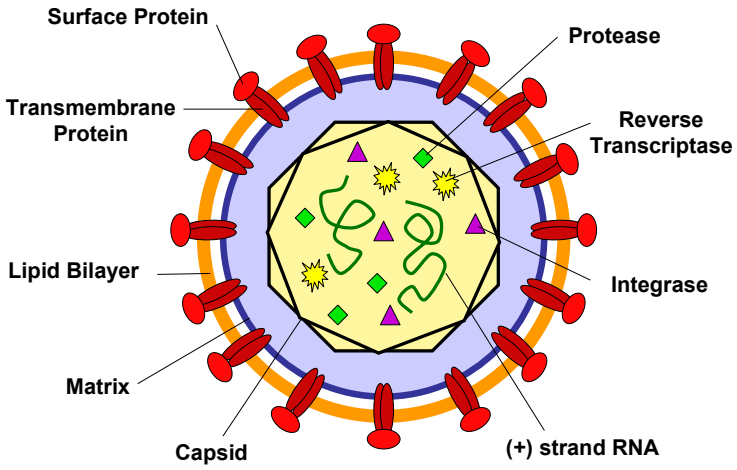

Figure 1.2. Basic structure of a retrovirus.

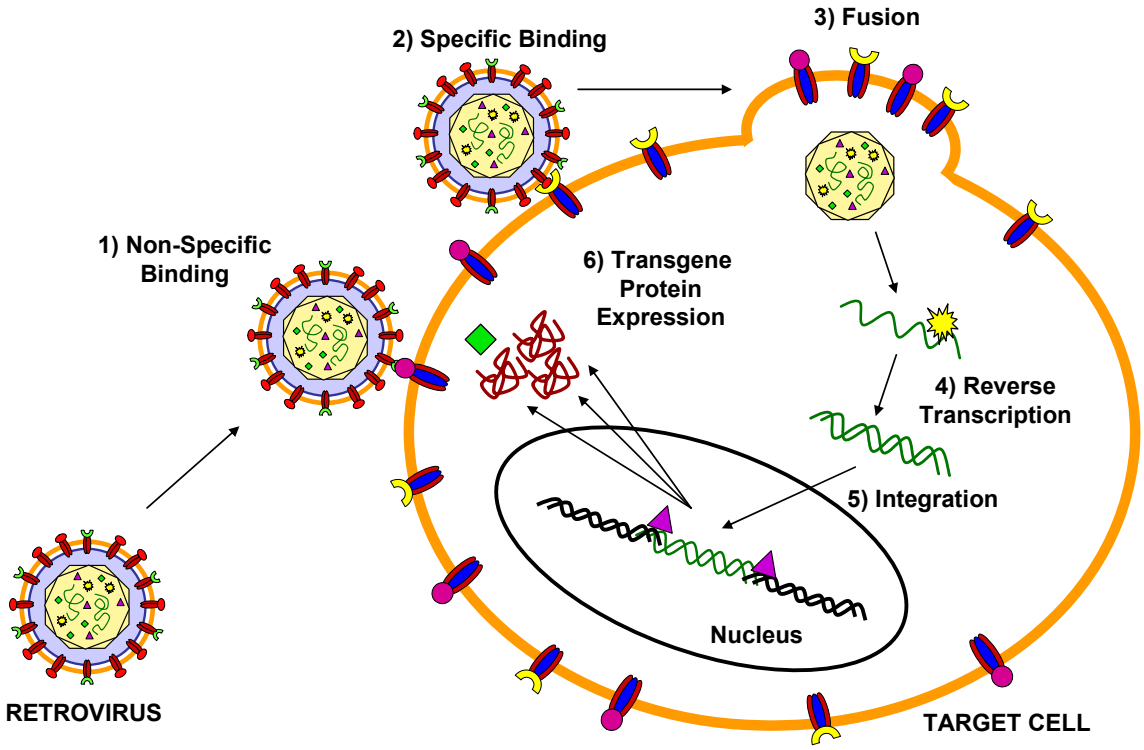

Figure 1.3. Transduction of target cells by recombinant retroviruses. A virus must complete several steps before it successfully inserts the ectopic gene into the genome of a target cell. The virion must first reach the cell surface by convection and/or diffusion where it binds nonspecifically and then attaches specifically to the cell surface viral receptors. The virion is subsequently removed from the extracellular environment (internalized), sheds its membrane, and releases its internal protein-RNA complex into the cytoplasm (un-coats). The uncoated RNA genome of the retrovirus is then reverse transcribed into DNA by reverse transcriptase (a virion associated enzyme) and the resultant protein DNA complex (pre-integration complex) is transported to the nucleus where it is integrated into the host cell genome by the virion associated enzyme integrase. After integration, the ectopic gene of interest is expressed.

Recombinant retroviruses are identical in structure to wild type virus except they carry a genetically engineered genome encoding the gene of interest instead of the viral *gag*, *pol*, and *env* structural genes necessary to form an infectious virion capable of replicating and producing progeny. As a result, recombinant retroviruses are incapable of self-replication, but still deliver genes in a manner similar to wild type virus [76, 77]. Recombinant retroviruses, however, retain the regulatory sequences necessary for their expression and the special packaging sequence (ψ^+) required for their encapsidation into an infectious particle [78]. Recombinant retroviruses are generally produced by transfecting the producer cell lines with separate expression plasmids encoding the *gag*, *pol*, and *env* structural genes (Figure 1.4) and the therapeutic vector with the gene of interest. The subsequently expressed structural gag, pol, and env proteins recognize the packaging sequence on the transcribed therapeutic vector and the retroviral and lentiviral RNAs are encapsidated into an infectious virion. These virions are released into the culture medium and harvested for future transductions.

When choosing a retroviral vector for transduction experiments, it is important to consider the properties of the target cell. For instance, recombinant lentiviruses differ from basic MLV-derived retroviruses in their ability to infect both dividing and non-dividing cells, while recombinant retroviruses can only infect actively dividing cells [79, 80]. This functional difference often makes the use of lentiviruses more advantageous in many gene therapy applications [81, 82]. Retroviral vectors have been useful for generating stable cell lines expressing a transgene of choice and for marking studies of cell lineage. Dependence on cell division restricts their *in vivo* applications to gene delivery to actively dividing tissues, stem cells and cancer cells. On the other hand, lentiviral vectors can be used for actively dividing cells or direct administration to many organs not actively dividing like the brain, eye, liver, and muscle.

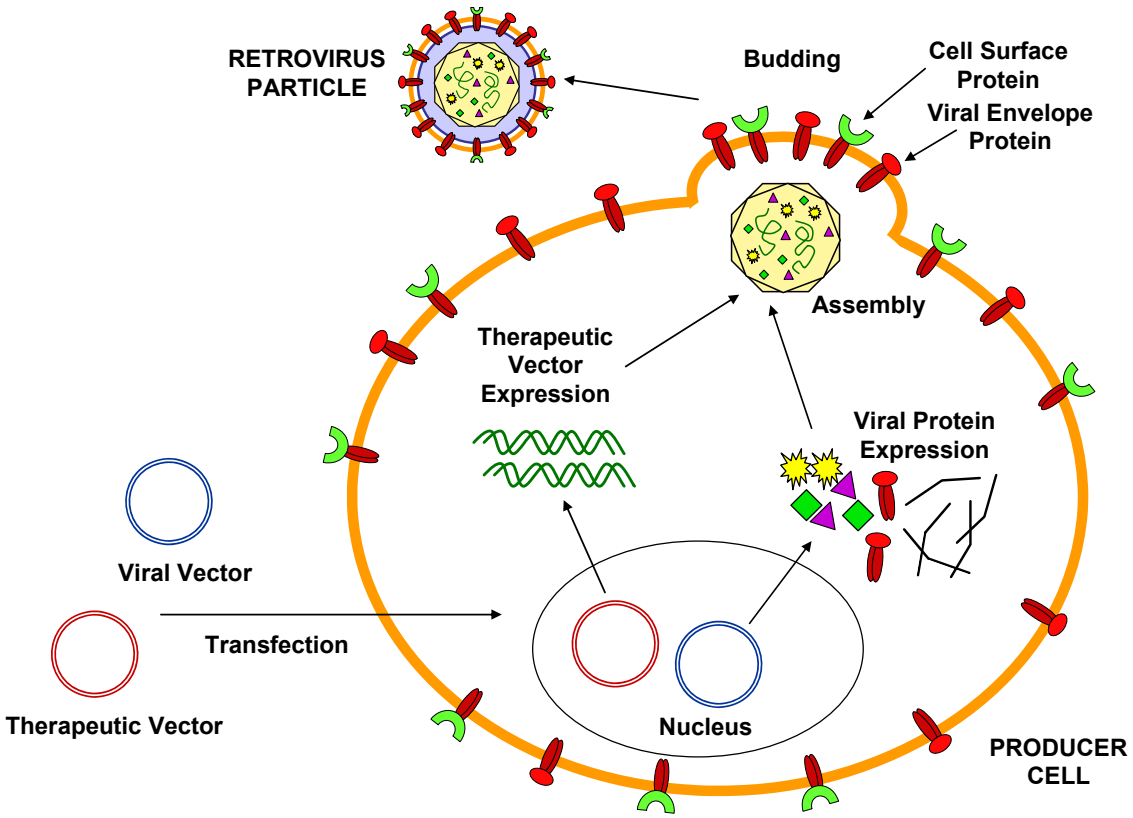

Figure 1.4. Production of recombinant retrovirus stock solutions by producer cell lines. Production of recombinant retroviruses involves the transfection of the producer cell line with viral vectors encoding the necessary structural and envelope proteins and the therapeutic vector containing the gene of interest and the packaging sequence. The therapeutic vector is encapsidated by the proteins encoded on the viral vector and buds from the cell to generate the recombinant viral vector. As the virus buds from the cell surface, it incorporates a lipid bilayer from the cell consisting of virus envelope proteins and other cell membrane proteins. Vector particles accumulate in the culture medium and are harvested for future use.

The ability of retroviruses and lentiviruses to infect actively dividing cells or nondividing cells stems from their routes of entry into the nucleus to integrate their genetic material [83, 84]. Because lentiviruses can infect both non-dividing and dividing cells, they are presumed to enter the intact nucleus through the nuclear pores [85-88]. The import of HIV-derived viruses into an intact nucleus remains unclear, but recent studies suggest that the HIV preintegration complex (PIC) can bind and use small host RNAs (including specific tRNAs or tRNA precursors) as carriers for transport to the nucleus [89]. For more simple retroviruses like MLV, successful infection can only occur when the cell is actively dividing and the nuclear membrane is dispersed during mitosis [90]. Retroviruses become included in the nucleus during the reformation of the nuclear membrane in the daughter cells [90]. Otherwise retroviral PICs cannot enter the nucleus in cells arrested in G1/G0 or in G2 and remain in the cytoplasm [91, 92].

Once inside the nucleus, retroviral and lentiviral PICs attack the host chromosomal DNA to integrate the viral DNA. It was previously thought that retroviruses and lentiviruses integrated randomly within the host genome [93]. However, recent studies have uncovered nonrandom integration patterns [94-98]. MLV-based retroviral vectors have been found to integrate predominantly around transcription start sites of cellular promoters [99]. In particular, CpG islands, chromosomal regions enriched with the CpG dinucleotide, are favorable sites of integration [96]. In contrast, lentiviral vectors favor transcription units of active genes and gene-dense regions of the genome [96]. These disparate integration patterns of retroviruses and lentiviruses may have implications for their safety in human therapies. Since MLV-based retroviral vectors integrate near the 5' ends of genes, they may be more likely to disrupt transcriptional control and expression of potentially oncogenic gene products and lead to the increased cancer risks associated with insertional mutagenesis [93, 99]. Insertion of lentiviruses within transcription units can lead to frame shifts and other events which interrupt the

production of a normal gene product, but lentiviruses may be less likely to induce tumorigenesis [93]. Whether lentiviruses offer a safer integrating vector for gene therapy, however, needs to be directly demonstrated and confirmed in several animal models [93, 99].

1.9 Limitations to retrovirus-mediated gene transfer to embryonic stem cells

Retrovirus-mediated gene transfer to embryonic stem cells has met with limited success, as gene silencing of retroviral vectors has compromised long-term expression. Gene silencing is the most widely discussed restriction inhibiting the use of retroviral vectors for gene transfer to embryonic stem cells. Gene silencing is a term used to include three related phenomena: 1) transcriptional *silencing* observed shortly after infection; 2) *variegation*, in which subsets of cells either express or are silent; and 3) *extinction*, whereby long-term culture or differentiation leads to the progressive silencing of retrovirus transgenes that were initially expressed [100, 101].

The two main molecular mechanisms responsible for gene silencing of retroviruses are *de novo* cytosine methylation and histone remodeling [102]. Methylation of DNA involves the addition of a methyl group to the 5' position of a cytosine in a cytosine-phosphate-guanine (CpG) dinucleotide [103]. CpG methylation is catalyzed by DNA methyltransferases (DNMTs) and is symmetrical along both DNA strands [103]. DNMTs can recognize isolated CpGs, clustered CpGs or clustered CpGs within a CpG island [103]. Frequency of cytosine greater than 0.6 with a GC dinucleotide content greater than 50% defines a CpG island [103]. In particular, DNMTs recognize the CpG nucleotides clustered in the U3 region and in the R region directly spanning the transcription start site of the long terminal repeat (LTR) promoter of retroviral vectors [104].

Histone modifications include acetylation, phosphorylation, ubiquitination, and methylation [105]. The condensed, inaccessible chromatin marking silenced genes is created by histone modifications involving the deacetylation of histones H3 and H4 by histone deacetylases HDAC1 and HDAC2 and the abundant presence of linker histone H1 [106].

Silencing of retrovirus transgenes was originally speculated to be due to DNA methylation of the CpG islands present in the retroviral LTR promoter. But more recently, two interesting models have emerged to explain retrovirus silencing [102, 107]. In the first model, DNA methylation has a causal role, whereby methylation acts as a genome defense mechanism. Following methylation of retroviral DNA, the methyl groups then become targets for methyl-binding proteins, like MeCP2 [108]. These proteins in turn recruit co-repressors such as histone deacetylases, which catalyze the deacetylation of histones H3 and H4, leading to chromatin condensation and silencing of the retroviral transgene [109].

In the second model, it is speculated that stem cell-specific factors act as negative *trans*-factors binding to the newly integrated provirus in the negative control region (NCR) of retroviral LTR [110]. YY1, ELP, and Factor A have been implicated as possible candidates [111-113]. In turn, these negative factors are targeted by histone deacetylases, leading to chromatin remodelling and modifications such as acetyl groups or methyl groups being attached to histones [102]. This new repressive histone code is subsequently targeted by *de novo* methylase to fully methylate the retroviral LTR. Therefore, the role of methylation in this model is to serve as a secondary or associated step to maintain and propogate a heritable silenced state.

With gene silencing as an extremely effective obstacle limiting the use of retroviral vectors to genetically modify ES cells, less attention has been paid to other possible rate-limiting steps in retrovirus-mediated gene transfer to ES cells. However,

multiple steps in the transduction process should be considered when evaluating the overall efficiency of gene transfer protocols for stem cells.

1.10 Enhancement of gene transfer using virus-polymer complexation

Studies have demonstrated that the use of anionic and cationic polymers increases the efficiency of retroviral gene transfer. By combining equal weight concentrations of cationic polymer Polybrene (PB) and anionic polymer Chondroitin Sulfate C (CSC) to retrovirus stocks, retrovirus-polymer complexes can be formed and rapidly pelleted by centrifugation in a table top centrifuge and resuspended in fresh culture medium [114]. Due to their large size, the virus-polymer complexes more rapidly sediment to the surface of the cells, thus increasing the rate that viruses reach the surfaces of cells before they decay and increasing the number of genes transferred [115]. Polymer complexation also offers a simplified means of concentrating and purifying retrovirus stocks. Resuspension of the virus-polymer pellet in smaller volumes concentrates the virus and has significantly increased the efficiency of gene transfer to cell types such as primary human fibroblasts and murine hematopoeitic progenitor cells [114-116]. Concentrating the virus by resuspending it in one-eighth its original volume can increase gene transfer 10- to 20-fold over original unconcentrated retrovirus stock in NIH3T3 murine fibroblasts [114, 115]. Interestingly, the polymer complexes selectively integrate more than 70-80% of retrovirus particles and less than 0.3-0.4% of all other proteins [114]. These virus-polymer complexes show no detectable levels of inhibitory activity due to their purification from inhibitors of transduction like negatively charged molecules such as proteoglycans and glycosaminoglycans, as well as free retrovirus envelope proteins [117-120]. When virus purified by complexation is used, transduction increases monotonically and is linearly proportional to virus concentration in NIH 3T3

murine fibroblasts [121]. Figure 1.5 outlines this procedure for gene transfer enhancement.

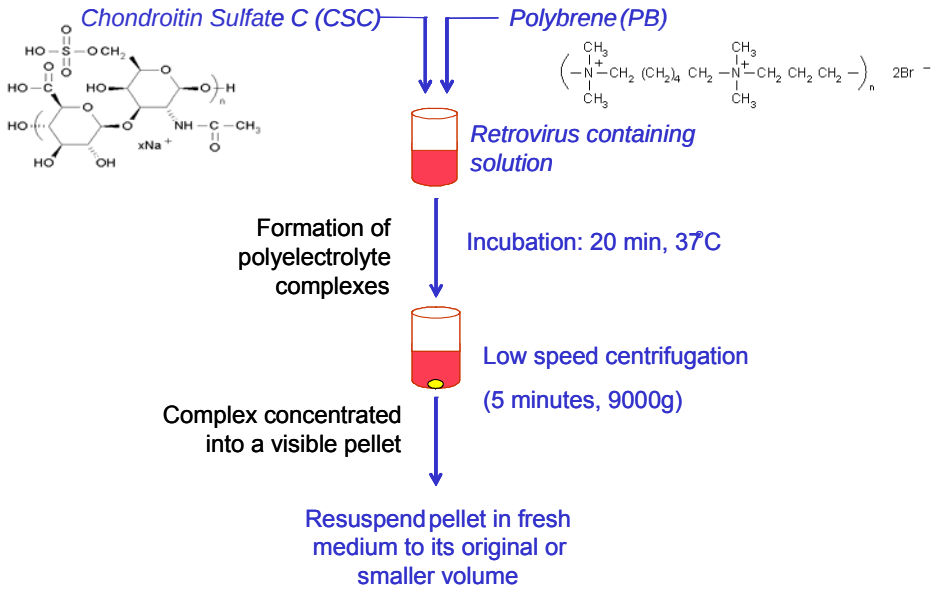

Figure 1.5. Procedure for enhancing gene transfer using anionic and cationic polymers.

1.11 Thesis objectives

The long term goal of this thesis was to ectopically express the proendocrine transcription factor Neurogenin 3 (ngn3) in murine embryonic stem (mES) cells using retroviral gene transfer in order to provide the genetic "push" to regulate their pancreatic differentiation and enhance beta cell phenotype expression, thereby improving methods to provide a physiologically functional cell source for pancreatic tissue engineering. Ngn3 expression in the developing mouse pancreas is essential for endocrine fate determination, without which the islets of Langerhans are unable to form. We hypothesized that sustained overexpression of ngn3 in murine embryonic stem cells in vitro will be an efficient trigger to enhance the differentiation and beta cell functionality of

ES cells, but that multiple steps in the retroviral transduction process restrict the efficient expression of such transgenes for therapeutic purposes.

The objectives of this thesis were to characterize and enhance the efficiency of transduction of murine embryonic stem (mES) cells, and to identify any additional restrictions to gene transfer in this cell type. To accomplish these objectives, we pursued the following aims:

1) Evaluate the ability of mES cells to respond to genetic modification with a retroviral vector encoding proendocrine transcription factor ngn3.
2) Determine the extent to which a polymer complexation method to increase the rate of transport of viruses to mES cells enhances gene transfer.
3) Determine the efficiency of major steps in the transduction process in mES cells.
4) Evaluate the effect that a specific genetic mutation in mES cells and chemical agent has on gene transfer.

In these studies, we evaluated gene transfer to ES cells in the mouse model, due to the availability of multiple mES cell lines. In addition, using a mouse model afforded us the ability to examine specific gene knockouts, otherwise unavailable in other animal or human models.

1.12 Organization of thesis

In chapter one, we emphasize that the motivation for our work is to derive a functional cell source for pancreatic transplantation from embryonic stem cells. We briefly introduce stem cells, gene therapy, the use of recombinant retroviruses as gene delivery vectors, and the limitations of employing retroviral-mediated gene transfer to embryonic stem cells.

In chapter two, we constructed two retroviral vectors encoding proendocrine transcription factors Neurogenin 3 (ngn3) and pancreatic duodenal homeobox 1 (PDX-1). We then genetically modified mES cells with a retroviral vector encoding proendocrine transcription factor ngn3 and examined the resulting pancreatic gene expression.

In chapter three, we evaluate a method for its ability to increase the efficiency of retroviral-mediated gene transfer to murine embryonic stem cells by increasing the rate and concentration that retroviruses are delivered to the cell surface. The method consists of aggregating retrovirus particles with charged polymers to form high molecular weight virus-polymer complexes which rapidly concentrates and purifies virus stocks, as well as increases sedimentation of virus particles to the cell surface. Also, we evaluate the utility of pseudotyping retroviruses with various envelope proteins to improve gene transfer to embryonic stem cells.

In chapter four, we examine the efficiency with which embryonic stem cells complete the major steps in the retrovirus and lentivirus transduction process in order to identify which steps in the virus lifecycle are restricted in mES cells. Specifically, we quantify the rate that viruses attach to and are absorbed by mES cells, integrate, and are expressed.

In chapter five, we examine the efficiency of gene transfer in mES cells using three different recombinant viral vectors. We also evaluate whether nonlethal genetic mutations can be made to mES cells to increase the efficiency of gene transfer.

In chapter six, we summarize our major conclusions and offer suggestions for future research.

1.13 References

[1] F. Levine, Gene therapy for diabetes: strategies for beta-cell modification and replacement, Diabetes Metab Rev 13 (1997) 209-246.

[2] B. Soria, A. Skoudy, F. Martin, From stem cells to beta cells: new strategies in cell therapy of diabetes mellitus, Diabetologia 44 (2001) 407-415.

[3] L. St-Onge, R. Wehr, P. Gruss, Pancreas development and diabetes, Curr Opin Genet Dev 9 (1999) 295-300.

[4] F. Levine, G. Leibowitz, Towards gene therapy of diabetes mellitus, Mol Med Today 5 (1999) 165-171.

[5] B. Soria, In-vitro differentiation of pancreatic beta-cells, Differentiation 68 (2001) 205-219.

[6] B. Soria, E. Andreu, G. Berna, E. Fuentes, A. Gil, T. Leon-Quinto, F. Martin, E. Montanya, A. Nadal, J.A. Reig, C. Ripoll, E. Roche, J.V. Sanchez-Andres, J. Segura, Engineering pancreatic islets, Pflugers Arch 440 (2000) 1-18.

[7] K. Docherty, Growth and development of the islets of Langerhans: implications for the treatment of diabetes mellitus, Curr Opin Pharmacol 1 (2001) 641-650.

[8] J. Gurdon, Developmental biology and the redirection or replacement of cells, Philos Trans R Soc Lond B Biol Sci 354 (1999) 1967-1976.

[9] P. Itkin-Ansari, I. Geron, E. Hao, C. Demeterco, B. Tyrberg, F. Levine, Cell-based therapies for diabetes: progress towards a transplantable human beta cell line, Ann N Y Acad Sci 1005 (2003) 138-147.

[10] P. Itkin-Ansari, F. Levine, Sources of beta-Cells for Human Cell-Based Therapies for Diabetes, Cell Biochem Biophys 40 (2004) 103-112.

[11] F.M. Watt, B.L. Hogan, Out of Eden: stem cells and their niches, Science 287 (2000) 1427-1430.

[12] M. Reyes, C.M. Verfaillie, Characterization of multipotent adult progenitor cells, a subpopulation of mesenchymal stem cells, Ann N Y Acad Sci 938 (2001) 231-233; discussion 233-235.

[13] M.J. Evans, M.H. Kaufman, Establishment in culture of pluripotential cells from mouse embryos, Nature 292 (1981) 154-156.

[14] G.R. Martin, Isolation of a pluripotent cell line from early mouse embryos cultured in medium conditioned by teratocarcinoma stem cells, Proc Natl Acad Sci U S A 78 (1981) 7634-7638.

[15] J.A. Thomson, J. Kalishman, T.G. Golos, M. Durning, C.P. Harris, R.A. Becker, J.P. Hearn, Isolation of a primate embryonic stem cell line, Proc Natl Acad Sci U S A 92 (1995) 7844-7848.

[16] P. Menendez, L. Wang, M. Bhatia, Genetic manipulation of human embryonic stem cells: a system to study early human development and potential therapeutic applications, Curr Gene Ther 5 (2005) 375-385.

[17] H. Niwa, J. Miyazaki, A.G. Smith, Quantitative expression of Oct-3/4 defines differentiation, dedifferentiation or self-renewal of ES cells, Nat Genet 24 (2000) 372-376.

[18] A.H. Hart, L. Hartley, M. Ibrahim, L. Robb, Identification, cloning and expression analysis of the pluripotency promoting Nanog genes in mouse and human, Dev Dyn 230 (2004) 187-198.

[19] K. Mitsui, Y. Tokuzawa, H. Itoh, K. Segawa, M. Murakami, K. Takahashi, M. Maruyama, M. Maeda, S. Yamanaka, The homeoprotein Nanog is required for maintenance of pluripotency in mouse epiblast and ES cells, Cell 113 (2003) 631-642.

[20] C. Hansis, J.A. Grifo, L.C. Krey, Oct-4 expression in inner cell mass and trophectoderm of human blastocysts, Mol Hum Reprod 6 (2000) 999-1004.

[21] A.G. Smith, J.K. Heath, D.D. Donaldson, G.G. Wong, J. Moreau, M. Stahl, D. Rogers, Inhibition of pluripotential embryonic stem cell differentiation by purified polypeptides, Nature 336 (1988) 688-690.

[22] J.S. Draper, C. Pigott, J.A. Thomson, P.W. Andrews, Surface antigens of human embryonic stem cells: changes upon differentiation in culture, J Anat 200 (2002) 249-258.

[23] J.S. Odorico, D.S. Kaufman, J.A. Thomson, Multilineage differentiation from human embryonic stem cell lines, Stem Cells 19 (2001) 193-204.

[24] L.C. Murtaugh, Pancreas and beta-cell development: from the actual to the possible, Development 134 (2007) 427-438.

[25] V.E. Papaioannou, Embryonic stem cells and mouse models of human syndromes: examples from the T-box gene family, Reprod Biomed Online 4 Suppl 1 (2002) 68-71.

[26] T.J. Allen, M.E. Cooper, H.Y. Lan, Use of genetic mouse models in the study of diabetic nephropathy, Curr Atheroscler Rep 6 (2004) 197-202.

[27] K.A. Sullivan, J.M. Hayes, T.D. Wiggin, C. Backus, S. Su Oh, S.I. Lentz, F. Brosius, 3rd, E.L. Feldman, Mouse models of diabetic neuropathy, Neurobiol Dis 28 (2007) 276-285.

[28] E.H. Leiter, C.H. Lee, Mouse models and the genetics of diabetes: is there evidence for genetic overlap between type 1 and type 2 diabetes?, Diabetes 54 Suppl 2 (2005) S151-158.

[29] D.J. Kaczorowski, E.S. Patterson, W.E. Jastromb, M.J. Shamblott, Glucose-responsive insulin-producing cells from stem cells, Diabetes Metab Res Rev 18 (2002) 442-450.

[30] K.S. O'Shea, Directed differentiation of embryonic stem cells: genetic and epigenetic methods, Wound Repair Regen 9 (2001) 443-459.

[31] S.K. Kim, R.J. MacDonald, Signaling and transcriptional control of pancreatic organogenesis, Curr Opin Genet Dev 12 (2002) 540-547.

[32] J. Peters, A. Jurgensen, G. Kloppel, Ontogeny, differentiation and growth of the endocrine pancreas, Virchows Arch 436 (2000) 527-538.

[33] J.M. Wells, Genes expressed in the developing endocrine pancreas and their importance for stem cell and diabetes research, Diabetes Metab Res Rev 19 (2003) 191-201.

[34] H. Edlund, Transcribing pancreas, Diabetes 47 (1998) 1817-1823.

[35] H. Edlund, Developmental biology of the pancreas, Diabetes 50 Suppl 1 (2001) S5-9.

[36] J. Jensen, Gene regulatory factors in pancreatic development, Dev Dyn 229 (2004) 176-200.

[37] G. Gradwohl, A. Dierich, M. LeMeur, F. Guillemot, neurogenin3 is required for the development of the four endocrine cell lineages of the pancreas, Proc Natl Acad Sci U S A 97 (2000) 1607-1611.

[38] T. Asano, Y. Hanazono, Y. Ueda, S. Muramatsu, A. Kume, H. Suemori, Y. Suzuki, Y. Kondo, K. Harii, M. Hasegawa, N. Nakatsuji, K. Ozawa, Highly efficient gene transfer into primate embryonic stem cells with a simian lentivirus vector, Mol Ther 6 (2002) 162-168.

[39] M. Jenny, C. Uhl, C. Roche, I. Duluc, V. Guillermin, F. Guillemot, J. Jensen, M. Kedinger, G. Gradwohl, Neurogenin3 is differentially required for endocrine cell fate specification in the intestinal and gastric epithelium, Embo J 21 (2002) 6338-6347.

[40] S.K. Kim, M. Hebrok, Intercellular signals regulating pancreas development and function, Genes Dev 15 (2001) 111-127.

[41] J.C. Lee, S.B. Smith, H. Watada, J. Lin, D. Scheel, J. Wang, R.G. Mirmira, M.S. German, Regulation of the pancreatic pro-endocrine gene neurogenin3, Diabetes 50 (2001) 928-936.

[42] V.M. Schwitzgebel, D.W. Scheel, J.R. Conners, J. Kalamaras, J.E. Lee, D.J. Anderson, L. Sussel, J.D. Johnson, M.S. German, Expression of neurogenin3 reveals an islet cell precursor population in the pancreas, Development 127 (2000) 3533-3542.

[43] S. Ashizawa, F.C. Brunicardi, X.P. Wang, PDX-1 and the pancreas, Pancreas 28 (2004) 109-120.

[44] A. Grapin-Botton, A.R. Majithia, D.A. Melton, Key events of pancreas formation are triggered in gut endoderm by ectopic expression of pancreatic regulatory genes, Genes Dev 15 (2001) 444-454.

[45] A.M. Holland, M.A. Hale, H. Kagami, R.E. Hammer, R.J. MacDonald, Experimental control of pancreatic development and maintenance, Proc Natl Acad Sci U S A 99 (2002) 12236-12241.

[46] H. Hanawa, P.F. Kelly, A.C. Nathwani, D.A. Persons, J.A. Vandergriff, P. Hargrove, E.F. Vanin, A.W. Nienhuis, Comparison of various envelope proteins for their ability to pseudotype lentiviral vectors and transduce primitive hematopoietic cells from human blood, Mol Ther 5 (2002) 242-251.

[47] M. Sander, M.S. German, The beta cell transcription factors and development of the pancreas, J Mol Med 75 (1997) 327-340.

[48] D.Q. Shih, M. Stoffel, Dissecting the transcriptional network of pancreatic islets during development and differentiation, Proc Natl Acad Sci U S A 98 (2001) 14189-14191.

[49] J. Jonsson, L. Carlsson, T. Edlund, H. Edlund, Insulin-promoter-factor 1 is required for pancreas development in mice, Nature 371 (1994) 606-609.

[50] C. Brink, Promoter elements in endocrine pancreas development and hormone regulation, Cell Mol Life Sci 60 (2003) 1033-1048.

[51] H. Kojima, M. Fujimiya, K. Matsumura, P. Younan, H. Imaeda, M. Maeda, L. Chan, NeuroD-betacellulin gene therapy induces islet neogenesis in the liver and reverses diabetes in mice, Nat Med 9 (2003) 596-603.

[52] S. Sharma, U.S. Jhala, T. Johnson, K. Ferreri, J. Leonard, M. Montminy, Hormonal regulation of an islet-specific enhancer in the pancreatic homeobox gene STF-1, Mol Cell Biol 17 (1997) 2598-2604.

[53] S. Miyazaki, E. Yamato, J. Miyazaki, Regulated expression of pdx-1 promotes in vitro differentiation of insulin-producing cells from embryonic stem cells, Diabetes 53 (2004) 1030-1037.

[54] S.K. Chakrabarti, R.G. Mirmira, Transcription factors direct the development and function of pancreatic beta cells, Trends Endocrinol Metab 14 (2003) 78-84.

[55] H. Edlund, Pancreatic organogenesis--developmental mechanisms and implications for therapy, Nat Rev Genet 3 (2002) 524-532.

[56] V.M. Schwitzgebel, Programming of the pancreas, Mol Cell Endocrinol 185 (2001) 99-108.

[57] Y. Heremans, M. Van De Casteele, P. in't Veld, G. Gradwohl, P. Serup, O. Madsen, D. Pipeleers, H. Heimberg, Recapitulation of embryonic neuroendocrine differentiation in adult human pancreatic duct cells expressing neurogenin 3, J Cell Biol 159 (2002) 303-312.

[58] P. Blyszczuk, J. Czyz, G. Kania, M. Wagner, U. Roll, L. St-Onge, A.M. Wobus, Expression of Pax4 in embryonic stem cells promotes differentiation of nestin-positive progenitor and insulin-producing cells, Proc Natl Acad Sci U S A 100 (2003) 998-1003.

[59] A. Vetere, E. Marsich, M. Di Piazza, R. Koncan, F. Micali, S. Paoletti, Neurogenin3 triggers beta-cell differentiation of retinoic acid-derived endoderm cells, Biochem J 371 (2003) 831-841.

[60] S. Assady, G. Maor, M. Amit, J. Itskovitz-Eldor, K.L. Skorecki, M. Tzukerman, Insulin production by human embryonic stem cells, Diabetes 50 (2001) 1691-1697.

[61] N. Lumelsky, O. Blondel, P. Laeng, I. Velasco, R. Ravin, R. McKay, Differentiation of embryonic stem cells to insulin-secreting structures similar to pancreatic islets, Science 292 (2001) 1389-1394.

[62] Y. Hori, I.C. Rulifson, B.C. Tsai, J.J. Heit, J.D. Cahoy, S.K. Kim, Growth inhibitors promote differentiation of insulin-producing tissue from embryonic stem cells, Proc Natl Acad Sci U S A 99 (2002) 16105-16110.

[63] K.A. D'Amour, A.G. Bang, S. Eliazer, O.G. Kelly, A.D. Agulnick, N.G. Smart, M.A. Moorman, E. Kroon, M.K. Carpenter, E.E. Baetge, Production of pancreatic hormone-expressing endocrine cells from human embryonic stem cells, Nat Biotechnol 24 (2006) 1392-1401.

[64] E. Kroon, L.A. Martinson, K. Kadoya, A.G. Bang, O.G. Kelly, S. Eliazer, H. Young, M. Richardson, N.G. Smart, J. Cunningham, A.D. Agulnick, K.A. D'Amour, M.K. Carpenter, E.E. Baetge, Pancreatic endoderm derived from human embryonic stem cells generates glucose-responsive insulin-secreting cells in vivo, Nat Biotechnol 26 (2008) 443-452.

[65] T. Friedman, The Development of Human Gene Therapy, Cold Spring Harbor Lab. Press, Cold Spring Harbor, NY, 1999.

[66] I.M. Verma, M.D. Weitzman, Gene therapy: twenty-first century medicine, Annu Rev Biochem 74 (2005) 711-738.

[67] N.J. Caplen, Gene therapy: different strategies for different applications. American Society of Gene Therapy: First Annual Meeting, Seattle, Washington, USA, 28-31 May 1998, Mol Med Today 4 (1998) 374-375.

[68] Y. Lai, I. Drobinskaya, E. Kolossov, C. Chen, T. Linn, Genetic modification of cells for transplantation, Adv Drug Deliv Rev 60 (2008) 146-159.

[69] F. Yates, G.Q. Daley, Progress and prospects: gene transfer into embryonic stem cells, Gene Ther 13 (2006) 1431-1439.

[70] P.W. Zandstra, C. Bauwens, T. Yin, Q. Liu, H. Schiller, R. Zweigerdt, K.B. Pasumarthi, L.J. Field, Scalable production of embryonic stem cell-derived cardiomyocytes, Tissue Eng 9 (2003) 767-778.

[71] M. Schuldiner, J. Itskovitz-Eldor, N. Benvenisty, Selective ablation of human embryonic stem cells expressing a "suicide" gene, Stem Cells 21 (2003) 257-265.

[72] A. Mountain, Gene therapy: the first decade, Trends Biotechnol 18 (2000) 119-128.

[73] C.E. Thomas, A. Ehrhardt, M.A. Kay, Progress and problems with the use of viral vectors for gene therapy, Nat Rev Genet 4 (2003) 346-358.

[74] G.H. Guibinga, A. Miyanohara, J.D. Esko, T. Friedmann, Cell surface heparan sulfate is a receptor for attachment of envelope protein-free retrovirus-like particles and VSV-G pseudotyped MLV-derived retrovirus vectors to target cells, Mol Ther 5 (2002) 538-546.

[75] P. Lei, B. Bajaj, S.T. Andreadis, Retrovirus-associated heparan sulfate mediates immobilization and gene transfer on recombinant fibronectin, J Virol 76 (2002) 8722-8728.

[76] R.D. Cone, R.C. Mulligan, High-efficiency gene transfer into mammalian cells: generation of helper-free recombinant retrovirus with broad mammalian host range, Proc Natl Acad Sci U S A 81 (1984) 6349-6353.

[77] R.D. Cone, R.C. Mulligan, High-efficiency gene transfer into mammalian cells: generation of helper-free recombinant retrovirus with broad mammalian host range. 1984, Biotechnology 24 (1992) 420-424.

[78] J.M. Le Doux, Morgan, J.R., and Yarmush, M.L., "Gene Therapy", CRC Handbook of Biomedical Engineering, 2nd ed., 106: 1-19 (2000).

[79] M.I. Bukrinsky, N. Sharova, M.P. Dempsey, T.L. Stanwick, A.G. Bukrinskaya, S. Haggerty, M. Stevenson, Active nuclear import of human immunodeficiency virus type 1 preintegration complexes, Proc Natl Acad Sci U S A 89 (1992) 6580-6584.

[80] J.D. Dvorin, P. Bell, G.G. Maul, M. Yamashita, M. Emerman, M.H. Malim, Reassessment of the roles of integrase and the central DNA flap in human immunodeficiency virus type 1 nuclear import, J Virol 76 (2002) 12087-12096.

[81] G.L. Buchschacher, Jr., F. Wong-Staal, Development of lentiviral vectors for gene therapy for human diseases, Blood 95 (2000) 2499-2504.

[82] L. Naldini, U. Blomer, F.H. Gage, D. Trono, I.M. Verma, Efficient transfer, integration, and sustained long-term expression of the transgene in adult rat brains injected with a lentiviral vector, Proc Natl Acad Sci U S A 93 (1996) 11382-11388.

[83] B.R. Cullen, Journey to the center of the cell, Cell 105 (2001) 697-700.

[84] R.A. Fouchier, M.H. Malim, Nuclear import of human immunodeficiency virus type-1 preintegration complexes, Adv Virus Res 52 (1999) 275-299.

[85] P. Lewis, M. Hensel, M. Emerman, Human immunodeficiency virus infection of cells arrested in the cell cycle, Embo J 11 (1992) 3053-3058.

[86] P.F. Lewis, M. Emerman, Passage through mitosis is required for oncoretroviruses but not for the human immunodeficiency virus, J Virol 68 (1994) 510-516.

[87] J.B. Weinberg, T.J. Matthews, B.R. Cullen, M.H. Malim, Productive human immunodeficiency virus type 1 (HIV-1) infection of nonproliferating human monocytes, J Exp Med 174 (1991) 1477-1482.

[88] L. Naldini, U. Blomer, P. Gallay, D. Ory, R. Mulligan, F.H. Gage, I.M. Verma, D. Trono, In vivo gene delivery and stable transduction of nondividing cells by a lentiviral vector, Science 272 (1996) 263-267.

[89] L. Zaitseva, R. Myers, A. Fassati, tRNAs promote nuclear import of HIV-1 intracellular reverse transcription complexes, PLoS Biol 4 (2006) e332.

[90] S.P. Goff, Host factors exploited by retroviruses, Nat Rev Microbiol 5 (2007) 253-263.

[91] T. Roe, T.C. Reynolds, G. Yu, P.O. Brown, Integration of murine leukemia virus DNA depends on mitosis, Embo J 12 (1993) 2099-2108.

[92] D.G. Miller, M.A. Adam, A.D. Miller, Gene transfer by retrovirus vectors occurs only in cells that are actively replicating at the time of infection, Mol Cell Biol 10 (1990) 4239-4242.

[93] P. Hematti, B.K. Hong, C. Ferguson, R. Adler, H. Hanawa, S. Sellers, I.E. Holt, C.E. Eckfeldt, Y. Sharma, M. Schmidt, C. von Kalle, D.A. Persons, E.M. Billings, C.M. Verfaillie, A.W. Nienhuis, T.G. Wolfsberg, C.E. Dunbar, B. Calmels, Distinct genomic integration of MLV and SIV vectors in primate hematopoietic stem and progenitor cells, PLoS Biol 2 (2004) e423.

[94] D. Elleder, A. Pavlicek, J. Paces, J. Hejnar, Preferential integration of human immunodeficiency virus type 1 into genes, cytogenetic R bands and GC-rich DNA regions: insight from the human genome sequence, FEBS Lett 517 (2002) 285-286.

[95] S. Laufs, B. Gentner, K.Z. Nagy, A. Jauch, A. Benner, S. Naundorf, K. Kuehlcke, B. Schiedlmeier, A.D. Ho, W.J. Zeller, S. Fruehauf, Retroviral vector integration occurs in preferred genomic targets of human bone marrow-repopulating cells, Blood 101 (2003) 2191-2198.

[96] R.S. Mitchell, B.F. Beitzel, A.R. Schroder, P. Shinn, H. Chen, C.C. Berry, J.R. Ecker, F.D. Bushman, Retroviral DNA integration: ASLV, HIV, and MLV show distinct target site preferences, PLoS Biol 2 (2004) E234.

[97] A.R. Schroder, P. Shinn, H. Chen, C. Berry, J.R. Ecker, F. Bushman, HIV-1 integration in the human genome favors active genes and local hotspots, Cell 110 (2002) 521-529.

[98] X. Wu, Y. Li, B. Crise, S.M. Burgess, Transcription start regions in the human genome are favored targets for MLV integration, Science 300 (2003) 1749-1751.

[99] M. De Palma, E. Montini, F.R. Santoni de Sio, F. Benedicenti, A. Gentile, E. Medico, L. Naldini, Promoter trapping reveals significant differences in integration site selection between MLV and HIV vectors in primary hematopoietic cells, Blood 105 (2005) 2307-2315.

[100] J. Ellis, Silencing and variegation of gammaretrovirus and lentivirus vectors, Hum Gene Ther 16 (2005) 1241-1246.

[101] S. Yao, T. Sukonnik, T. Kean, R.R. Bharadwaj, P. Pasceri, J. Ellis, Retrovirus silencing, variegation, extinction, and memory are controlled by a dynamic interplay of multiple epigenetic modifications, Mol Ther 10 (2004) 27-36.

[102] D. Pannell, J. Ellis, Silencing of gene expression: implications for design of retrovirus vectors, Rev Med Virol 11 (2001) 205-217.

[103] P. Collas, A. Noer, S. Timoskainen, Programming the genome in embryonic and somatic stem cells, J Cell Mol Med 11 (2007) 602-620.

[104] C.S. Swindle, H.G. Kim, C.A. Klug, Mutation of CpGs in the murine stem cell virus retroviral vector long terminal repeat represses silencing in embryonic stem cells, J Biol Chem 279 (2004) 34-41.

[105] B.D. Strahl, C.D. Allis, The language of covalent histone modifications, Nature 403 (2000) 41-45.

[106] D. Schubeler, M.C. Lorincz, D.M. Cimbora, A. Telling, Y.Q. Feng, E.E. Bouhassira, M. Groudine, Genomic targeting of methylated DNA: influence of methylation on transcription, replication, chromatin structure, and histone acetylation, Mol Cell Biol 20 (2000) 9103-9112.

[107] D. Pannell, C.S. Osborne, S. Yao, T. Sukonnik, P. Pasceri, A. Karaiskakis, M. Okano, E. Li, H.D. Lipshitz, J. Ellis, Retrovirus vector silencing is de novo methylase independent and marked by a repressive histone code, Embo J 19 (2000) 5884-5894.

[108] X. Nan, F.J. Campoy, A. Bird, MeCP2 is a transcriptional repressor with abundant binding sites in genomic chromatin, Cell 88 (1997) 471-481.

[109] P.L. Jones, G.J. Veenstra, P.A. Wade, D. Vermaak, S.U. Kass, N. Landsberger, J. Strouboulis, A.P. Wolffe, Methylated DNA and MeCP2 recruit histone deacetylase to repress transcription, Nat Genet 19 (1998) 187-191.

[110] J.R. Flanagan, A.M. Krieg, E.E. Max, A.S. Khan, Negative control region at the 5' end of murine leukemia virus long terminal repeats, Mol Cell Biol 9 (1989) 739-746.

[111] J.R. Flanagan, K.G. Becker, D.L. Ennist, S.L. Gleason, P.H. Driggers, B.Z. Levi, E. Appella, K. Ozato, Cloning of a negative transcription factor that binds to the upstream conserved region of Moloney murine leukemia virus, Mol Cell Biol 12 (1992) 38-44.

[112] N.A. Speck, D. Baltimore, Six distinct nuclear factors interact with the 75-base-pair repeat of the Moloney murine leukemia virus enhancer, Mol Cell Biol 7 (1987) 1101-1110.

[113] R. Petersen, G. Kempler, E. Barklis, A stem cell-specific silencer in the primer-binding site of a retrovirus, Mol Cell Biol 11 (1991) 1214-1221.

[114] J.M. Le Doux, N. Landazuri, M.L. Yarmush, J.R. Morgan, Complexation of retrovirus with cationic and anionic polymers increases the efficiency of gene transfer, Hum Gene Ther 12 (2001) 1611-1621.

[115] N. Landazuri, J.M. Le Doux, Complexation of retroviruses with charged polymers enhances gene transfer by increasing the rate that viruses are delivered to cells, J Gene Med 6 (2004) 1304-1319.

[116] D.W. McMillin, N. Landazuri, B. Gangadharan, B. Hewes, D.R. Archer, H.T. Spencer, J.M. Le Doux, Highly efficient transduction of repopulating bone marrow cells using rapidly concentrated polymer-complexed retrovirus, Biochem Biophys Res Commun 330 (2005) 768-775.

[117] J.M. Le Doux, J.R. Morgan, R.G. Snow, M.L. Yarmush, Proteoglycans secreted by packaging cell lines inhibit retrovirus infection, J Virol 70 (1996) 6468-6473.

[118] R.K. Batra, J.C. Olsen, D.K. Hoganson, B. Caterson, R.C. Boucher, Retroviral gene transfer is inhibited by chondroitin sulfate proteoglycans/glycosaminoglycans in malignant pleural effusions, J Biol Chem 272 (1997) 11736-11743.

[119] J.H. Slingsby, D. Baban, J. Sutton, M. Esapa, T. Price, S.M. Kingsman, A.J. Kingsman, A. Slade, Analysis of 4070A envelope levels in retroviral preparations and effect on target cell transduction efficiency, Hum Gene Ther 11 (2000) 1439-1451.

[120] Y. Yu, P.K. Wong, Studies on compartmentation and turnover of murine retrovirus envelope proteins, Virology 188 (1992) 477-485.

[121] N. Landazuri, J.M. Le Doux, Complexation with chondroitin sulfate C and Polybrene rapidly purifies retrovirus from inhibitors of transduction and substantially enhances gene transfer, Biotechnol Bioeng 93 (2006) 146-158.

CHAPTER 2

ECTOPIC EXPRESSION OF PROENDOCRINE TRANSCRIPTION FACTOR NEUROGENIN 3 IN MURINE EMBRYONIC STEM CELLS

2.1 Introduction

Complete autoimmune destruction of pancreatic beta cells, where the patient exhibits relative or absolute insulin deficiency, characterizes type 1 diabetes, also known as insulin-dependent diabetes mellitus (IDDM) [1]. The patient's pancreatic β-cells can no longer produce insulin in response to high blood glucose levels following meals [1]. Clinical studies suggest, however, that the manifestations of type 1 diabetes could potentially be reversed if a renewable source of β-cells or pancreatic islets was available for cell replacement therapy [2]. With their capacity for self-renewal and differentiation into derivatives of all three germ layers, embryonic stem (ES) cells represent an attractive choice for the development of cell therapies for the treatment of diabetes. In order to develop protocols which efficiently differentiate ES cells into pancreas progenitor cells or fully differentiated endocrine cell types, understanding the genetic networks and extracellular signals involved in endocrine pancreas differentiation is essential.

Several efforts have been made to derive β-cells from ES cells through different culturing techniques, but such techniques have been proven unreliable and difficult to reproduce [3, 4]. Thus research has refocused on investigating whether the signaling pathways of master regulatory genes during embryonic development can be recapitulated in ES cells *in vitro* [5]. A key pancreatic regulatory gene is Neurogenin 3 (Ngn3), whose expression and functions in the developing pancreas have been more extensively characterized. Ngn3 plays a central role in determining the endocrine

lineage in the pancreas, defining which cells are islet progenitor cells. Homozygous ngn3 null mutations in mice result in the complete lack of formation of the islets of Langerhans or any of the four islet cell types, leading to the development of diabetes and death 1-3 days after birth [6-11]. Direct downstream factors of Ngn3 essential in β-cell formation are NeuroD1/Beta2 and Pax4, as Ngn3 binds to and activates their promoters. NeuroD1/Beta2 is required for proper morphogenesis of pancreatic islets, and Pax4 has been implicated in committing early pancreatic endocrine cells to a β-cell fate [12-14]. In the absence of Ngn3, expression of both NeuroD1/Beta2 and Pax4 is lost. Another transcription factor, pancreatic duodenal homeobox 1 (PDX-1), plays a prominent role early in the development of the entire pancreas and later on for maintaining normal β-cell function and activating β-specific genes [15]. NeuroD1/Beta2 has been shown to interact cooperatively with PDX-1 to promote insulin transcription in β-cells [16, 17]. Without NeuroD1/Beta2 or PDX-1 expression, insulin transcription in β-cells is severely compromised.

We hypothesized that sustained ectopic expression of proendocrine transcription factor Ngn3 via retroviral genetic modification would be an efficient trigger to enhance the expression of downstream regulatory genes in β-cell differentiation. To evaluate if murine ES cells are capable of responding to ectopic expression of Ngn3, we constructed an MSCV-derived retroviral vector encoding the expression of Ngn3, transduced EFC1 mES cells and a mouse fibroblast cell line as control with Ngn3 retrovirus, and quantified the resulting gene expression of endocrine pancreas transcription factors.

2.2 Materials and Methods

Chemicals. Chondroitin sulfate C (CSC) (shark cartilage), gluteraldehyde, 1,5-dimethyl-1,5-diazaundecamethylene polymethobromide (Polybrene, PB), ANTI-FLAG®

M2 monoclonal antibody-Cy3 conjugate and gelatin from porcine skin (Type A) were from Sigma Chemical Co. (St. Louis, MO, USA).

Plasmids. The expression plasmid encoding the ecotropic (pFBMOSALF) and amphotropic (pFB4070ASALF) envelope proteins were from Stephen Russell [18]. The expression plasmids encoding proendocrine transcription factors Neurogenin 3 (Ngn3) and pancreatic duodenal homeobox 1 (PDX-1) were from David Anderson and Kevin Doherty, respectively. The murine stem cell virus retroviral vector (pMSCV-Gateway-IRES-eGFP) was from Catherine Verfaillie [19, 20].

Retroviral vector construction. The MSCV-FTngn3-eGFP and MSCV-PDX1cmyc-eGFP retroviral vectors based on the MSCV LTR were constructed, according to manufacturer's instructions, with Gateway® Technology (Invitrogen Corp., Carlsbad, CA, USA), which allows DNA segments flanked by a recombination site to be transferred into the corresponding site in a Gateway vector. The entire coding sequence of flag-tagged Ngn3 and c-myc-tagged PDX-1 were PCR amplified from their expression plasmids and topo cloned into a Gateway® entry vector. These sequences were then transferred via the Invitrogen LR Clonase® reaction to a parent Gateway MSCV retrovirus vector (MSCV-Gateway-ires-eGFP), a kind gift from Catherine Verfaillie (University of Minnesota). The final vector sequences were verified by restriction digest and DNA sequencing.

Cell culture. NIH 3T3 mouse fibroblasts, were cultured in Dulbecco's modified Eagle's medium (DMEM; Mediatech, Inc., Herndon, VA, USA) with 10% bovine calf serum (BCS; Hyclone Labs, Inc., Logan, UT, USA), and 100 U of penicillin and 100 µg of streptomycin (Hyclone Labs, Inc., Logan, UT, USA) per mL. The packaging cell line GP2-293 was cultured on collagen-coated plates (BD Biosciences Discovery Labware, Bedford, MA, USA) in DMEM (Mediatech, Inc., Herndon, VA, USA) with 10% fetal bovine serum (FBS; Hyclone Labs, Inc., Logan, UT, USA) and 100 U of penicillin and 100 µg of

streptomycin per mL. HeLa (human cervical cancer) cells were cultured in DMEM with 10% FBS and 100 U of penicillin and 100 µg of streptomycin per mL and 110 µg of sodium pyruvate (Hyclone Labs, Inc., Logan, UT, USA) per mL.

Undifferentiated EFC1 mES cells, a kind gift from David Archer (Emory University), were cultured on 0.1% porcine gelatin-coated tissue culture flasks and plated in ES Complete Medium (ES-DMEM; ATCC, Manassas, VA, USA) supplemented with 4mM L-glutamine (Invitrogen Corp., Carlsbad, CA, USA), 150 M β-mercaptoethanol (Sigma Chemical Co., St. Louis, MO, USA), 10% heat-inactivated fetal (ES Cell-Qualified FBS; Invitrogen Corp., Carlsbad, CA, USA), 1% MEM non-essential amino acids (Invitrogen Corp., Carlsbad, CA, USA), 100 U of penicillin and 100 µg of streptomycin (Invitrogen Corp., Carlsbad, CA, USA) per mL, and 10^3 U of leukemia inhibitory factor (LIF; Chemicon International Inc., Ternecula, CA, USA) per mL. To induce embyroid body (EB) formation, mES cells were plated as 20 µL droplets on the cover of nonadherent bacterial culture dishes at a density of 150 cells per µL. The EBs were formed for 6 days in ES Complete Medium without LIF before collection.

Production of recombinant retroviruses. To generate retrovirus stocks, GP2-293 cells, a HEK 293-based packaging cell line that stably expresses the retroviral gag and pol genes (Clontech Laboratories, Inc., Mountain View, CA, USA) [21], were plated in 10 cm dishes ($4x10^6$ cells) in DMEM that contained heat inactivated FBS (10%) but no antibiotics. The next day, Lipofectamine™ 2000 (Invitrogen Corp., Carlsbad, CA, USA), was used according to the manufacturer's recommendations to cotransfect the cells with 12 µg of a viral envelope expression plasmid (either ecotropic (Eco) or amphotropic (Ampho)) and 12 µg of the constructed MSCV-FTngn3 retroviral vector that encoded eGFP. Six hours after transfection, the medium was replaced with fresh 10 mL DMEM/FBS with antibiotics. Virus-laden tissue culture medium was harvested 24, 48,

72, and 96 hours post-transfection, filter-sterilized (0.45 μm), and then frozen (-80ºC) for later single harvest or combined harvest use.

Transduction with polymers. EFC1 mES and NIH 3T3 cells were plated at 3.5 x 10^5 and 1.5 x 10^5 cells per well, respectively, in gelatinized 6-well tissue culture plates. HeLa cells were plated at 5 x 10^4 cells per well on coverslips in 12-well plates. The next day, equal weight concentrations of 80 μg per mL of cationic polymer Polybrene (PB) and anionic polymer chondroitin sulfate C (CSC) were added to ecotropic or amphotropic MSCV-FTngn3-eGFP retrovirus stocks and mixed by vortexing. Virus and polymers were incubated together for 20 min, and then centrifuged for 10 min at 10,300 g at room temperature. The visible virus-polymer pellets were resuspended in the appropriate fresh medium to the desired virus concentration (either in the same volume or in one-fifth the volume). Cells were transduced with 1 mL virus per well, and plates were centrifuged for 30 min at 1,100 g at room temperature. The viral supernatants were removed 24 hours later and replaced with fresh medium. Transduced cells were evaluated by fluorescence microscopy, flow cytometry, immunochemistry and real-time PCR.

Fluorescence microscopy. Three days after transduction, epifluorescent images (10X) of EFC1 mES, NIH 3T3 cells and HeLa cells were taken with an inverted epifluorescence microscope (IX-50; Olympus America, Inc., Melville, NY, USA). Images represent three independent experiments.

Flow cytometry. The percentage of eGFP+ cells and the mean fluorescence intensity of eGFP transgene expression in transduced EFC1 mES and NIH 3T3 cells was determined 3 days post transduction via flow cytometry using a BD LSR analyzer (BD Biosciences, San Jose, CA, USA). Nontransduced control and MSCV-FTngn3-eGFP-transduced EFC1 mES and NIH 3T3 cells were trypsinized, pelleted, washed, and resuspended in 1X PBS plus 10% FBS to achieve a single-cell suspension. Ten

thousand events were collected per sample. Nontransduced cells served as negative controls and were used to monitor autofluorescence and set fluorescence thresholds. Viable cells were gated using forward and side scatter properties. The mean fluorescence intensity of eGFP was determined by gating the eGFP+ cells in each sample. Results are representative of three independent experiments.

Immunofluorescence Microscopy. To determine if transduction with MSCV-FTngn3-eGFP lead to stable integration of the FTngn3 sequence and translation of the FTngn3 protein, HeLa cells were immunostained by plating them on coverslips (no. 1.5 12mm, Fisher Scientific; Suwanee, GA, USA) in 12-well plates (50,000 cells per well). Three days after transduction, the cells were fixed with 2% paraformaldehyde (1 mL/well) for 10 min. Next the cells were washed 3 times with PBS and incubated with ANTI-FLAG® M2 monoclonal antibody-Cy3 conjugate (diluted 800-fold in Tris Buffered Saline (TBS), 0.05 M Tris, pH 7.4, with 0.15 M NaCl) for 1 hour at room temperature, washed 3 times with PBS and once with double distilled water, and then their nuclei were stained with DAPI (300nM in PBS) for 1 min at room temperature. The cells were subsequently washed with double distilled water (1 mL/well), and the coverslips were mounted on glass slides with gelvatol [22]. All cells were examined by epifluorescence microscopy (IX-50; Olympus America, Inc., Melville, NY, USA; 60 X oil objective).

Determination of proendocrine transcription factor and reporter gene mRNA expression by real-time PCR. Extraction of total RNA from cell cultures was performed using RNeasy® Mini Kit and QIAamp® Columns (Qiagen Inc., Valencia, CA, USA). DNase treatment of RNA was performed on-column using RNase-free DNase Kit (Qiagen Inc., Valencia, CA, USA). Reverse transcription of RNA into cDNA was performed using 3 µg of total RNA in a final volume of 20 µL, using oligo dT primers and SuperScript™ III First-Strand Synthesis System for RT-PCR (Invitrogen Corp., Carlsbad, CA, USA). Ngn3, NeuroD1, Pax4, Dll-1, and PDX-1 transcription factors, eGFP

(reporter) and 18SrRNA (endogenous reference) gene-specific primer pair sequences (Applied Biosystems, Foster City, CA, USA or Integrated DNA Technologies, Inc., Coralville, IA, USA) were as follows: Ngn3 forward primer 5'-GCGCAAGAAGGCCAATGA-3' and Ngn3 reverse primer 5'-AGCGCCGAGTTGAGGTTG-3'; NeuroD1 forward primer 5'-ACCAATTTGGTCGCCGG-3' and NeuroD1 reverse primer 5'-GGGTTCTGCTCAGGCAAGAA-3'; Pax4 forward primer 5'-GGGACTGCCAATCCCTCC-3' and Pax4 reverse primer 5'-GGCAGGGCCAGGCAA-3'; Dll-1 forward primer 5'-TACCCCTAACCCATGCGAGA-3' and Dll-1 reverse primer 5'-GGCAACGGAAGTCACCCC-3'; PDX-1 forward primer 5'-AAATCCACCAAAGCTCACGC-3' and PDX-1 reverse primer 5'-CTCGGGTTCCGCTGTGTAAG-3'; eGFP forward primer 5'-AGCAAAGACCCCAACGAGAA-3' and eGFP reverse primer 5'-GGCGGCGGTCACGAA-3'; and 18SrRNA forward primer 5'-CGCCGCTAGAGGTGAAATTC-3' and 18SrRNA reverse primer 5'-TTGGCAAATGCTTTCGCTC-3'. Standards for eGFP, Ngn3, and 18SrRNA were prepared from amplifications purified using an E.Z.N.A® Gel Extraction Kit (Omega Bio-tek, Inc., Doraville, GA, USA) and serially diluted. All real-time PCR reactions were performed by amplifying 1 µL of cDNA in a 30 µL total volume with SYBR® Green PCR Master Mix (Applied Biosystems, Inc., Foster City, CA, USA) in an ABI PRISM™ 7700 Sequence Detector (2 min at 50ºC, 10 min at 95ºC, and then 40 cycles of 15 sec at 95°C and 1 min at 60°C) [23-28]. Detection limits for each gene were determined by no template control. The relative standard curve method, as described in ABI User Bulletin #2 Rev B: ABI Prism 7700 Sequence Detection System [29], was used to quantify the level of mRNA expression of eGFP in EFC1 mES cells, and the results were expressed as relative to the expression levels of endogenous 18SrRNA, the reference gene. Quantification of mRNA gene expression of transcription factors Ngn3, NeuroD1, Pax4,

Dll-1, and PDX-1 in EFC1 mES cells was based on the comparative C_T method for each sample, as described in ABI User Bulletin #2 Rev B: ABI Prism 7700 Sequence Detection System [29], and expressed as relative expression normalized to the 18SrRNA endogenous reference gene and depicted as an *n*-fold difference relative to nontransduced cells. Values are the mean ± the standard deviation for triplicate samples.

Data analysis. Data are summarized as the mean ± the standard deviation for at least triplicate samples. Statistical analysis was performed with MINITAB® Release 12.23 software (Minitab, Inc., State College, PA, USA) using a one-way analysis of variance (ANOVA) for repeated measurements of the same variable. The Tukey multiple comparison test was used to conduct pair wise comparisons between means. Differences at $p < 0.05$ were considered statistically significant.

2.3 Results

Technologies are in great demand to efficiently generate insulin-producing β-like cells in sufficient quantities for the treatment of type 1 diabetes. As most culturing methods alone are not adequate to generate β-cells, we speculated that ectopic expression of key proendocrine transcription factors, Neurogenin 3 (Ngn3) in particular, would be a more efficient trigger than culturing methods for initiating the subsequent signal cascades that lead to pancreatic β-cell formation.

In order to assess the ability of murine embryonic stem (ES) cells to respond to ectopic expression of proendocrine transcription factor Neurogenin 3 (Ngn3), we constructed two murine stem cell virus (MSCV) retroviral vectors encoding for proendocrine transcription factors Neurogenin 3 (Ngn3) and pancreatic duodenal homeobox-1 (PDX-1) (Figure 2.1).

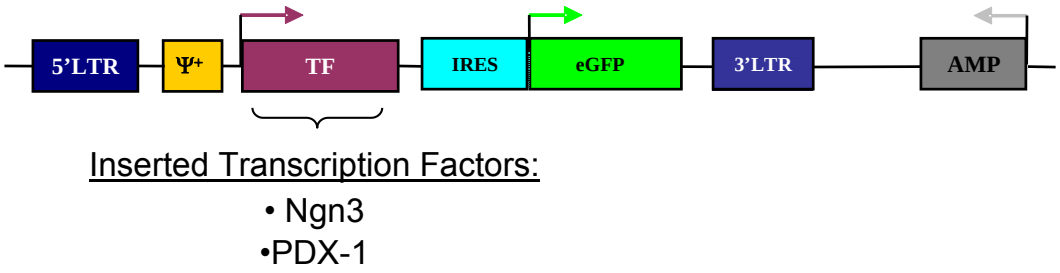

Figure 2.1. Schematic diagram of the two MSCV retroviral vectors constructed, containing the MSCV long terminal repeat (LTR) promoter followed by a packaging sequence (Ψ^+). One vector encodes for the flag-tagged proendocrine transcription factor Neurogenin 3 (FTngn3), the other for the cmyc-tagged pancreatic duodenal homeobox-1 (PDX-1-cmyc). The enhanced green fluorescent protein (eGFP) is downstream of an internal ribosome entry site (IRES).

To examine the effect of ectopic expression of Ngn 3 in mES cells, we first generated stocks of ecotropic MSCV-FTngn3-eGFP virus by transfecting GP2 packaging cells that stably express the *gag* and *pol* genes and evaluated the efficiency of gene transfer. EFC1 mES cells and NIH 3T3 cells were transduced with ecotropic MSCV-FTngn3-eGFP retrovirus that had been precipitated with 80 μg/mL each of Polybrene (PB) and chondroitin sulfate C (CSC) and resuspended in the same volume. Three days later we visualized the cells by epifluorescence microscopy (Figure 2.2A and 2.2B), used flow cytometry to quantify the number of transduced cells (Figure 2.2C and 2.2D), and used real-time PCR to quantify the level of eGFP mRNA.

We found that our MSCV-FTngn3-eGFP virus successfully transduced both EFC1 mES cells and NIH 3T3 cells, as demonstrated by the presence of eGFP+ cells in transduced cultures (Figure 2.2A and 2.2B). However, the number of transduced NIH 3T3 cells was significantly higher than the number of transduced EFC1 mES cells (Figure 2.2C and 2.2D). Typically, NIH 3T3 cells showed transduction efficiencies of 70-80%, while the highest transduction efficiencies achieved in EFC1 mES cells were 3-4%. In addition, eGFP expression in individual transduced NIH 3T3 cells was much higher than in individual transduced EFC1 mES cells (Figure 2.2A and Figure 2.2B). We conducted real-time PCR to quantify the level of eGFP mRNA in transduced cultures. We found that transduced EFC1 mES cells expressed significantly lower levels of eGFP mRNA than transduced NIH 3T3 cells, about 7-fold lower ($p<0.05$) (Figure 2.2E).

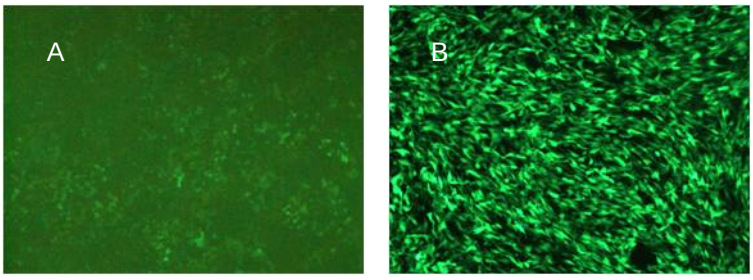

Figure 2.2. Expression of eGFP can be detected in EFC1 mES cells and NIH 3T3 cells. Fluorescent images detecting eGFP expression in EFC1 mES cells (A) and NIH3T3 cells (B) that were seeded in gelatinized 6-well plates at 3.5 x 10^5 and 1.5 x 10^5, respectively, and transduced the next day with ecotropic MSCV-FTngn3-eGFP virus precipitated with polymers and resuspended in the same volume. Three days later the cells were visualized by epifluorescence (A, B), the number of transduced cells determined by flow cytometry (C, D), and the levels of eGFP mRNA quantified by real-time PCR (E). Flow cytometry histograms of non transduced control (black) and transduced (red) NIH 3T3 cells (C) and EFC1 mES cells (D). Statistically significant difference ($p<0.05$) in the level of eGFP mRNA (E) in EFC1 mES cells from NIH 3T3 cells is denoted with an asterisk.

C

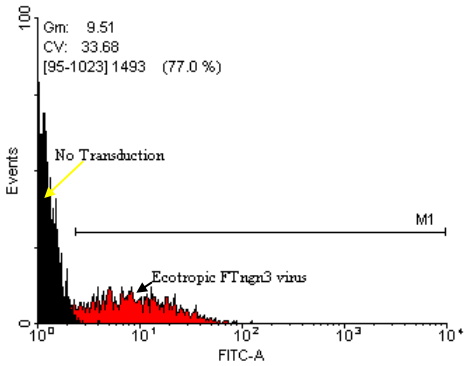

D

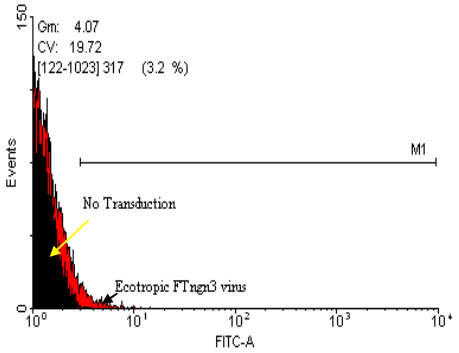

E

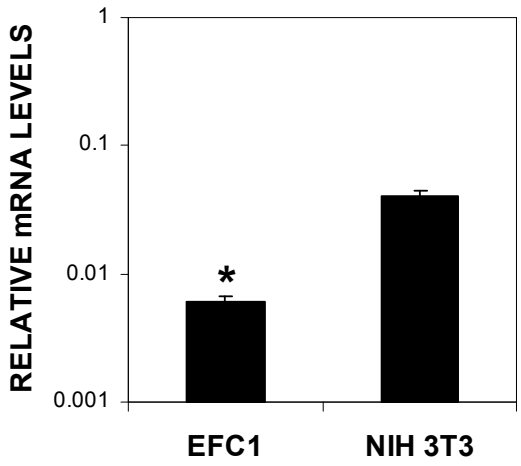

Figure 2.2 continued

A HeLa human cervical carcinoma cell line was next examined to verify that transduction with MSCV-FTngn3-eGFP virus leads to stable integration of the FTngn3 sequence within the host genome and to translation of an FTngn3 protein. HeLa cells were transduced with 5-fold polymer concentrated amphotropic MSCV-FTngn3-eGFP virus (Figure 2.3H). Three days post transduction, immunoreactivity of an ANTI-FLAG® M2 monoclonal antibody-Cy3 conjugate to the flag tag fusion protein (FT) of the exogenous FTngn3 was used to detect cells making functional FTngn3 protein. HeLa cells stained positive for the FTngn3 protein in eGFP+ cells (Figure 2.3 A and 2.3B), demonstrating translation of the FTngn3 protein in transduced cells. Staining of cell nuclei (Figure 2.3C) also revealed that FTngn3 protein expression in HeLa cells was localized to cell nuclei, as would be expected for transcription factors (Figure 2.3D).

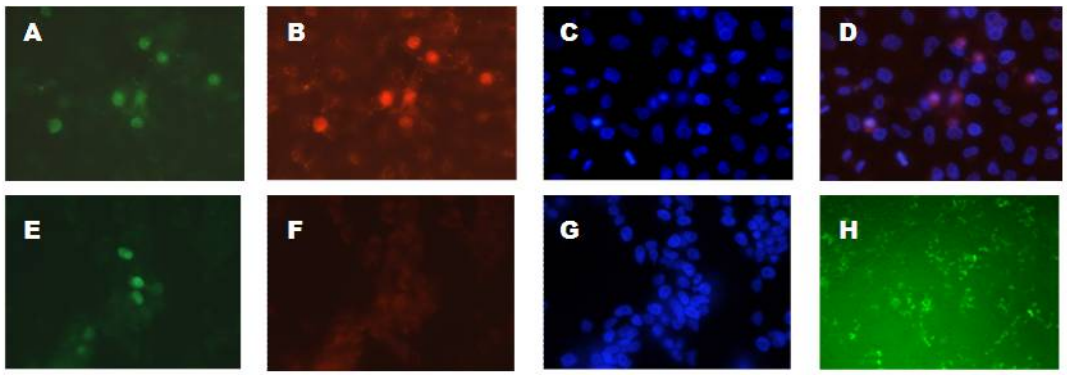

Figure 2.3. Transduced eGFP+ HeLa cells stain positive for FTngn3 protein expression. Fluorescent image detecting eGFP expression in transduced HeLa cells incubated with antibody (A, H) and nontreated control (E). Immunofluorescence staining for flag tag fusion protein in transduced HeLa cells incubated with antibody (B) and nontreated control (F). DAPI staining of nuclei (C, G). Overlay (D) of (B) and (C) to show immunostaining of flag tag occurs in the cell nucleus. (A-G, 60X magnification; H, 10X magnification).

As a first step towards analyzing the effect of ngn3 expression on mES cell fate, we transduced EFC1 mES cells, and NIH 3T3 murine fibroblasts as a control, with ecotropic MSCV-FTngn3-GFP virus, then quantified the level of expression of Ngn3 by real-time PCR 3 and 5 days following transduction (Figure 2.4). Ngn3 expression was detected at high levels in transduced NIH3T3 cells 3 and 5 days after transduction. However, Ngn3 expression in transduced mES cells was about 700-fold lower at day 3 and about 500-fold lower at day 5 than in NIH 3T3 cells.

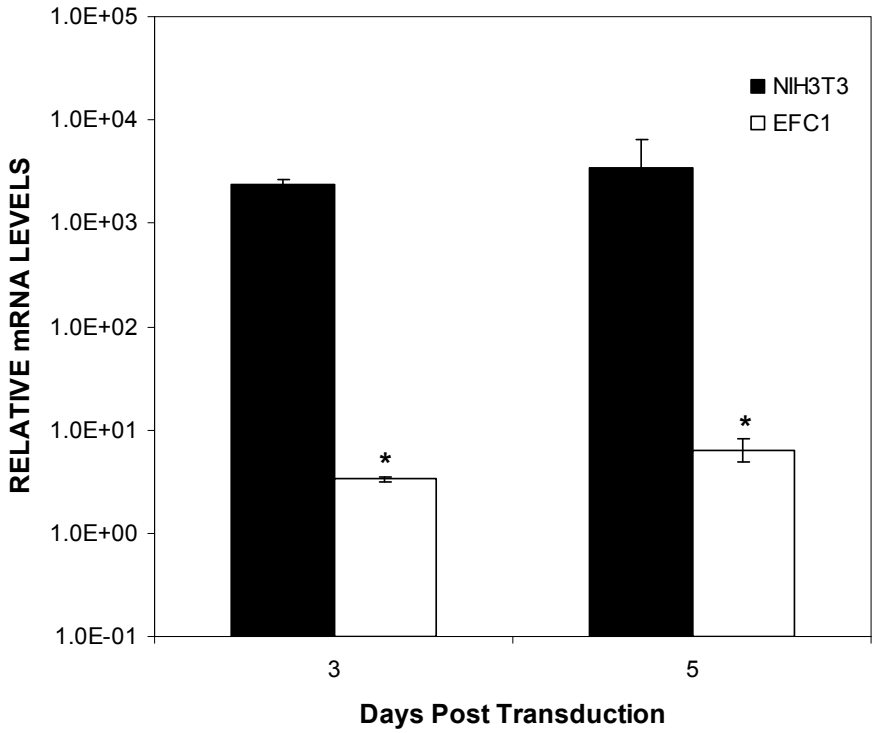

Figure 2.4. Expression of the Ngn3 transgene is signicantly lower in transduced EFC1 mES cells than in NIH 3T3 cells. EFC1 mES and NIH 3T3 cells were plated (350,000 cells/well and 150,000 cells/well, respectively) in gelatinized 6-well tissue culture plates, and then transduced the next day with ecotropic MSCV-FTngn3-eGFP virus precipitated with polymers and resuspended in the same volume. Three and five days later, total RNA was extracted from the lysates of EFC1 mES (white bars) and NIH 3T3 (black bars) cells and reverse transcribed using oligo dT primers, and the relative amount of cDNA was quantified by real-time PCR and is reported as *n*-fold differences relative to cells that were not transduced. Each bar represents the mean ± standard deviation of three replicates. Statistically significant ($p<0.05$) differences of Ngn3 expression levels in EFC1 mES cells from NIH 3T3 cells are denoted with an asterisk (*).

To next determine if mES cells were competent to respond to ectopic expression of Ngn3 and regulate additional factors in the proendocrine transcription factor cascade, we transduced EFC1 mES cells and NIH 3T3 cells with ecotropic MSCV-FTngn3-GFP virus, and then used real-time PCR to quantify the level of expression of Ngn3, as well as NeuroD1, Pax-4, Dll-1, and PDX-1, transcription factors whose *in vivo* expression is regulated by Ngn3 (Figure 2.5). Ngn3 expression was significantly higher in transduced cells than in nontransduced cells for both 3 and 5 days post transduction (Figure 2.5). Ngn3 expression in transduced EFC1 mES cells was 3-fold higher than nontransduced cells at 3 days post transduction and 6-fold higher at 5 days post transduction ($p<0.05$). For NeuroD1, Pax-4, Dll-1, and PDX-1, gene expression was about 2-fold higher in the transduced cells than in the non transduced cells (Figure 2.5) by 5 days post transduction ($p<0.05$). These results suggest that the product of the FTngn3 transgene may upregulate the expression of transcription factors in mES cells that it is known to regulate in development *in vivo*. Levels of expression of NeuroD1, Pax-4, Dll-1, and PDX-1 did not increase when, as a negative control, NIH 3T3 murine fibroblasts were transduced to express Ngn3 (data not shown).

Next, we wondered if expression of proendocrine factors could be maintained during continued culture and into differentiation. We transduced EFC1 mES cells with ecotropic MSCV-FTngn3-eGFP virus, cultured them for 16 days in monolayer and then iniated differentiation by embryoid body (EB) formation, with nontransduced control mES cells cultured in parallel. We used real-time PCR to quantify the level of expression of Ngn3, NeuroD1, Pax-4 and PDX-1 following EB formation (Figure 2.6) as compared to two days post transduction. We found that expression of Ngn3 significantly decreased by about 30-fold ($p<0.05$) after EB formation in comparison to 2 days post transduction. Expression of all other proendocrine transcription factors also decreased, except for Pax4.

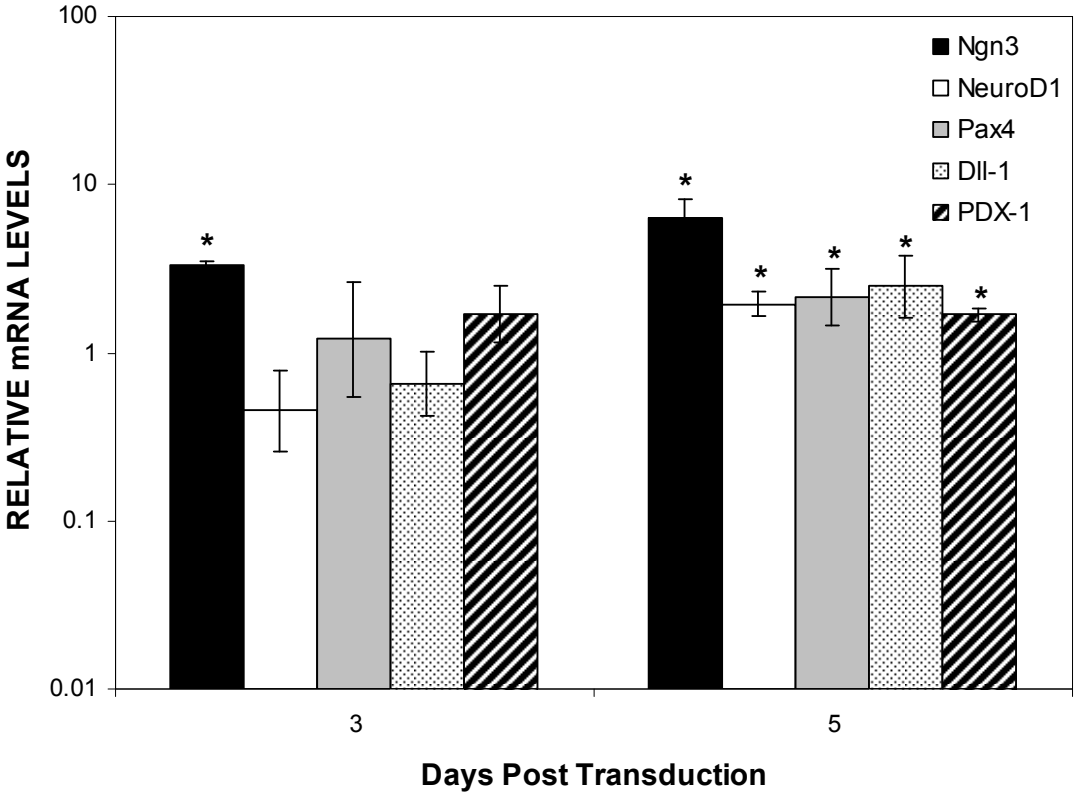

Figure 2.5. Transduction of EFC1 mES cells with MSCV-FTngn3-eGFP leads to increased expression of Ngn3 and its downstream factors. EFC1 mES cells were plated (350,000 cells/well) in gelatinized 6-well tissue culture plates, and then transduced the next day with ecotropic MSCV-FTngn3-eGFP virus precipitated with polymers and resuspended in the same volume. Three and five days later, total RNA was extracted from the lysates of EFC1 mES cells and reverse transcribed using oligo dT primers, and the relative amount of cDNA was quantified by real-time PCR and is reported as *n*-fold differences relative to cells that were not transduced. Each bar represents the mean ± standard deviation of three replicates. Statistically significant ($p<0.05$) differences of transcription factor expression levels in transduced EFC1 mES cells from nontransduced EFC1 mES cells are denoted with an asterisk (*).

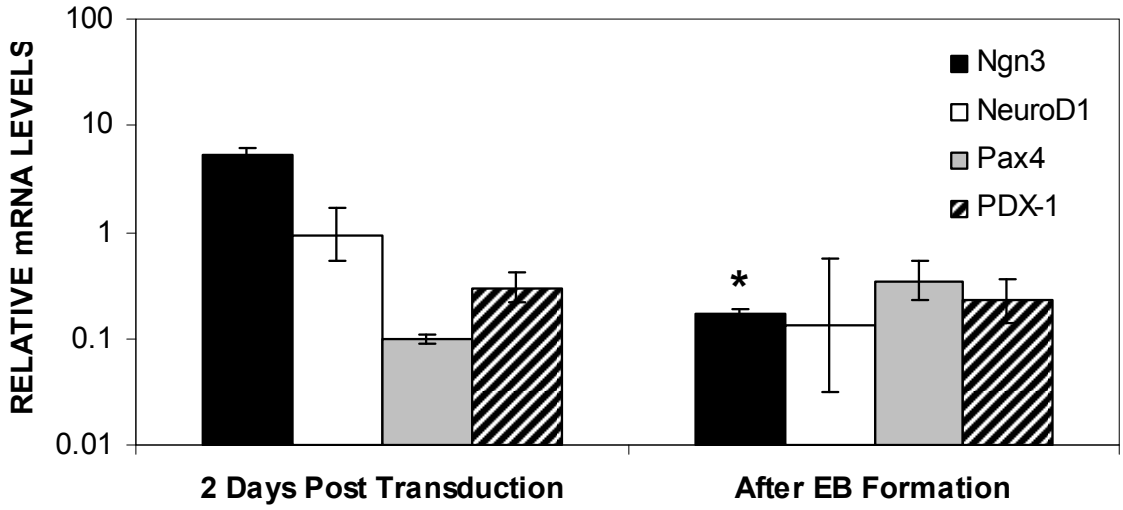

Figure 2.6. Following embryoid body (EB) formation, expression of Ngn3 is sigficantly lower than 2 days post transduction of EFC1 mES cells. . EFC1 mES cells were plated (350,000 cells/well) in gelatinized 6-well tissue culture plates, and then transduced the next day with ecotropic MSCV-FTngn3-eGFP virus precipitated with polymers and resuspended in the same volume. Three and five days later, total RNA was extracted from the lysates of EFC1 mES cells and reverse transcribed using oligo dT primers, and the relative amount of cDNA was quantified by real-time PCR and is reported as *n*-fold differences relative to cells that were not transduced. Each bar represents the mean ± standard deviation of three replicates. Statistically significant ($p<0.05$) differences of transcription factor expression levels in transduced EFC1 mES cells from nontransduced EFC1 mES cells are denoted with an asterisk (*).

2.4 Discussion

In order to determine the effect of ectopic expression of Ngn3 in murine ES cells we employed retroviruses as our gene delivery vehicle. We constructed two MSCV-derived retroviral vectors encoding for proendocrine transcription factors Ngn3 and PDX-1. We genetically modified mES cells with our Ngn3 retrovirus to ectopically express Ngn3, and we found its overexpression was followed by a 2-fold upregulation at 5 days post transduction of NeuroD1/Beta2, Pax4, Dll-1, and PDX-1, other important proendocrine transcription factors whose expression is regulated by or downstream of

Ngn3. These results suggest that pluripotent mES cells may be competent to respond to Ngn3 and support our hypothesis that ectopic expression of these factors can be used to induce mES cells to adopt an endocrine fate. However, following long-term culture and embryoid body differentiation, expression of most proendocrine transcription factors decreased. In addition, our retrovirus transduction methods were inefficient for gene transfer to mES cells, demonstrated by low transgene expression levels of both Ngn3 and the eGFP reporter gene in EFC1 mES cells in comparison to NIH 3T3 fibroblasts, an easy to transduce cell type.

We found our observation that retroviral transgenes were expressed at a very low level in EFC1 mES cells in comparison to NIH 3T3 expression levels rather surprising, considering that the retroviral vectors we constructed were based on the state- of- the- art murine embryonic stem cell virus (MSCV). MSCV vectors contain CpG mutations in their long terminal repeats (LTR) designed to eliminate cis-acting repressor elements that serve as binding sites for methyltransferases that, when bound to retroviral DNA, methylate it and silence its [30]. Considering the degree of transgene silencing observed, it will be necessary to develop more efficient methods for genetically modifying mES cells with retroviruses.

After transducing EFC1 mES cells with our retroviruses encoding Ngn3, we evaluated the gene expression of the entire transduced culture which included a mixed population of successfully transduced and nontransduced EFC1 mES cells. Considering retroviral transgene silencing and mixed populations of transduced and nontransduced cells, the resulting effects of ectopic Ngn3 expression may not be as pronounced. Future work regarding overexpression of Ngn3 and evaluating its effects in ES cells should include isolating only successfully transduced cells by fluorescent activated cell sorting (FACS).

Another point of interest for future studies is the temporal effects of ectopic expression of master proendocrine transcription factors. For these studies we only evaluated the effects on ectopic expression on Ngn3 although we constructed two retroviral vectors encoding both Ngn3 and PDX-1. Further studies should perhaps include transduction of ES cells with both retroviral vectors for a combined effect or transduction with first one and then the other vector at different time points to better determine how to manipulate overexpression of proendocrine transcription factors to more naturally recapitulate their expression patterns during differentiation *in vivo*. Other efforts could be spent examining overexpression of Ngn3 from an inducible system in the event that constitutive overexpression appears undesireable.

Interestingly we observed that expression of almost all transcription factors (except Pax4) decreased following continued culture and initiation of differentiation through EB formation. This decrease could possibly be due to the further silencing of the Ngn3 transgene upon ES cell differentiation, which has been observed when using retroviral vectors. This decrease could also be due to the choice of culture condition. EB formation may be counteractive to any pancreatic transcription factor cascades possibly initiated. Investigating culture conditions for differentiating ES cells that are complimentary to overexpression of proendocrine factors may warrant further effort.

In summar, we focused on pancreatic gene expression following ectopic Ngn3 expression. To further characterize how genetic modification of ES cells influences their cell fate decisions, ES cells should be immunostained for pancreatic-specific markers including insulin (beta cells), glucagon (alpha cells), somatostatin (delta cells), and pancreatic polypeptide (PP cells). The level of beta cell physiological function should also be assessed determining the total insulin content of the cells, and the amount of insulin secreted in response to perturbations in the extracellular concentrations of glucose by cells precultured in regular or insulin-free medium in the presence or

absence of agonists (tolbutamide, IBMX, and carbachol) and antagonists (diazoxide and nifedipine) of insulin secretion. Such work would improve our knowledge to establish improved methods to produce cells in greater quantities that more closely resemble mature β-cells in physiological function.

2.5 Acknowledgements

We thank David Archer for the EFC1 mES cell line and for helpful discussions and technical assistance, Stephen Russell for the ecotropic Env constructs, Kevin Doherty for the PDX-1 construct, David Anderson for the Ngn3 construct and Catherine Verfaillie for the MSCV-gateway retroviral vector. This work was supported by the Georgia Tech/Emory Center for the Engineering of Living Tissues (NSF Engineering Research Center: EEC-9731643).

2.6 References

[1] B. Soria, In-vitro differentiation of pancreatic beta-cells, Differentiation 68 (2001) 205-219.

[2] I. Serafimidis, I. Rakatzi, V. Episkopou, M. Gouti, A. Gavalas, Novel effectors of directed and Ngn3-mediated differentiation of mouse embryonic stem cells into endocrine pancreas progenitors, Stem Cells 26 (2008) 3-16.

[3] J. Rajagopal, W.J. Anderson, S. Kume, O.I. Martinez, D.A. Melton, Insulin staining of ES cell progeny from insulin uptake, Science 299 (2003) 363.

[4] M. Hansson, A. Tonning, U. Frandsen, A. Petri, J. Rajagopal, M.C. Englund, R.S. Heller, J. Hakansson, J. Fleckner, H.N. Skold, D. Melton, H. Semb, P. Serup, Artifactual insulin release from differentiated embryonic stem cells, Diabetes 53 (2004) 2603-2609.

[5] C.G. Liew, N.N. Shah, S.J. Briston, R.M. Shepherd, C.P. Khoo, M.J. Dunne, H.D. Moore, K.E. Cosgrove, P.W. Andrews, PAX4 enhances beta-cell differentiation of human embryonic stem cells, PLoS ONE 3 (2008) e1783.

[6] G. Gradwohl, A. Dierich, M. LeMeur, F. Guillemot, neurogenin3 is required for the development of the four endocrine cell lineages of the pancreas, Proc Natl Acad Sci U S A 97 (2000) 1607-1611.

[7] T. Asano, Y. Hanazono, Y. Ueda, S. Muramatsu, A. Kume, H. Suemori, Y. Suzuki, Y. Kondo, K. Harii, M. Hasegawa, N. Nakatsuji, K. Ozawa, Highly efficient gene transfer into primate embryonic stem cells with a simian lentivirus vector, Mol Ther 6 (2002) 162-168.

[8] M. Jenny, C. Uhl, C. Roche, I. Duluc, V. Guillermin, F. Guillemot, J. Jensen, M. Kedinger, G. Gradwohl, Neurogenin3 is differentially required for endocrine cell fate specification in the intestinal and gastric epithelium, Embo J 21 (2002) 6338-6347.

[9] S.K. Kim, M. Hebrok, Intercellular signals regulating pancreas development and function, Genes Dev 15 (2001) 111-127.

[10] J.C. Lee, S.B. Smith, H. Watada, J. Lin, D. Scheel, J. Wang, R.G. Mirmira, M.S. German, Regulation of the pancreatic pro-endocrine gene neurogenin3, Diabetes 50 (2001) 928-936.

[11] V.M. Schwitzgebel, D.W. Scheel, J.R. Conners, J. Kalamaras, J.E. Lee, D.J. Anderson, L. Sussel, J.D. Johnson, M.S. German, Expression of neurogenin3 reveals an islet cell precursor population in the pancreas, Development 127 (2000) 3533-3542.

[12] B. Sosa-Pineda, K. Chowdhury, M. Torres, G. Oliver, P. Gruss, The Pax4 gene is essential for differentiation of insulin-producing beta cells in the mammalian pancreas, Nature 386 (1997) 399-402.

[13] A.L. Greenwood, S. Li, K. Jones, D.A. Melton, Notch signaling reveals developmental plasticity of Pax4(+) pancreatic endocrine progenitors and shunts them to a duct fate, Mech Dev 124 (2007) 97-107.

[14] F.J. Naya, H.P. Huang, Y. Qiu, H. Mutoh, F.J. DeMayo, A.B. Leiter, M.J. Tsai, Diabetes, defective pancreatic morphogenesis, and abnormal enteroendocrine differentiation in BETA2/neuroD-deficient mice, Genes Dev 11 (1997) 2323-2334.

[15] S. Ashizawa, F.C. Brunicardi, X.P. Wang, PDX-1 and the pancreas, Pancreas 28 (2004) 109-120.

[16] C. Brink, Promoter elements in endocrine pancreas development and hormone regulation, Cell Mol Life Sci 60 (2003) 1033-1048.

[17] H. Kojima, M. Fujimiya, K. Matsumura, P. Younan, H. Imaeda, M. Maeda, L. Chan, NeuroD-betacellulin gene therapy induces islet neogenesis in the liver and reverses diabetes in mice, Nat Med 9 (2003) 596-603.

[18] F.L. Cosset, Y. Takeuchi, J.L. Battini, R.A. Weiss, M.K. Collins, High-titer packaging cells producing recombinant retroviruses resistant to human serum, J Virol 69 (1995) 7430-7436.

[19] R.C. Zhao, Y. Jiang, C.M. Verfaillie, A model of human p210(bcr/ABL)-mediated chronic myelogenous leukemia by transduction of primary normal human CD34(+) cells with a BCR/ABL-containing retroviral vector, Blood 97 (2001) 2406-2412.

[20] J.C. Pui, D. Allman, L. Xu, S. DeRocco, F.G. Karnell, S. Bakkour, J.Y. Lee, T. Kadesch, R.R. Hardy, J.C. Aster, W.S. Pear, Notch1 expression in early lymphopoiesis influences B versus T lineage determination, Immunity 11 (1999) 299-308.

[21] Retroviral Gene Transfer and Expression User Manual, Clontech Laboratories, Inc., Mountain View, 2006.

[22] R.F. Smith, Microscopy and Photomicrography, CRC Press, Boca Raton, 1994.

[23] S.A. Bustin, Absolute quantification of mRNA using real-time reverse transcription polymerase chain reaction assays, J Mol Endocrinol 25 (2000) 169-193.

[24] S.A. Bustin, Real-time, fluorescence-based quantitative PCR: a snapshot of current procedures and preferences, Expert Rev Mol Diagn 5 (2005) 493-498.

[25] S.A. Bustin, V. Benes, T. Nolan, M.W. Pfaffl, Quantitative real-time RT-PCR--a perspective, J Mol Endocrinol 34 (2005) 597-601.

[26] J.H. Marino, P. Cook, K.S. Miller, Accurate and statistically verified quantification of relative mRNA abundances using SYBR Green I and real-time RT-PCR, J Immunol Methods 283 (2003) 291-306.

[27] M.L. Wong, J.F. Medrano, Real-time PCR for mRNA quantitation, Biotechniques 39 (2005) 75-85.

[28] J.S. Yuan, A. Reed, F. Chen, C.N. Stewart, Jr., Statistical analysis of real-time PCR data, BMC Bioinformatics 7 (2006) 85.

[29] Relative Quantitation Of Gene Expression: ABI PRISM 7700 Sequence Detection System: User Bulletin #2: Rev B Applied Biosystems, Inc., Foster City, 1997

[30] C.S. Swindle, H.G. Kim, C.A. Klug, Mutation of CpGs in the murine stem cell virus retroviral vector long terminal repeat represses silencing in embryonic stem cells, J Biol Chem 279 (2004) 34-41.

CHAPTER 3

COMPLEXATION OF RETROVIRUSES WITH POLYMERS SIGNIFICANTLY INCREASES THE NUMBER OF GENES TRANSFERRED TO MURINE EMBRYONIC STEM CELLS BUT DOES NOT RAISE TRANSGENE EXPRESSION LEVELS[1]

3.1 Introduction

Embryonic stem (ES) cells hold great promise for use in regenerative medicine and in the treatment of disease because of their capacity to self-renew, and their potential, when provided with appropriate cues, to differentiate into all cell types of the body. To help realize the full potential of ES cells, it is essential that an effective means to genetically modify them is developed. Genetic modification of ES cells can be used to explore basic questions in stem cell biology and development, to track or direct their differentiation, to develop strategies to down-regulate their immunogenicity, and to create cellular therapies for the treatment of disease [1-3]. Recombinant retroviruses derived from the Moloney murine leukemia virus (MoMLV) are one of the most effective means for genetically modifying most cell types because they efficiently and permanently integrate their genetic material into the chromosomal DNA of the cells, which gives rise to high levels of sustained expression of the integrated transgene in the transduced cells and their progeny [4]. Unfortunately, MoMLV-derived retroviruses have proven less useful for the genetic modification of ES cells because ES cells employ multiple mechanisms to partially or completely silence their expression [5]. To overcome this limitation, retrovirus vectors have been developed that are less susceptible to silencing. For example, retroviruses derived from the murine stem cell virus (MSCV) contain CpG mutations in their long terminal repeats (LTR). These mutations eliminate cis-acting repressor elements that serve as binding sites for methyltransferases that,

[1] Modified from Biotechnology and Applied Biochemistry, 2008 Feb 11 (Epub ahead of print)

when bound to retroviral DNA, methylate it and silence its expression [5-11]. Despite these improvements in vector design, expression from integrated retrovirus transgenes is still low and variable in ES cells [12, 13].

Most efforts to solve this problem continue to focus on increasing the resistance of retrovirus vectors to ES cell silencing mechanisms [9, 14]. As an alternative approach, we wondered to what extent retrovirus transgene expression could be improved by increasing the number of transgenes that are integrated into the chromosomal DNA of ES cells. To evaluate the effectiveness of this approach, we first developed a method to substantially increase the efficiency of retrovirus gene transfer to ES cells. To accomplish this, we identified which of four commonly used retrovirus pseudotypes transduce ES cells most efficiently and then rapidly delivered high doses of that virus to ES cells as a complex with the cationic polymer Polybrene (PB) and the anionic polymer chondroitin sulfate C (CSC). We have previously shown that retrovirus-polymer complexes transfer genes to cells more efficiently than neat retrovirus stocks because they contain fewer inhibitory substances, can be suspended in culture medium that is optimized for the cell type being transduced, and rapidly deliver large numbers of active retroviruses to the surfaces of the cells being transduced [15-18]. Using this method for transducing ES cells, we significantly increased the level of gene transfer to D3 and R1 murine embryonic stem cells, and to NIH 3T3 murine fibroblasts as a control, and then quantitatively examined the relationship between the number of integrated transgenes per cell and the overall level to which the integrated transgenes were expressed.

3.2 Materials And Methods

Chemicals. Chondroitin sulfate C (CSC) (shark cartilage), gluteraldehyde, 1,5-dimethyl-1,5-diazaundecamethylene polymethobromide (Polybrene, PB), Alkaline

Phosphatase Yellow (pNPP) Liquid Substrate System for ELISA (p-nitrophenyl phosphate), alkaline phosphatase from bovine intestinal mucosa (Type VII-S), 1-(4,5-Dimethylthiazol-2-yl)-3,5-diphenylformazan (MTT) and gelatin from porcine skin (Type A) were from Sigma Chemical Co. (St. Louis, MO, USA). Hydrogen peroxide 30%, bovine serum albumin fraction V (BSA), polyoxyethylene 20-sorbitan monolaurate (Tween 20), Triton-X and sodium dodecyl sulfate (SDS) were from Fisher Scientific (Pittsburg, PA, USA). Non-fat dry milk (blotting grade) was from Bio-Rad Laboratories (Hercules, CA, USA). Mouse anti-p30 antibody was purified from the supernatant of the CRL-1219 (ATCC, Rockville, MD, USA) hybridoma cell line, following standard procedures [19]. The goat polyclonal anti-p30 antibody (78S221) was from Quality Biotech (Camden, NJ, USA). The horseradish peroxidase conjugated rabbit anti-goat immunoglobulin G polyclonal antibody was from Zymed Laboratories (South San Francisco, CA).

Plasmids. The expression plasmids encoding the ecotropic (pFBMOSALF) and amphotropic (pFB4070ASALF) envelope proteins were from Stephen Russell [20]. The expression plasmids encoding the 10A1 (pIK.MCV.10A1.env.uTd) [21], and VSV-G (pMD.G) [22, 23] envelope proteins were from Maribeth Eiden and Scott Case, respectively. The murine stem cell virus retroviral vector (pMSCV-IRES-eGFP) was from Catherine Verfaillie [24, 25].

Cell culture. NIH 3T3 mouse fibroblasts, were cultured in Dulbecco's modified Eagle's medium (DMEM; Mediatech, Inc., Herndon, VA, USA) with 10% bovine calf serum (BCS; Hyclone Labs, Inc., Logan, UT, USA), and 100 U of penicillin and 100 µg of streptomycin (Hyclone Labs, Inc., Logan, UT, USA) per mL. The packaging cell line GP2-293 was cultured on collagen-coated plates (BD Biosciences Discovery Labware, Bedford, MA, USA) in DMEM (Mediatech, Inc., Herndon, VA, USA) with 10% fetal bovine serum (FBS; Hyclone Labs, Inc., Logan, UT, USA) and 100 U of penicillin and 100 µg of streptomycin per mL. Undifferentiated D3 murine embryonic stem (mES) cells, obtained

from ATCC, and undifferentiated R1 mES cells, a kind gift from Todd McDevitt (Georgia Tech), were cultured on 0.1% porcine gelatin-coated tissue culture flasks and plated in ES Complete Medium (ES-DMEM; ATCC, Manassas, VA, USA) supplemented with 4mM L-glutamine (Invitrogen Corp., Carlsbad, CA, USA), 150 M β-mercaptoethanol (Sigma Chemical Co., St. Louis, MO, USA), 10% heat-inactivated fetal (ES Cell-Qualified FBS; Invitrogen Corp., Carlsbad, CA, USA), 1% MEM non-essential amino acids (Invitrogen Corp., Carlsbad, CA, USA), 100 U of penicillin and 100 µg of streptomycin (Invitrogen Corp., Carlsbad, CA, USA) per mL, and 10^3 U of leukemia inhibitory factor (LIF; Chemicon International Inc., Ternecula, CA, USA) per mL.

Production of recombinant retroviruses. To generate retrovirus stocks, GP2-293 cells, a HEK 293-based packaging cell line that stably expresses the retroviral gag and pol genes (Clontech Laboratories, Inc., Mountain View, CA, USA) [26], were plated in 10 cm dishes ($4x10^6$ cells) or T175 flasks ($12.5x10^6$ cells) in DMEM that contained heat inactivated FBS (10%) but no antibiotics. The next day, Lipofectamine™ 2000 (Invitrogen Corp., Carlsbad, CA, USA), was usesd according to the manufacturer's recommendations to transfect the cells with one of the expression plasmids (12 µg in 10 cm dishes or 38 µg in T175 flasks) for the following viral envelope proteins: ecotropic (Eco), amphotropic (Ampho), 10A1, or VSV-G, and a MSCV-derived retroviral vector that encoded eGFP (12 µg in 10 cm dishes or 38 µg in T175 flasks). Six hours after transfection, the medium was replaced with fresh 10 mL or 40 mL DMEM/FBS with antibiotics. Virus-laden tissue culture medium was harvested 24, 48, 72, and 96 hours post-transfection, filter-sterilized (0.45 µm), and then frozen (-80ºC) for later single harvest or combined harvest use. The concentration of virus capsid protein (p30) in the virus stocks was determined using a previously described enzyme-linked immunosorbent assay (ELISA) [15].

Diluted titer assay. To determine virus titer, ten-fold serial dilutions of MSCV-eGFP virus stock (from 48 hr harvests) were made in ES Complete Medium and Polybrene (8μg per mL). Serially diluted virus (1 mL per dish) was used to transduce D3 and R1 mES and NIH 3T3 cells that had been seeded at 3.5 x 10^5 and 1.5 x 10^5 cells per dish, respectively, in 35 mm gridded (2 mm) dishes (Nalge Nunc International, Rochester, NY, USA). The viral supernatants were removed 24 hours later and replaced with fresh medium. Three days post transduction, the number of clusters of eGFP+ mES and NIH 3T3 cells (typically in clusters of 2, 4, 8, or 16 green cells) were counted with the aid of an inverted epifluorescence microscope (IX-50; Olympus America, Inc., Melville, NY, USA), and multiplied by the dilution factor to determine the titer (i.e., the number of eGFP+ colony forming units (CFU) per mL). Typical titers measured with NIH 3T3 cells were 1.2 ± 0.17 x 10^5 (amphotropic), 6.9 ± 0.73 x 10^5 (ecotropic), 1.0 ± 0.12 x 10^5 (10A1), and 7.1 ± 0.15 x 10^5 CFU/mL (VSV-G) CFU/mL. Results are representative of three independent experiments.

Determination of viral receptor and pluripotency marker mRNA expression by real-time PCR. Extraction of total RNA from cell cultures was performed using RNeasy® Mini Kit and QIAamp® Columns (Qiagen Inc., Valencia, CA, USA). DNase treatment of RNA was performed on-column using RNase-free DNase Kit (Qiagen Inc., Valencia, CA, USA). Reverse transcription of RNA into cDNA was performed using 3 μg of total RNA in a final volume of 20 μL, using oligo dT primers and SuperScript™ III First-Strand Synthesis System for RT-PCR (Invitrogen Corp., Carlsbad, CA, USA). MCAT-1 (ecotropic receptor), Pit-2 (amphotropic receptor), Oct-4 (mES pluripotency marker), Nanog (mES pluripotency marker) and GAPDH (endogenous reference) gene-specific primer pair sequences (Integrated DNA Technologies, Inc., Coralville, IA, USA) were as follows: MCAT-1 forward primer 5'-TGCCATCGTCATCTCCTTCTT-3' and MCAT-1 reverse primer 5'-CGTAGCACAGGCCGGC-3'; Pit-2 forward primer 5'-

CTTTCAGAGCCTCGGACACC-3' and Pit-2 reverse primer 5'-CACACTGTCACCCACCAGCT-3'; Oct-4 forward primer 5'-CCAGGCTCAGAGGTATTGGG-3' and Oct-4 reverse primer 5'-ATCCCTCCGCAGAACTCGTA-3'; Nanog forward primer 5'-GCATCCATTGCAGCTATCCC-3' and Nanog reverse primer 5'-GCCCCACATGGAAAGGC-3'; and GAPDH forward primer 5'-TCACTGGCATGGCCTTCC-3' and GAPDH reverse primer 5'-GGCGGCACGTCAGATCC-3'. Standards for MCAT-1, Pit-2, and GAPDH were prepared from amplifications purified using an E.Z.N.A® Gel Extraction Kit (Omega Bio-tek, Inc., Doraville, GA, USA) and serially diluted. All real-time PCR reactions were performed by amplifying 1 µL of cDNA in a 30 µL total volume with SYBR® Green PCR Master Mix (Applied Biosystems, Inc., Foster City, CA, USA) in an ABI PRISM™ 7700 Sequence Detector (2 min at 50ºC, 10 min at 95ºC, and then 40 cycles of 15 sec at 95°C and 1 min at 60°C) [27-32]. Detection limits for each gene were determined by no template control. The relative standard curve method, as described in ABI User Bulletin #2 Rev B: ABI Prism 7700 Sequence Detection System [33], was used to quantify the level of mRNA expression of the viral receptors MCAT-1 and Pit-2, and the results were expressed as relative to the expression levels of endogenous GAPDH, the reference gene. Quantification of mRNA gene expression of MCAT-1 and Pit-2 viral receptors was conducted for each cell type at three different passages in triplicate for each passage. Results represent the average expression over the three separate passages. Quantification of mRNA gene expression of pluripotency markers Oct-4 and Nanog was based on the comparative C_T method for each sample, as described in ABI User Bulletin #2 Rev B: ABI Prism 7700 Sequence Detection System [33], and expressed as relative expression normalized to the GAPDH endogenous reference gene and depicted as an

n-fold difference relative to the nonexposed. Results represent the average expression over three separate exposure experiments.

MTT assay for cell number. To determine the effect of polymer exposure on growth rate, D3 and R1 mES and NIH 3T3 cells were plated in gelatin-coated 96-well tissue culture plates at 10,000 and 5,000 cells per well, respectively. After two days of exposure at 37ºC to varying concentrations of PB and CSC, the number of viable cells was determined by an MTT assay, as previously described.[34] Values for each point are the averages of triplicate wells. Results are representative of three independent experiments.

Alkaline phosphatase activity assay. To measure the level of alkaline phosphatase activity in cells that had been incubated with polymer complexes, D3 and R1 mES cells and NIH 3T3 were plated in gelatin-coated 96-well tissue culture plates at 10,000 and 5,000 cells per well, respectively, incubated (2 d, 37°C) with varying doses of Polybrene and chondroitin sulfate C, washed with PBS (100 µL per well), lysed for 10 min with 0.1% Triton-X (100 µL per well), and then the alkaline phosphatase (ALP) activity in the lysates was quantified using the Alkaline Phosphatase Yellow (pNPP) Liquid Substrate System [35]. Incubation with pNPP (37ºC for 3-4 min) led to the development of a visible yellow color, the optical density of which was measured with an absorbance plate reader (VERSAmax; Molecular Devices, Sunnyvale, CA, USA) at 405 nm. Values for each point are the averages of triplicate wells. Results are representative of three independent experiments.

Transduction with polymers. To measure the effect of the polymers on the efficiency of retrovirus transduction, D3 and R1 mES and NIH 3T3 cells were plated at 3.5×10^5 and 1.5×10^5 cells per well, respectively, in gelatinized 6-well tissue culture plates. The next day, equal weight concentrations of 80 µg per mL of cationic polymer

Polybrene (PB) and anionic polymer chondroitin sulfate C (CSC) were added to ecotropic MSCV-eGFP retrovirus stocks (from combined harvests with titers of 2.7×10^5 and 4.1×10^5) and mixed by vortexing. Virus and polymers were incubated together for 20 min, and then centrifuged for 10 min at 10,300 g at room temperature. The visible virus-polymer pellets were resuspended in fresh complete ES medium to the desired virus concentration. Cells were transduced with 1 mL of concentrated virus per well, and plates were centrifuged for 30 min at 1,100 g at room temperature. The viral supernatants were removed 24 hours later and replaced with fresh medium. Two days later the level of gene transfer was evaluated by fluorescence microscopy, flow cytometry, and real-time PCR.

Fluorescence microscopy. Three days after transduction, epifluorescent and phase contrast images (10X) of D3 and R1 mES and NIH 3T3 cells were taken with an inverted epifluorescence microscope (IX-50; Olympus America, Inc., Melville, NY, USA). Images represent three independent experiments.

Flow cytometry. The percentage of eGFP+ cells and the mean fluorescence intensity of eGFP transgene expression in transduced D3 and R1 mES and NIH 3T3 cells was determined 3 days post transduction via flow cytometry using a BD LSR analyzer (BD Biosciences, San Jose, CA, USA). Nontransduced control and MSCV-eGFP-transduced D3 and R1 mES and NIH 3T3 cells were trypsinized, pelleted, washed, and resuspended in 1X PBS plus 10% FBS to achieve a single-cell suspension. Ten thousand events were collected per sample. Nontransduced cells served as negative controls and were used to monitor autofluorescence and set fluorescence thresholds. Viable cells were gated using forward and side scatter properties. The mean fluorescence intensity of eGFP was determined by gating the eGFP+ cells in each sample. Results are representative of two independent experiments.

Determination of relative transgene copy number by real-time PCR. To determine the number of integrated eGFP transgenes per cell, the genomic DNA of transduced D3 and R1 mES and NIH 3T3 cells was extracted 3 days post transduction using the DNeasy® Tissue Kit (Qiagen Inc., Valencia, CA, USA), with RNase (Qiagen Inc., Valencia, CA, USA) treatment of DNA performed prior to lysis. The sequences of the primers (Integrated DNA Technologies, Inc., Coralville, IA, USA) used to amplify the DNA were as follows: eGFP forward primer 5'-AGCAAAGACCCCAACGAGAA-3' and eGFP reverse primer 5'-GGCGGCGGTCACGAA-3'; genomic GAPDH forward primer 5'-CTCTGGCTCAGAGGGTTTGG-3' and genomic GAPDH reverse primer 5'-ACAGAAACCAGTGGGCTTTGA-3'. Standards for genomic GAPDH and eGFP transgene were prepared from serially diluted amplicons purified using an E.Z.N.A® Gel Extraction Kit (Omega Bio-tek, Inc., Doraville, GA, USA). All real-time PCR reactions were performed by loading 150 ng of DNA per tube in a 30 µL total volume with SYBR® Green Master Mix (Applied Biosystems, Inc., Foster City, CA, USA) in an ABI PRISM™ 7700 Sequence Detector (2 min at 50ºC, 10 min at 95ºC, and then 40 cycles of 15 sec at 95°C and 1 min at 60°C). No template control reactions were used to determine the detection limits for each gene. Quantification of the relative number of integrated transgenes was based on the relative standard curve method and expressed as the relative eGFP copy number normalized to the GAPDH endogenous reference gene with relative copy number in nontransduced control subtracted as background [33, 36]. Values for each point are the averages of triplicate PCR tubes. Results are representative of three independent experiments.

Data analysis. Data for all studies are representative of three independent experiments. Data are summarized as the mean ± the standard deviation for at least triplicate samples. Statistical analysis was performed with MINITAB® Release 12.23 software (Minitab, Inc., State College, PA, USA) using a one-way analysis of variance

(ANOVA) for repeated measurements of the same variable. The Tukey multiple comparison test was used to conduct pair wise comparisons between means. Differences at $p < 0.05$ were considered statistically significant.

3.3 Results

Technologies are needed to efficiently genetically modify embryonic stem cells. Recombinant retroviruses are one of the most promising gene transfer technologies currently available, yet they have proven relatively ineffective for genetically modifying ES cells. One key reason is that expression of integrated retrovirus transgenes is often variegated or completely silenced. As a result, most research efforts have focused on understanding and overcoming the mechanisms that ES cells use to shutdown retrovirus gene expression. We wondered if retroviruses were also limited in their ability to transduce ES cells.

We first asked which of four commonly used retrovirus pseudotypes - amphotropic, ecotropic, 10A1 or vesicular stomatitis virus G (VSV-G) - most efficiently transduce ES cells. To answer this question, we generated the four types of murine leukemia retrovirus (MLV) stocks by transfecting GP2-293 packaging cells with the appropriate envelope protein expression vector and a murine stem cell retrovirus (MSCV) vector that encoded eGFP (Figure 3.1), and then measured their titers on D3 and R1 murine embryonic stem cells (mES), and on murine NIH 3T3 fibroblasts as a positive control. We found that both D3 and R1 mES cells were transduced most efficiently by ecotropic and VSV-G pseudotyped retroviruses, which had titers about two to four-fold higher than amphotropic and 10A1 pseudotyped viruses (Figure 3.2A). We verified by an ELISA for the virus capsid protein (p30) that the number of particles in each virus stock was similar (Figure 3.2B), which eliminated the possibility that the differences in titer were simply due to differences in the number of particles applied to

the cells. In all cases, virus titers were substantially lower (by 300 to 1000-fold) on ES cells than on NIH 3T3 cells (the titers of the amphotropic, ecotropic, 10A1, and VSV-G pseudotyped viruses on NIH 3T3 cells were 1.2 x 10^5 CFU/ml, 6.9 x 10^5 CFU/ml, 1.0 x 10^5 CFU/ml, and 7.1 x 10^5 CFU/ml, respectively).

To determine if mES cells express fewer amphotropic receptors (Pit-2; inorganic phosphate transporter 2) or ecotropic receptors (MCAT-1; mouse cationic amino acid transporter 1) than NIH 3T3 cells, we used real-time PCR to quantify the relative number of Pit-2 and MCAT-1 mRNA transcripts in D3, R1, and NIH 3T3 cells. We found no statistically significant ($p<0.05$) differences in the expression of MCAT-1 and Pit-2 in the three cell types tested (Figure 3.3).

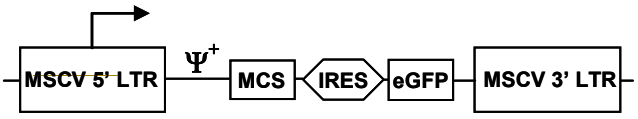

Figure 3.1. Schematic diagram of the bicistronic MSCV-eGFP retroviral vector containing the MSCV long terminal repeat (LTR) promoter followed by a packaging sequence (Ψ^+) , a multiple cloning site (MCS), the enhanced green fluorescent protein (eGFP), and an internal ribosome entry site (IRES).

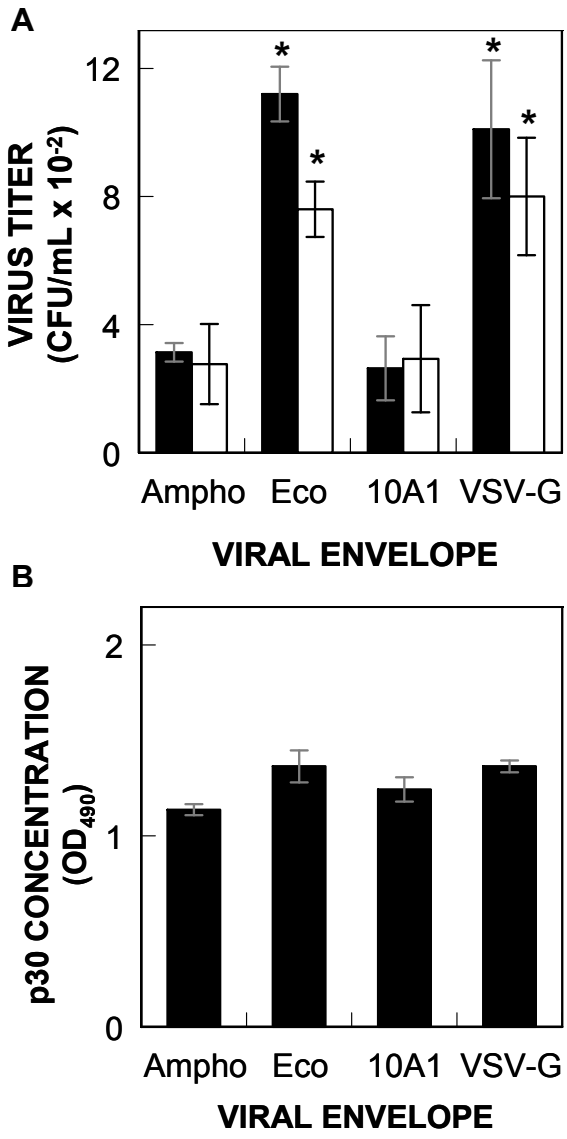

Figure 3.2. Retroviruses, when used to transduce D3 and R1 murine embryonic stem cells (mES), have significantly higher titers when they are pseudotyped with ecotropic or VSV-G envelope proteins than when they are pseudotyped with amphotropic or 10A1 envelope proteins. (A) D3 (black bars) and R1 (white bars) cells, plated (350,000 cells/dish) the previous day in gelatinized 35mm gridded dishes, were transduced with stocks of amphotropic (Ampho), ecotropic (Eco), 10A1, or VSV-G pseudotyped retroviruses that had been serially diluted in fresh medium and brought to 8 μg/mL Polybrene (PB). Three days later, the number of clusters of transduced cells (eGFP+) was counted by epifluorescence microscopy and multiplied by the dilution factor to determine the virus titer. Statistically significant differences ($p<0.05$) from the titers of both amphotropic and 10A1-pseudotyped viruses are denoted by an asterisk (*). Ecotropic and VSV-G titers were not significantly different statistically from one another. (B) The number of virus particles in each stock was quantified by an ELISA for the viral capsid protein (p30). Each bar shows the mean ± standard deviation of three replicates.

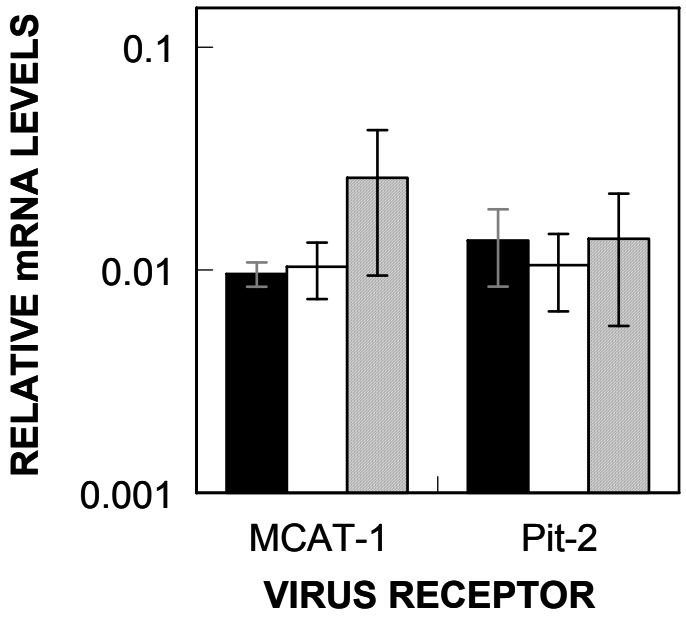

Figure 3.3. D3, R1, and NIH 3T3 cells express similar levels of mRNA for the ecotropic (MCAT-1) and amphotropic (Pit-2) retrovirus receptors. Total RNA was extracted from lysates of D3 (black bars), R1 (white bars), and NIH 3T3 (cross hatch) cells, reverse transcribed using oligo dT primers, and real-time PCR used to quantify the relative amount of cDNA normalized to GAPDH. Each bar represents the mean ± standard deviation of three experiments with three replicates. No statistically significant ($p<0.05$) differences in mRNA expression were detected.

These results indicate that retrovirus transduction of mES cells is not limited by the number of receptors they express, and suggest that increasing receptor expression is not likely to be an effective strategy for improving ES cell transduction. We have previously found in other cell types (e.g., NIH 3T3 and HeLa cells) that retrovirus transduction is limited, in part, by the slow rate that retroviruses are delivered to the surfaces of the cells [37-39]. The rate that retroviruses reach the cells, and the efficiency of transduction, can be significantly increased by forming retrovirus-polymer complexes, which due to their large size, sediment rapidly onto the cells and significantly increase the number of genes transferred [15-17]. Transduction can be further improved by increasing the concentration of virus, which is accomplished by pelleting the virus-polymer complexes and resuspending them in a smaller volume of cell culture medium.

Based on these previous successes, we decided to determine if we could improve retrovirus transduction of mES cells by using retrovirus-polymer complexation to increase the number and rate that the viruses were delivered to the cells. Given the sensitivity of mES cells to the conditions used to culture them, and the need to maintain their pluripotency, we first determined the doses of the polymers (Polybrene (PB) and chondroitin sulfate C (CSC)) that could be used without significantly reducing the viability or pluripotency of the cells. To determine if PB and CSC were cytotoxic, we plated D3, R1, and NIH 3T3 cells in 96-well plates, exposed them to a range of equal weight concentrations of PB and CSC for two days, and then quantified the number of viable cells using the MTT assay (Figure 3.4A). We found, that, in all cases, the number of viable cells present after two days of culture was significantly higher than the number of viable cells that were present immediately after they were plated, which indicates that the polymers were not cytotoxic, even at the highest doses tested. Nevertheless, the growth rates of the cells did appear to decline with increasing doses of the polymers.

The number of viable cells was 40 percent lower in wells that contained 3200 μg/mL of each polymer than in wells that did not contain any polymer (Figure 3.4A).

Next we tested if the polymers affected the pluripotency of the mES cells. We plated D3, R1, and NIH 3T3 cells in 96-well and 6-well plates, incubated them for 2 days with a range of equal weight concentrations of PB and CSC, and then measured the amount of alkaline phosphatase (ALP) activity present in extracts of the cells (Figure 3.4B, 96-well plates). Interestingly, ALP activity was slightly higher ($p<0.05$) in cells that had been incubated with intermediate doses (80 to 1600 μg/mL) of the polymers than in cells that were incubated with 0 or 3200 μg/mL of each polymer (Figure 3.4B). Cells that were incubated with the highest dose of polymers tested (3200 μg/mL) exhibited about the same amount of ALP activity as the cells that were not incubated with the polymers. As expected, ALP activity was much lower in NIH 3T3 cells than in mES cells. To more fully assess the effect of the polymer complexes on their pluripotency, we incubated mES cells with a range of concentrations of the polymer complexes for two days, and then used real-time PCR to quantify the level of mRNA within the cells of the pluripotency markers Oct-4 and Nanog. We found that Oct-4 expression did not change, regardless of how much polymer was added to the cells (Figure 3.4C). Interestingly, Nanog expression increased ($p<0.05$) by as much as 4.5-fold in mES cells that were exposed to the polymers as compared to non-exposed control cells (Figure 3.4D). Taken together, these data suggest that the polymers do not adversely affect the pluripotency of mES cells.

From these data, we concluded that virus-polymer complexes (which are formed using 80 μg/mL each of PB and CSC) could be concentrated up to 40-fold (for a final polymer concentration of 3200 μg/mL each) and used to transduce mES cells without significantly reducing their viability or pluripotency. To test this, we incubated stocks of

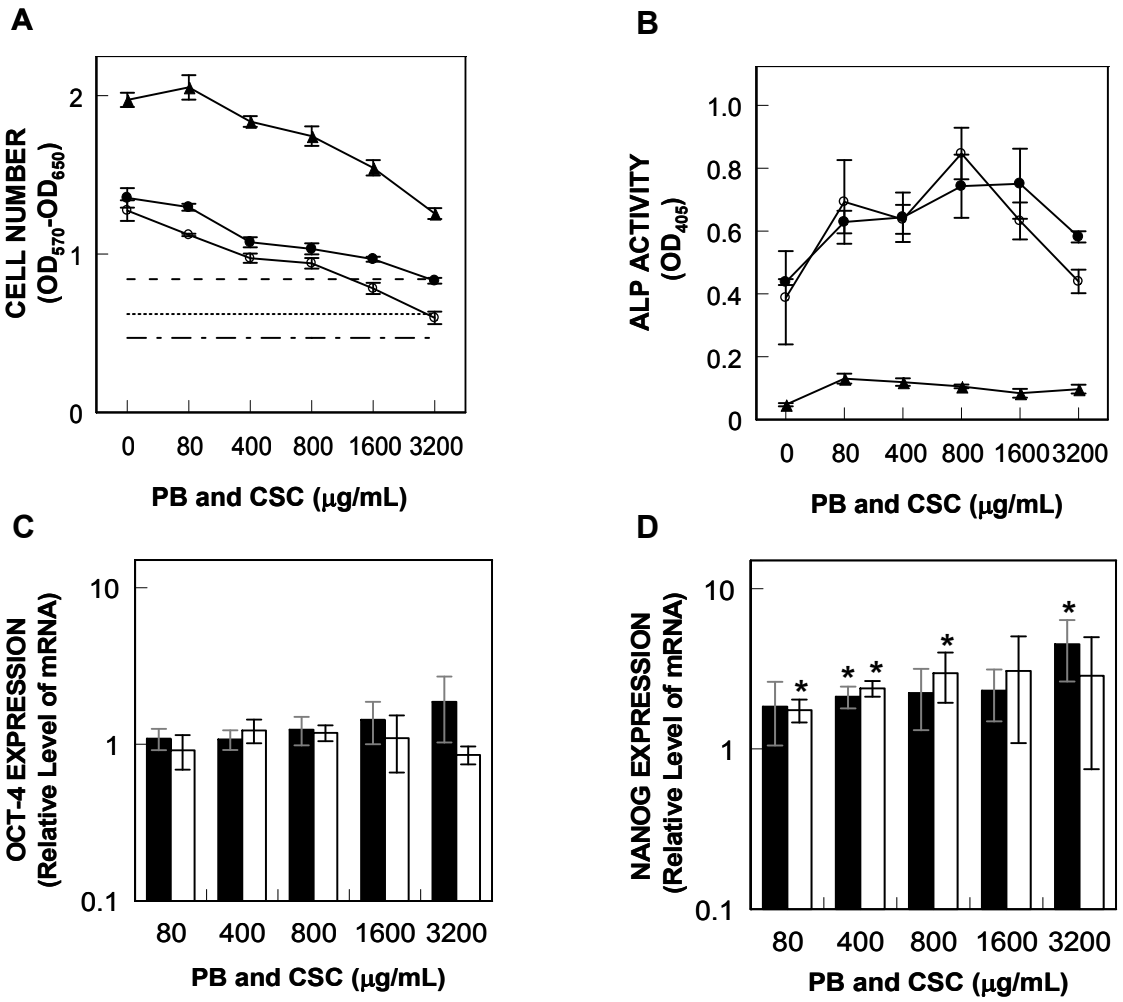

Figure 3.4. High doses of Polybrene (PB) and chondroitin sulfate C (CSC) reduces the growth rate, but not the pluripotency, of D3 and R1 mESC. D3 and R1 mES cells were plated (10,000 and 5,000 cells/well, respectively) in gelatinized 96-well tissue culture plates. The next day, the number of D3 (▪▪▪▪), R1 (– ——), and NIH 3T3 (– –) cells was determined using the MTT assay, after which the cells were cultured with a range of equal weight concentrations of CSC and PB. Two days later, the (A) number and (B) pluripotency of D3 (●), R1 (○), and NIH 3T3 (▲) cells was determined using the MTT and alkaline phosphatase (ALP) assays, respectively. Each point represents the mean ± standard deviation of triplicate wells. For both D3 and R1 mES cells, ALP activity in cells exposed to 80, 400, 800, and 1600 μg/ml of polymers was significantly different ($p<0.05$) from cells cultured without the polymers (i.e., 0 μg/ml). Oct-4 (C) and Nanog (D) mRNA expression levels were also quantified. D3 and R1 mES cells were plated (350,000 cells/well) in gelatinized 6-well tissue culture plates, and then cultured the next day with a range of equal weight concentrations of CSC and PB. Two days later, total RNA was extracted from lysates of D3 (black bars) and R1 (white bars) cells and reverse transcribed using oligo dT primers, and the relative amount of cDNA was quantified by real-time PCR and is reported as *n*-fold differences relative to cells that were cultured without the polymers (i.e., 0 μg/mL). Each bar represents the mean ± standard deviation of three independent experiments. Statistically significant ($p<0.05$) differences from cells that were not cultured with polymers are denoted with an asterisk (*).

ecotropic MSCV-eGFP retroviruses with 80 μg/mL each of PB and CSC at 37°C for 20 minutes to form virus-polymer complexes, pelleted the complexes and resuspended them in a range of reduced volumes of fresh ES complete medium, and then used them to transduce D3, R1, and NIH 3T3 cells. The cells were cultured in gelatin coated dishes in the presence of leukemia inhibitory factor (LIF) to maintain the embryonic stem cells in an undifferentiated state. Three days later we visualized the cells by epifluorescence microscopy (Figure 3.5) and used flow cytometry to quantify the mean fluorescent intensity of the transduced cells (Figure 3.6) as a function of virus concentration.

We found that for all the cell types tested, the number of eGFP+ cells increased with increasing concentrations of virus (Figure 3.5). In D3 and R1 mES cells, however, eGFP expression in individual cells (i.e., their mean fluorescence intensity) remained consistently low and did not change when the concentration of virus was increased (Figure 3.6). In contrast, both the number of transduced NIH 3T3 cells, (Figure 3.5) and the intensity of fluorescence within individual NIH 3T3 cells (Figure 3.6) increased with increasing doses of virus, although the amount of eGFP expressed per cell appeared to reach a maximum at the highest doses of virus tested. For all concentrations of virus used, however, the mean fluorescence intensity of eGFP in NIH 3T3 was significantly higher ($p<0.05$) than in D3 and R1 mES cells.

Given their low levels of eGFP expression, we wondered if mES cells contained fewer integrated transgenes than the NIH 3T3 cells. To determine if this was the case, we transduced D3, R1, and NIH 3T3 cells with virus-polymer complexes that had been concentrated up to 40-fold, and then three days later used real-time PCR to quantify the number of integrated eGFP transgenes. We found that the number of integrated eGFP transgenes in all the cell types increased as the dose of virus used to transduce them increased (Figure 3.7). Interestingly, at all doses of virus tested, we found that mES contained up to 13-fold fewer integrated transgenes than NIH 3T3 cells.

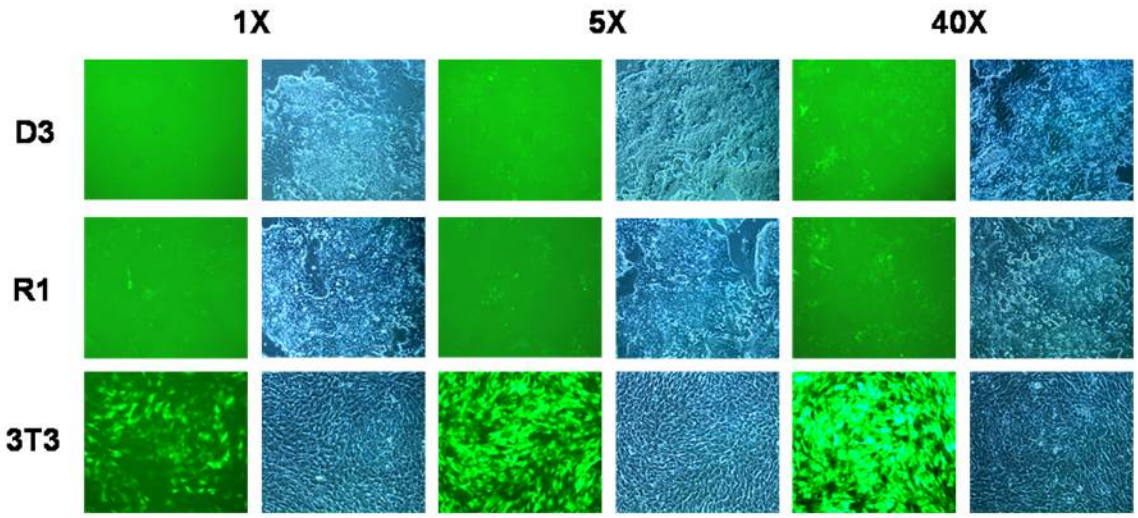

Figure 3.5. The number of transduced cells increases when ecotropic retrovirus is concentrated by complexation with Polybrene and chondroitin sulfate C. Retrovirus-polymer complexes were formed, pelleted, resuspended in fresh ES cell culture medium to their original volume (1X), or to one-fifth (5X) or to one-fortieth (40X) their original volume, added to gelatinized 6-well tissue culture plates that had been seeded the previous day with mES (D1 and R3; 350,000 per well) or NIH 3T3 (150,000 per well) cells, centrifuged (1,100 g, 30 min, 25°C), and then cultured at 37°C in a humidified tissue culture incubator. Three days later the cells were visualized by phase contrast and epifluorescence microscopy.

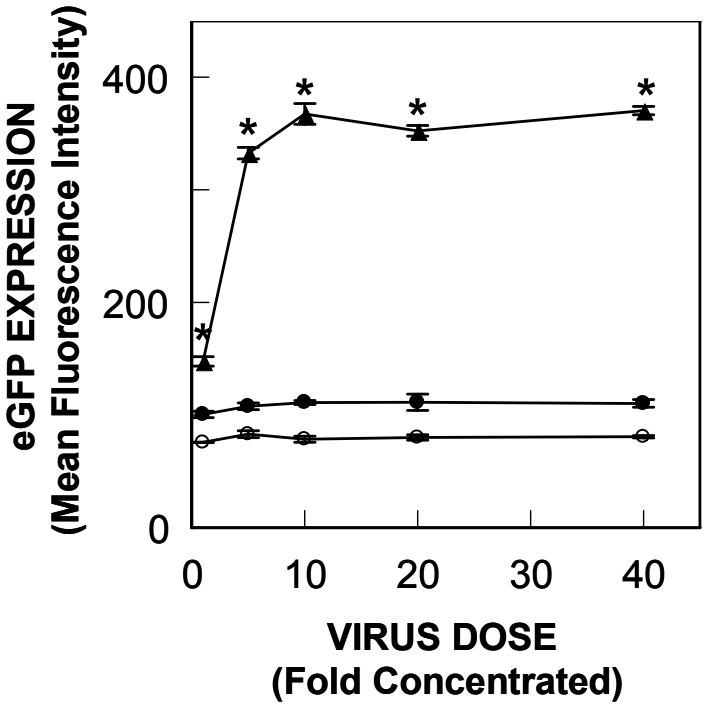

Figure 3.6. Delivery of ecotropic virus, concentrated up to 40-fold by complexation with PB and CSC, increases transgene expression in NIH 3T3 cells, but not in D3 or R1 mES cells. Retrovirus-polymer complexes were formed, pelleted, resuspended in fresh ES cell culture medium to their original volume (1X), or to one-fifth (5X), one-tenth (10X), one-twentieth (20X) or one-fortieth (40X) their original volume, added to gelatinized 6-well tissue culture plates that had been seeded the previous day with mES (D3 and R1; 350,000 per well) or NIH 3T3 (150,000 per well) cells, centrifuged (1,100 g, 30 min, 25°C), and then cultured at 37°C in a humidified tissue culture incubator. Three days later flow cytometry was used to quantify the mean fluorescence intensity of the transduced D3 (●) and R1 (○) mES cells and NIH3T3 cells (▲). For all concentrations of virus used, the mean fluorescence intensity of eGFP in NIH 3T3 was significantly higher ($p<0.05$) than in D3 and R1 mES cells and denoted with an asterisk (*). Each point represents the mean ± standard deviation of three replicates.

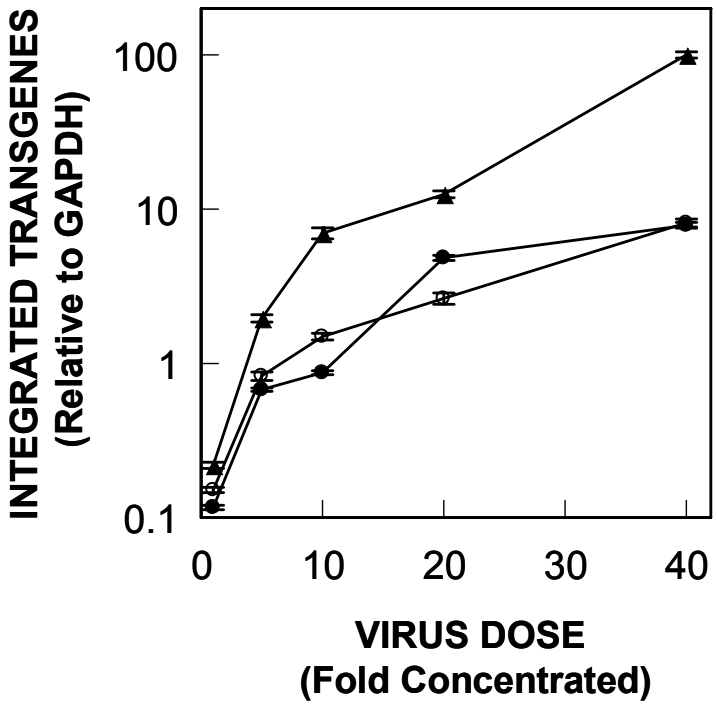

Figure 3.7. Ecotropic retrovirus transfers fewer genes to mES cells than to NIH 3T3 cells. Retrovirus-polymer complexes were formed, pelleted, resuspended in fresh ES cell culture medium to their original volume, or to one-fifth (5X), one-tenth (10X), one-twentieth (20X), or one-fortieth (40X) their original volume, added to gelatinized 6-well tissue culture plates that had been seeded the previous day with mES (D3 and R1; 350,000 per well) or NIH 3T3 (150,000 per well) cells, centrifuged (1,100 g, 30 min, 25°C), and then cultured at 37°C in a humidified tissue culture incubator. Three days later the chromosomal DNA of D3 (●), R1 (○), and NIH 3T3 cells (▲) was isolated, and real-time PCR was used to quantify the number of integrated eGFP transgenes relative to the number of endogenous GAPDH genes. Each point represents the mean ± standard deviation of three replicates.

3.4 Discussion

Embryonic stem (ES) cells are difficult to genetically modify with recombinant retroviruses, largely because they employ multiple mechanisms to silence retrovirus gene expression [40]. As a result, most strategies to improve retrovirus transduction of ES cells have focused on developing retroviral vectors that are resistant to silencing [14]. As a potential complimentary strategy, we decided to determine to what extent retrovirus gene expression could be improved in ES cells by increasing the number of genes transferred. To test this strategy, we formed ecotropic retrovirus – polymer complexes, concentrated them up to 40-fold, and then used them to transduce D3 and R1 murine ES cells, and NIH 3T3 murine fibroblasts as a control. Gene transfer was highest when the most concentrated virus-polymer complexes were used, with increases in the number of integrated transgenes as high as 150-fold in D3 cells, 50-fold in R1 cells, and 120-fold in NIH 3T3 murine fibroblasts. Despite these large increases in gene transfer, gene expression increased only in NIH 3T3 murine fibroblasts. Gene expression in D3 and R1 cells remained low and virtually constant. Interestingly, even though an equivalent amount of retrovirus was delivered to each cell type, up to ten-fold fewer transgenes integrated into D3 and R1 cells than in NIH 3T3 fibroblasts. These results indicate that retrovirus gene expression in ES cells cannot be substantially increased by simply increasing the number of genes transferred.

The observation that D3 and R1 cells integrated fewer transgenes than NIH 3T3 cells suggests that ES cells are more restrictive than other cell types to steps in the retrovirus lifecycle that lead to integration of the retrovirus genome. It is interesting to consider which step of transduction is restricted in ES cells. Previous work has shown that the number of retrovirus genes transferred to cells is proportional to 1) the number of active viruses delivered to the cells, and 2) the overall efficiency with which post-

delivery steps of transduction are completed [37]. Mathematically, this relationship can be expressed as follows:

$$G = A\eta$$

where G is the number of genes integrated per cell, A is the number of active viruses delivered per cell, and η is the fraction of active viruses that successfully complete post-binding steps of transduction. Andreadis et al showed that the number of active viruses delivered per cell (A) can be estimated from the following relationship:

$$A = 4a_c DC_{vo} l$$

where a_c is the average radius of the target cells, D is the diffusion coefficient of the virus, C_{vo} is the initial concentration of active retrovirus at the start of the infection, and l is an integrated function of time, the diffusion coefficient, the half-life of the virus, and the radius of the target cells [37, 41]. Based on this relationship, we conclude that the differences we observed in gene transfer to ES and NIH 3T3 cells were most likely not due to differences in the amount of virus delivered to the cells. This is because each cell type was incubated with exactly the same formulation of virus, which rules out the possibility that the cells were exposed to different concentrations of virus, or to viruses with different half-lives or diffusion coefficients. Also, the radii of ES (4-7 μM) and NIH 3T3 (7 μM) cells are similar, and could account for at most a 1.75-fold difference in the number of active viruses delivered per cell [37, 42]. Since ES cells are transduced up to 10-fold less efficiently than NIH 3T3 cells, it is likely that ES cells significantly inhibit one or more post-delivery steps of transduction.

We do not know which post-delivery step of transduction is inhibited. One possibility is that ES cells express fewer retrovirus receptors than NIH 3T3 cells. Our data suggests this is unlikely since we found that ES and NIH 3T3 cells express similar levels of mRNA for the ecotropic retrovirus receptor. Nevertheless, we cannot exclude

the formal possibility that ES cells express fewer functional receptors on their surfaces than NIH 3T3 cells due to differences in the post-transcriptional regulation of the receptor. Another possibility is that ES cells divide more slowly than NIH 3T3 cells, or that a smaller fraction of ES cells are in mitosis at any given time. This would reduce the susceptibility of ES cells to transduction since retroviruses can only gain access to the nuclei of cells during mitosis, when their nuclear envelopes are disassembled [43, 44]. Since retroviruses rapidly lose their activity within cells over time due to 'intracellular decay', the longer they are excluded from access to the nucleus, the less likely they will be able to successfully transduce a cell [45]. However, this is not likely to be the case in our experimental system since 1) both ES and NIH 3T3 cells rapidly divide (ES cells double every 12 to 17 hours [46-48] and NIH 3T3 cells double every 12 hours [37]), and 2) similar percentages of ES (about 18%) and NIH 3T3 (21.5%) cells are in the G_2/M phase of the cell cycle when they are rapidly dividing [42, 49]. Taken together, it seems likely that ES cells are more resistant to transduction than NIH 3T3 cells because they restrict one or more post-fusion steps of the retrovirus lifecycle, rather than because they bind fewer viruses, express fewer receptors, or divide more slowly than NIH 3T3 cells. Further experimentation is needed to identify the mechanisms by which ES cells restrict retrovirus infection.

Although it is of interest to understand and overcome the mechanisms by which ES cells restrict retrovirus integration, our results clearly show that the most significant obstacle that currently hampers the successful use of retroviruses with ES cells is the ability of ES cells to silence retrovirus transgene expression. This conclusion is supported by our rather surprising finding that that even though the number of genes transferred to ES cells increased monotonically with an increase of up to 40-fold in virus concentration (which suggests that the ES cells did not become saturated with virus even at the highest doses tested), transgene expression remained virtually constant.

These findings suggest that the mechanisms by which ES cells silence transgene expression are not saturable and are not overcome by large increases in the number of integrated transgenes. For these studies, we used MSCV-derived retrovirus vectors that have had their LTR regions modified to reduce their susceptibility to DNA methylation. But ES cells use multiple mechanisms to silence gene expression, each of which can act independently of one another, that include DNA methylation, histone deacetylation, and the binding of negative trans-acting factors [50] to regulatory and coding regions of the integrated transgenes [40, 51]. MSCV-derived retroviruses are resistant to DNA methylation, but they still retain a negative control region (NCR) and an enhancer direct repeat (DR) that are probably acted upon by ES cell encoded repressive transcription factors and trans-acting factors [11]. Retrovirus vectors are needed that are resistant to all the mechanisms used by ES cells to silence transgene expression.

Interestingly, we noticed that ES cells, when exposed to increasing doses of retrovirus-polymer complexes, expressed higher levels of ALP activity and Nanog expression, both makers of ES cell pluripotency [52, 53]. In contrast, Oct-4 expression, another marker of ES cell pluripotency, did not change [54]. Although we can only speculate, it is possible that the virus-polymer complexes stimulate ES cells to upregulate expression of these pluripotency markers because they contain high levels of chondroitin sulfate glycosaminoglycans. Several recent studies suggest that chondroitin sulfate proteoglycans and glycosaminoglycans play important roles in directing the fate of ES cells. For example, Emami and Chaudhry found that chondroitin sulfate, when added to the gelatin used to culture murine ES cells in the absence of a feeder layer, increased ES cell self-renewal as evidenced by a 57% increase in the cell population and a 32% increase in the number of embryoid bodies they were able to form [55]. Sirko et al found that chondroitin sulfate proteoglycans play an essential role in proliferation, self-renewal and cell fate of neural stem cells [56]. In our studies, ES cells

expressed higher levels of Nanog when they were incubated with virus-polymer complexes that contained chondroitin sulfate. Nanog is a master regulator of self-renewal and pluripotency in ES cells, and is rapidly downregulated when ES cells differentiate *in vitro* [57]. Interestingly, ES cells that overexpress Nanog maintain their pluripotency even in the absence of leukemia inhibitory factor (LIF), a growth factor that is normally required to prevent their differentiation [52, 53, 57]. These observations suggest that it may be possible to maintain ES cells in a pluripotent state while they are being genetically modified - without the need for LIF - by coupling gene transfer vectors to a carrier composed of chondroitin sulfate glycosaminoglycans or other compounds with similar properties.

In summary, we have shown that retroviruses transfer significantly fewer genes to murine ES cells than to NIH 3T3 fibroblasts. Future work should determine the specific mechanisms by which ES cells restrict retrovirus transduction. Such work would improve our understanding of retrovirus-cell interactions, provide the basis for the design of more efficient retrovirus vectors, and may suggest novel strategies for inhibiting infectious diseases such as HIV-1.

3.5 Acknowledgements

We thank Todd McDevitt for the R1 mES cell line and for helpful discussions, David Archer for technical assistance, Scott Case for the VSV-G Env construct, Stephen Russell for the ecotropic and amphotropic Env constructs, MariBeth Eiden and Lorraine Albritton for the 10A1 Env construct, and Catherine Verfaillie for the MSCV retroviral vector. This work was supported by the Georgia Tech/Emory Center for the Engineering of Living Tissues (NSF Engineering Research Center: EEC-9731643).

3.6 References

[1] N. Kobayashi, J.D. Rivas-Carrillo, A. Soto-Gutierrez, T. Fukazawa, Y. Chen, N. Navarro-Alvarez, N. Tanaka, Gene delivery to embryonic stem cells, Birth Defects Res C Embryo Today 75 (2005) 10-18.

[2] S.Y. Moon, Y.B. Park, D.S. Kim, S.K. Oh, D.W. Kim, Generation, culture, and differentiation of human embryonic stem cells for therapeutic applications, Mol Ther 13 (2006) 5-14.

[3] A.M. Wobus, K.R. Boheler, Embryonic stem cells: prospects for developmental biology and cell therapy, Physiol Rev 85 (2005) 635-678.

[4] R.G. Vile, S.J. Russell, Retroviruses as vectors, Br Med Bull 51 (1995) 12-30.

[5] D. Pannell, J. Ellis, Silencing of gene expression: implications for design of retrovirus vectors, Rev Med Virol 11 (2001) 205-217.

[6] C.S. Swindle, H.G. Kim, C.A. Klug, Mutation of CpGs in the murine stem cell virus retroviral vector long terminal repeat represses silencing in embryonic stem cells, J Biol Chem 279 (2004) 34-41.

[7] M. Grez, E. Akgun, F. Hilberg, W. Ostertag, Embryonic stem cell virus, a recombinant murine retrovirus with expression in embryonic stem cells, Proc Natl Acad Sci U S A 87 (1990) 9202-9206.

[8] B.C. Guild, M.H. Finer, D.E. Housman, R.C. Mulligan, Development of retrovirus vectors useful for expressing genes in cultured murine embryonal cells and hematopoietic cells in vivo, J Virol 62 (1988) 3795-3801.

[9] R.G. Hawley, Progress toward vector design for hematopoietic stem cell gene therapy, Curr Gene Ther 1 (2001) 1-17.

[10] C.S. Osborne, P. Pasceri, R. Singal, T. Sukonnik, G.D. Ginder, J. Ellis, Amelioration of retroviral vector silencing in locus control region beta-globin-transgenic mice and transduced F9 embryonic cells, J Virol 73 (1999) 5490-5496.

[11] A. Ramezani, T.S. Hawley, R.G. Hawley, Stable gammaretroviral vector expression during embryonic stem cell-derived in vitro hematopoietic development, Mol Ther 14 (2006) 245-254.

[12] T. Asano, Y. Hanazono, Y. Ueda, S. Muramatsu, A. Kume, H. Suemori, Y. Suzuki, Y. Kondo, K. Harii, M. Hasegawa, N. Nakatsuji, K. Ozawa, Highly efficient gene transfer into primate embryonic stem cells with a simian lentivirus vector, Mol Ther 6 (2002) 162-168.

[13] S.R. Cherry, D. Biniszkiewicz, L. van Parijs, D. Baltimore, R. Jaenisch, Retroviral expression in embryonic stem cells and hematopoietic stem cells, Mol Cell Biol 20 (2000) 7419-7426.

[14] J. Ellis, S. Yao, Retrovirus silencing and vector design: relevance to normal and cancer stem cells?, Curr Gene Ther 5 (2005) 367-373.

[15] N. Landazuri, J.M. Le Doux, Complexation of retroviruses with charged polymers enhances gene transfer by increasing the rate that viruses are delivered to cells, J Gene Med 6 (2004) 1304-1319.

[16] N. Landazuri, J.M. Le Doux, Complexation with chondroitin sulfate C and Polybrene rapidly purifies retrovirus from inhibitors of transduction and substantially enhances gene transfer, Biotechnol Bioeng 93 (2006) 146-158.

[17] J.M. Le Doux, N. Landazuri, M.L. Yarmush, J.R. Morgan, Complexation of retrovirus with cationic and anionic polymers increases the efficiency of gene transfer, Hum Gene Ther 12 (2001) 1611-1621.

[18] D.W. McMillin, N. Landazuri, B. Gangadharan, B. Hewes, D.R. Archer, H.T. Spencer, J.M. Le Doux, Highly efficient transduction of repopulating bone marrow cells using rapidly concentrated polymer-complexed retrovirus, Biochem Biophys Res Commun 330 (2005) 768-775.

[19] H. Harlow, D. Lane, Antibodies: A laboratory manual., Cold Spring Harbor Laboratory Press, Cold Spring Harbor, 1998.

[20] F.L. Cosset, Y. Takeuchi, J.L. Battini, R.A. Weiss, M.K. Collins, High-titer packaging cells producing recombinant retroviruses resistant to human serum, J Virol 69 (1995) 7430-7436.

[21] J.Y. Han, P.M. Cannon, K.M. Lai, Y. Zhao, M.V. Eiden, W.F. Anderson, Identification of envelope protein residues required for the expanded host range of 10A1 murine leukemia virus, J Virol 71 (1997) 8103-8108.

[22] S.S. Case, M.A. Price, C.T. Jordan, X.J. Yu, L. Wang, G. Bauer, D.L. Haas, D. Xu, R. Stripecke, L. Naldini, D.B. Kohn, G.M. Crooks, Stable transduction of quiescent CD34(+)CD38(-) human hematopoietic cells by HIV-1-based lentiviral vectors, Proc Natl Acad Sci U S A 96 (1999) 2988-2993.

[23] L. Naldini, U. Blomer, P. Gallay, D. Ory, R. Mulligan, F.H. Gage, I.M. Verma, D. Trono, In vivo gene delivery and stable transduction of nondividing cells by a lentiviral vector, Science 272 (1996) 263-267.

[24] R.C. Zhao, Y. Jiang, C.M. Verfaillie, A model of human p210(bcr/ABL)-mediated chronic myelogenous leukemia by transduction of primary normal human CD34(+) cells with a BCR/ABL-containing retroviral vector, Blood 97 (2001) 2406-2412.

[25] J.C. Pui, D. Allman, L. Xu, S. DeRocco, F.G. Karnell, S. Bakkour, J.Y. Lee, T. Kadesch, R.R. Hardy, J.C. Aster, W.S. Pear, Notch1 expression in early lymphopoiesis influences B versus T lineage determination, Immunity 11 (1999) 299-308.

[26] Retroviral Gene Transfer and Expression User Manual, Clontech Laboratories, Inc., Mountain View, 2006.

[27] S.A. Bustin, Absolute quantification of mRNA using real-time reverse transcription polymerase chain reaction assays, J Mol Endocrinol 25 (2000) 169-193.

[28] S.A. Bustin, Real-time, fluorescence-based quantitative PCR: a snapshot of current procedures and preferences, Expert Rev Mol Diagn 5 (2005) 493-498.

[29] S.A. Bustin, V. Benes, T. Nolan, M.W. Pfaffl, Quantitative real-time RT-PCR--a perspective, J Mol Endocrinol 34 (2005) 597-601.

[30] J.H. Marino, P. Cook, K.S. Miller, Accurate and statistically verified quantification of relative mRNA abundances using SYBR Green I and real-time RT-PCR, J Immunol Methods 283 (2003) 291-306.

[31] M.L. Wong, J.F. Medrano, Real-time PCR for mRNA quantitation, Biotechniques 39 (2005) 75-85.

[32] J.S. Yuan, A. Reed, F. Chen, C.N. Stewart, Jr., Statistical analysis of real-time PCR data, BMC Bioinformatics 7 (2006) 85.

[33] Relative Quantitation Of Gene Expression: ABI PRISM 7700 Sequence Detection System: User Bulletin #2: Rev B Applied Biosystems, Inc., Foster City, 1997

[34] J.R. Morgan, J.M. LeDoux, R.G. Snow, R.G. Tompkins, M.L. Yarmush, Retrovirus infection: effect of time and target cell number, J Virol 69 (1995) 6994-7000.

[35] P.W. Zandstra, H.V. Le, G.Q. Daley, L.G. Griffith, D.A. Lauffenburger, Leukemia inhibitory factor (LIF) concentration modulates embryonic stem cell self-renewal and differentiation independently of proliferation, Biotechnol Bioeng 69 (2000) 607-617.

[36] L. Sastry, T. Johnson, M.J. Hobson, B. Smucker, K. Cornetta, Titering lentiviral vectors: comparison of DNA, RNA and marker expression methods, Gene Ther 9 (2002) 1155-1162.

[37] S. Andreadis, T. Lavery, H.E. Davis, J.M. Le Doux, M.L. Yarmush, J.R. Morgan, Toward a more accurate quantitation of the activity of recombinant retroviruses: alternatives to titer and multiplicity of infection, J Virol 74 (2000) 3431-3439.

[38] A.S. Chuck, M.F. Clarke, B.O. Palsson, Retroviral infection is limited by Brownian motion, Hum Gene Ther 7 (1996) 1527-1534.

[39] J.M. Le Doux, H.E. Davis, J.R. Morgan, M.L. Yarmush, Kinetics of retrovirus production and decay, Biotechnol Bioeng 63 (1999) 654-662.

[40] S. Yao, T. Sukonnik, T. Kean, R.R. Bharadwaj, P. Pasceri, J. Ellis, Retrovirus silencing, variegation, extinction, and memory are controlled by a dynamic interplay of multiple epigenetic modifications, Mol Ther 10 (2004) 27-36.

[41] S.T. Andreadis, J.R. Morgan, Quantitative measurement of the concentration of active recombinant retrovirus, Methods Mol Med 69 (2002) 161-172.

[42] Q. Zhou, A. Jouneau, V. Brochard, P. Adenot, J.P. Renard, Developmental potential of mouse embryos reconstructed from metaphase embryonic stem cell nuclei, Biol Reprod 65 (2001) 412-419.

[43] R.A. Katz, J.G. Greger, A.M. Skalka, Effects of cell cycle status on early events in retroviral replication, J Cell Biochem 94 (2005) 880-889.

[44] T. Roe, T.C. Reynolds, G. Yu, P.O. Brown, Integration of murine leukemia virus DNA depends on mitosis, Embo J 12 (1993) 2099-2108.

[45] S.T. Andreadis, D. Brott, A.O. Fuller, B.O. Palsson, Moloney murine leukemia virus-derived retroviral vectors decay intracellularly with a half-life in the range of 5.5 to 7.5 hours, J Virol 71 (1997) 7541-7548.

[46] M. Amit, M.K. Carpenter, M.S. Inokuma, C.P. Chiu, C.P. Harris, M.A. Waknitz, J. Itskovitz-Eldor, J.A. Thomson, Clonally derived human embryonic stem cell lines maintain pluripotency and proliferative potential for prolonged periods of culture, Dev Biol 227 (2000) 271-278.

[47] S.J. Field, R.S. Johnson, R.M. Mortensen, V.E. Papaioannou, B.M. Spiegelman, M.E. Greenberg, Growth and differentiation of embryonic stem cells that lack an intact c-fos gene, Proc Natl Acad Sci U S A 89 (1992) 9306-9310.

[48] E.Y. Fok, P.W. Zandstra, Shear-controlled single-step mouse embryonic stem cell expansion and embryoid body-based differentiation, Stem Cells 23 (2005) 1333-1342.

[49] M.R. Smith, D.W. Court, H.K. Kim, J.B. Park, S.G. Rhee, J.S. Rhim, H.F. Kung, Overexpression of phosphoinositide-specific phospholipase Cgamma in NIH 3T3 cells promotes transformation and tumorigenicity, Carcinogenesis 19 (1998) 177-185.

[50] J. Ellis, Silencing and variegation of gammaretrovirus and lentivirus vectors, Hum Gene Ther 16 (2005) 1241-1246.

[51] D. Pannell, C.S. Osborne, S. Yao, T. Sukonnik, P. Pasceri, A. Karaiskakis, M. Okano, E. Li, H.D. Lipshitz, J. Ellis, Retrovirus vector silencing is de novo methylase independent and marked by a repressive histone code, Embo J 19 (2000) 5884-5894.

[52] I. Chambers, D. Colby, M. Robertson, J. Nichols, S. Lee, S. Tweedie, A. Smith, Functional expression cloning of Nanog, a pluripotency sustaining factor in embryonic stem cells, Cell 113 (2003) 643-655.

[53] R.L. Williams, D.J. Hilton, S. Pease, T.A. Willson, C.L. Stewart, D.P. Gearing, E.F. Wagner, D. Metcalf, N.A. Nicola, N.M. Gough, Myeloid leukaemia inhibitory factor maintains the developmental potential of embryonic stem cells, Nature 336 (1988) 684-687.

[54] J. Nichols, B. Zevnik, K. Anastassiadis, H. Niwa, D. Klewe-Nebenius, I. Chambers, H. Scholer, A. Smith, Formation of pluripotent stem cells in the mammalian embryo depends on the POU transcription factor Oct4, Cell 95 (1998) 379-391.

[55] S.H. Emami, M.A.S. Chaudhry, Self-renewal and Proliferation of Murine Embryonic Stem Cells: A Study of Glycosaminoglycans Effect on Feeder-Free Cultures, Journal of Bioactive and Compatible Polymers 22 (2007) 314-322.

[56] S. Sirko, A. von Holst, A. Wizenmann, M. Gotz, A. Faissner, Chondroitin sulfate glycosaminoglycans control proliferation, radial glia cell differentiation and neurogenesis in neural stem/progenitor cells, Development 134 (2007) 2727-2738.

[57] K. Mitsui, Y. Tokuzawa, H. Itoh, K. Segawa, M. Murakami, K. Takahashi, M. Maruyama, M. Maeda, S. Yamanaka, The homeoprotein Nanog is required for maintenance of pluripotency in mouse epiblast and ES cells, Cell 113 (2003) 631-642.

CHAPTER 4

QUANTITATIVE ANALYSIS OF RETROVIRAL AND LENTIVIRAL GENE TRANSFER TO MURINE EMBRYONIC STEM CELLS

4.1 Introduction

Embryonic stem (ES) cells are a promising source of cells for cellular therapy because they are capable of differentiating into virtually any cell type in the body [1, 2]. The genetic modification of ES cells further broadens their range of potential applications [3]. For example, genetic modification of ES cells can be used to study their development and differentiation, or to induce them to differentiate into a specific cell type, or to adopt a desired therapeutic phenotype [4, 5]. Genetic modification is also likely to prove useful for improving the efficacy and safety of ES cell transplantation. Genetic modification of ES cells could be used to reduce their immunogenicity, or to make them susceptible to a prodrug that could be administered to the patient should the transplanted cells form a tumor or teratoma [6, 7].

Recombinant retroviruses are an attractive tool for genetically modifying ES cells because they stably integrate their genetic material into the host cell genome, which makes long-term transgene expression possible, both *in vitro* and *in vivo*. Unfortunately, it has proven difficult to successfully genetically modify ES cells with retroviruses, primarily because ES cells shutdown expression of the integrated transgenes [8]. The mechanisms by which ES cells silence gene expression include DNA methylation, histone deacetylation, and the binding of negative trans-acting factors to regulatory and coding regions of the integrated transgenes [8-10]. Silencing of retrovirus transgene expression can manifest itself shortly after transduction or after long-term culture or differentiation of modified ES cells.

Lentivirus vectors (derived from HIV) may not be as susceptible to silencing in ES cells as traditional retrovirus vectors (derived from the murine leukemia virus) [11]. Pfeifer et al reported stable expression from lentivirus transgenes in proliferating murine ES cells [12]. Expression was maintained in the cells, even when they were cultured *in vitro* as embryoid bodies, or *in vivo* as teratomas. Nevertheless, recent work suggests that lentiviruses are not entirely resistant to ES cell silencing mechanisms. For example, Yao et al isolated ES cell clones, each of which contained a single copy of an integrated lentivirus transgene, and observed three distinct patterns of gene expression. One clone expressed the transgene, another exhibited variegated expression, and in a third expression was silenced. Chromatin immunoprecipitation experiments suggested that expression in the silent clone was most likely shutdown by the same mechanisms used to shutdown retrovirus transgene expression [10].

Clearly, the silencing of integrated transgenes is a significant limitation of using retroviruses or lentiviruses to genetically modify ES cells. Recently, we found that ES cells integrate fewer retrovirus transgenes than NIH 3T3 mouse fibroblasts, which suggests that inefficient transduction may be another limitation of using retroviruses to genetically modify ES cells [13]. Several cellular factors (e.g., Fv1, moesin, and TRIM5α) are known to impede or block one or more intracellular steps of retrovirus infection [14-19] in other cell types. We do not know if these or other factors restrict transduction in ES cells.

As a first step towards identifying the factors that impede transduction of ES cells, we examined the efficiency with which three key steps of transduction are completed in R1 murine ES cells and in NIH 3T3 murine fibroblasts, a cell type that is much more easily transduced. Using recombinant murine leukemia virus (MLV)-derived retrovirus and HIV-1-derived lentivirus vectors, we quantitatively compared 1) the

amount of virus binding, 2) the number of integrated transgenes, and 3) the resulting level of gene expression.

4.2 Materials and Methods

Chemicals. Gluteraldehyde, poly-L-lysine, 1,5-dimethyl-1,5-diazaundecamethylene polymethobromide (Polybrene, PB), 1-(4,5-dimethylthiazol-2-yl)-3,5-diphenylformazan (MTT), 5-bromo-4-chloro-3-indolyl-β-D-galactopyranoside (X-Gal), IGEPAL CA-630, trypsin inhibitor (soybean), gelatin from bovine skin (Type B) and gelatin from porcine skin (Type A) were purchased from Sigma Chemical Co. (St. Louis, MO, USA). Complete mini protease inhibitor cocktail tablets were purchased from Roche Diagnostics (Indianapolis, IN, USA). Hydrogen peroxide 30%, bovine serum albumin fraction V (BSA), polyoxyethylene 20-sorbitan monolaurate (Tween 20), Triton-X and sodium dodecyl sulfate (SDS) were from Fisher Scientific (Pittsburg, PA, USA). Non-fat dry milk (blotting grade) was from Bio-Rad Laboratories (Hercules, CA, USA). Mouse anti-p30 antibody was purified from the supernatant of the CRL-1219 (ATCC, Rockville, MD, USA) hybridoma cell line, following standard procedures [20]. The goat polyclonal anti-p30 antibody (78S221) was from Quality Biotech (Camden, NJ, USA). The horseradish peroxidase conjugated rabbit anti-goat immunoglobulin G polyclonal antibody was from Zymed Laboratories (South San Francisco, CA).

Plasmids. The expression plasmid encoding the VSV-G (pMD.G) [21, 22] was from Scott Case. The expression plasmid encoding the ecotropic (pFBMOSALF) envelope protein was from Stephen Russell [23]. The lacZ retroviral vector (pCMMP-nlsLacZ) was from Michael Conte (Harvard Institute of Human Genetics). The expression plasmid encoding the MLV RFP-Gag protein (pmRFP-N1) was purchased from Addgene (Addgene plasmid 1814; Cambridge, MA, USA) [24]. The lentiviral packaging construct (pCMVΔR8.91) was from Scott Case [21]. The lacZ lentiviral vector

(pTY-EFnlacZ) was purchased from NIH AIDS Research and Reference Reagent Program (Bethesda, MD, USA). The expression plasmid encoding the GFP-Vpr protein (peGFPC3) was from Thomas Hope [25].

Cell culture. NIH 3T3 mouse fibroblasts were cultured in Dulbecco's modified Eagle's medium (DMEM; Mediatech, Inc., Herndon, VA, USA) with 10% bovine calf serum (BCS; Hyclone Labs, Inc., Logan, UT, USA), and 100 U of penicillin and 100 µg of streptomycin (Hyclone Labs, Inc., Logan, UT, USA) per mL. The packaging cell line GP2-293 was cultured on collagen-coated plates (BD Biosciences Discovery Labware, Bedford, MA, USA) in DMEM (Mediatech, Inc., Herndon, VA, USA) with 10% fetal bovine serum (FBS; Hyclone Labs, Inc., Logan, UT, USA) and 100 U of penicillin and 100 µg of streptomycin per mL. The packaging cell line 293T was cultured in DMEM (Mediatech, Inc., Herndon, VA, USA) with 10% fetal bovine serum (FBS; Hyclone Labs, Inc., Logan, UT, USA) and 100 U of penicillin and 100 µg of streptomycin per mL. Undifferentiated R1 murine embryonic stem (mES) cells, a kind gift from Todd McDevitt (Georgia Tech), were cultured on 0.1% porcine gelatin-coated tissue culture flasks and plated in ES Complete Medium (ES-DMEM; ATCC, Manassas, VA, USA) supplemented with 4mM L-glutamine (Invitrogen Corp., Carlsbad, CA, USA), 150 M β-mercaptoethanol (Sigma Chemical Co., St. Louis, MO, USA), 10% heat-inactivated fetal bovine serum (ES Cell-Qualified FBS; Invitrogen Corp., Carlsbad, CA, USA), 1% MEM non-essential amino acids (Invitrogen Corp., Carlsbad, CA, USA), 100 U of penicillin and 100 µg of streptomycin (Invitrogen Corp., Carlsbad, CA, USA) per mL, and 10^3 U of leukemia inhibitory factor (LIF; Chemicon International Inc., Ternecula, CA, USA) per mL.

Production of recombinant retroviruses. To generate stocks of *RFP-lacZ* retrovirus, GP2-293 cells, a HEK 293-based packaging cell line that stably expresses the retroviral *gag* and *pol* genes (Clontech Laboratories, Inc., Mountain View, CA, USA) [26], were plated in 0.01% poly-L-lysine-coated T175 flasks ($12.5x10^6$ cells) in DMEM that

contained heat inactivated FBS (10%) but no antibiotics. The next day, Lipofectamine™ 2000 (Invitrogen Corp., Carlsbad, CA, USA) was used according to the manufacturer's recommendations to cotransfect the cells with 24 µg each of 3 plasmids: the VSV-G envelope glycoprotein expression plasmid (pMD.G), the RFP-Gag protein expression plasmid (pmRFP-N1) and the retrovirus vector pCMMP-nlsLacZ. Six hours after transfection, the medium was replaced with fresh 30 mL DMEM/FBS with antibiotics and again at 36 hours after transfection. Virus-laden tissue culture medium was harvested every 12 hours at 48, 60, 72, and 84 hours post-transfection, filter-sterilized (0.45 µm), combined, aliquotted and then frozen (-80ºC) for later use. Two separate rounds of *RFP-lacZ* retrovirus stock were generated. To generate stocks of *GFP-lacZ* lentivirus, we followed the same procedure to cotransfect 293T cells, except with 18 µg each of 4 plasmids: the VSV-G envelope glycoprotein expression plasmid (pMD.G), the GFP-Vpr protein expression plasmid (peGFPC3), the lentivirus packaging construct pCMVΔR8.91 and the lentivirus vector pTY-EFnlacZ.

Measurement of lentivirus decay. Frozen VSV-G and ecotropic *lacZ* lentivirus in culture medium was thawed and then incubated at 37ºC and 10% CO_2. Samples were taken approximately every 10 hrs and frozen at -80ºC. At later times, the samples were thawed and used to transduce NIH 3T3 cells in the diluted titer assay. Briefly, ten-fold serial dilutions of the incubated virus were made in DMEM/BCS and PB (8 µg per mL). A 1-mL amount per well was used to transduce NIH 3T3 cells that had been plated (7×10^4 per well) the previous day in 12-well plates. The next day the viral supernatant was removed and the cells replenished with fresh medium. Three days post transduction, the cells were fixed and stained for β-galactosidase activity with X-Gal. The number of colonies of *lacZ*+ NIH 3T3 cells (typically in clusters of 2, 4, 8, or 16 blue cells) was counted with the aid of a dissecting microscope. At appropriate dilutions of virus, the clusters of blue cells were sufficiently spread over the well such that each

cluster arose from a single transduction event. The number of clusters counted was multiplied by the dilution factor to determine CFU (i.e., the number of *lacZ*+ colony forming units) per mL. Values for each point are the averages of triplicate wells. Results are representative of two independent experiments for each *lacZ* lentivirus pseudotype. The best-fit value for the virus decay rate (k_d) was determined by using the method of least squares to fit experimental data for decay (Figure 1) to the following equation:

$$\frac{dV}{dt} = -k_d V \qquad [27]$$

where

$$k_d = \frac{\ln(2)}{t^{1/2}}$$

as previously described [28].

Diluted titer assay. To determine virus titer, two-fold serial dilutions of VSV-G *RFP-lacZ* retrovirus and VSV-G *GFP-lacZ* lentivirus stocks were made in DMEM/BCS and Polybrene (8μg per mL). Serially diluted virus (1 mL per well) was used to transduce NIH 3T3 cells that had been seeded at 2 x 10^4 cells per well in 6-well plates the previous day. The viral supernatants were removed 5 hours later and replaced with fresh medium. Three days post transduction, the cells were fixed and stained for β-galactosidase activity with X-Gal [29]. The number of colonies of *lacZ*+ NIH 3T3 cells were counted with the aid of a dissecting microscope, and multiplied by the dilution factor to determine CFU (i.e., the number of *lacZ*+ colony forming units) per mL. Titers for *RFP-lacZ* retrovirus stock #1, *RFP-lacZ* retrovirus stock #2 and *GFP-lacZ* lentivirus stock #1 were 4.57 ± 0.57 x 10^5 CFU/mL, 1.20 ± 0.61 x 10^5 CFU/mL, and 3.92 ± 1.04 x 10^3 CFU/mL, respectively. Results are the average of three independent experiments.

Cell-associated virus assay. Cell-associated and adsorbed VSV-G *RFP-lacZ* retrovirus and VSV-G *GFP-lacZ* lentivirus were analyzed by ELISA. R1 mES cells and

NIH 3T3 cells were plated in gelatinized 6-well plates (3.5×10^5 and 1.0×10^5 per well, respectively). The next day after plating, cells were transduced with 1 mL per well of either *RFP-lacZ* retrovirus or *GFP-lacZ* lentivirus and Polybrene (8 µg per mL) and LIF (10^3 U per mL), and plates were centrifuged for 30 min at 1,100 g at room temperature. Cells were incubated with virus for a range of times – immediately following centrifugation (0.5 hr), 1 hr, 2 hrs, and 7 hrs. The virus supernatant was then collected, and the cells were washed once with PBS. To remove loosely bound virus, cells were then treated with 1.25 mL non-enzymatic dissociation buffer (Sigma Chemical Co., St. Louis, MO, USA) for 10 min at room temperature. Cells were collected from wells and centrifuged, and then the dissociation buffer supernatant was collected. To determine levels of cell-associated virus (tightly-bound or absorbed virus), cell pellets were resuspended in 0.5 mL lysis buffer (1% Igepal, 150 mM NaCl and 50 mM Tris, pH 8) containing protease inhibitor (Complete Mini; Roche Diagnostics GmbH, Germany) and incubated on ice for 30 min, then centrifuged at 20,000 g for 10 min at 4°C to remove cellular debris. The resulting supernatant was collected. The virus supernatant, the dissociation buffer supernatant, and the cell lysate supernatant samples were stored at -80°C for later analysis by ELISA.

An enzyme-linked immunosorbent assay (ELISA) was used to determine the concentration of retrovirus p30 capsid protein or lentivirus p24 capsid protein in the supernatant samples collected above. The p30 ELISA was conducted as described by Landázuri and Le Doux [30]. Values for replicate wells without virus were subtracted as background. Values for each point are the average of triplicate wells. Values for each point account for dilution factor and collection sample volume. Results are representative of three independent experiments.

For the p24 ELISA, an HIV-1 p24 Antigen ELISA kit (Zeptometrix Corp., Buffalo, NY, USA) was used according to manufacturer's instructions. The optical density of the

wells at 450 nm (OD_{450}) was measured using an absorbance plate reader. Values for replicate wells without virus were subtracted as background. Optical density of the wells was converted to picograms of p24 using a standard curve. Values for each point account for dilution factor and collection sample volume. Results are the average of three independent experiments done in duplicate.

Confocal microscopy. To quantify the number of virus particles associated with cells over time, R1 mES and NIH 3T3 cells were labeled for imaging by plating them on 0.4% bovine gelatin-coated 12-well glass-bottom tissue culture plates (MatTek Corp., Ashland, MA, USA) at 350,000 and 70,000 cells per well, respectively. Before plating, the glass-bottom plates were first treated with 1 mL per well of 1 N HCl for 15 min, rinsed three times with PBS, rinsed twice with distilled, deionized H_2O and then coated with gelatin. The next day after plating, cells were transduced with 1 mL per well of either *RFP-lacZ* retrovirus or *GFP-lacZ* lentivirus and Polybrene (8 μg per mL) and LIF (10^3 U per mL), and plates were centrifuged for 30 min at 1,100 g at room temperature. Transductions were stopped immediately following centrifugation, 1, 2, 7, and 14 hrs post transduction by placing the plates on ice. After 30 min, the cells were incubated on ice with 1 mL per well of either ConcanavalinA$_{488}$ (green) or ConcanavalinA$_{594}$ (red) (diluted 1:750 in PBS) to stain the cell surface. After 30 min, ConA was removed and cells were rinsed twice with PBS, then fixed with 4% paraformaldehyde (1 mL per well) for 10 min at room temperature. The cells were washed twice with PBS, and then their nuclei were stained with DAPI (300nM in PBS) for 2 min at room temperature. The cells were then washed twice with PBS. All cells were visualized by confocal microscopy (Zeiss LSM 510, 40X oil objectives) and images were captured in z-series. Three random z-series of cells were taken per well, and each time point was done in triplicate wells for each virus for each cell type. 3D projections were created for each z-series and ImageJ software analysis was used to count the number of cell-associated viruses for

two z-series per well and two wells per time point. Results are the average of three independent experiments.

Transduction assays. To measure the level of *lacZ* expression per cell, R1 mES and NIH 3T3 cells were plated in 0.1% porcine gelatin-coated, black/clear bottom 96-well Costar® tissue culture treated assay plates (Fisher Scientific, Pittsburg, PA, USA) at 10,000 and 5,000 cells per well, respectively. The next day, cells were transduced with 100 µL per well of either *RFP-lacZ* retrovirus or *GFP-lacZ* lentivirus mixed with 8 µg per mL of Polybrene and 10^3 U of LIF per mL, and plates were centrifuged for 30 min at 1,100 g at room temperature. The viral supernatants were removed 24 hours later and replaced with fresh medium (200 µL per well). Three days post transduction, the level of *lacZ* expression per cell was evaluated by alamarBlue® and FluoReporter® lacZ/Galactosidase Quantitation Kit assays (Invitrogen Corp., Carlsbad, CA, USA). The day before conducting the assays, cells were replenished with 100 µL per well of fresh medium. To determine the relative number of cells per well, 3 hours prior to conducting the FluoReporter® assay, 25 µL per well of alamarBlue® reagent was added to the cells. After three hours, absorbance values of the reduced alamarBlue® reagent (now red) due to cellular metabolic activity were read at 570 and 600 nm using an absorbance plate reader (VERSAmax; Molecular Devices, Sunnyvale, CA, USA). The percent reduction of alamarBlue® was then calculated according to manufacturer's instructions. Values for each point are the averages of triplicate wells. Results are representative of three independent experiments.

Following the alamarBlue® assay, the levels of β-galactosidase activity per well were evaluated using the FluoReporter® assay. The alamarBlue®-containing medium was removed and the cells washed once with 100 µL of PBS containing 1 mM $MgCl_2$. After removal of the wash solution, 50 µL of lysis buffer (PBS with 1 mM $MgCl_2$ and 0.5% IGEPAL) was added to each well, and the plate incubated at 37ºC. After 30 min, 100 µL

of a 1.1 mM working solution of the 3-carboxy-umbelliferyl β-D-galactopyranoside (CUG) substrate reagent was added to each well, according to manufacturer's instructions, and the plate incubated at room temperature up to 30 min. The reactions were halted by addition of 50 µL per well of stop buffer (1 M Na_2CO_3). The fluorescence of the solution in each well was measured using a fluorescent plate reader (Modulus™ Microplate Reader; Turner Biosystems, Sunnyvale, CA, USA). Values for replicate wells without virus were subtracted as background. To compare plates, a reference standard (provided by kit) was run on each plate. Fluorescence values of the transduced samples were divided by the fluorescence of the reference standard on each individual plate. A standard curve of serially diluted β-galactosidase was also used to determine the actual amount of β-galactosidase in each experimental well. Values for each point are the averages of triplicate wells. Results are representative of three independent experiments.

Determination of relative transgene copy number by real-time PCR. To determine the number of integrated nlacZ transgenes per cell, the genomic DNA of transduced R1 mES and NIH 3T3 cells was extracted 5 days post transduction using the DNeasy® Tissue Kit (Qiagen Inc., Valencia, CA, USA), with RNase (Qiagen Inc., Valencia, CA, USA) treatment of DNA performed prior to lysis. The sequences of the primers (Integrated DNA Technologies, Inc., Coralville, IA, USA) used to amplify the DNA were as follows: nLacZ forward primer 5'-TTCGCTACCTGGAGAGACGC -3' and nLacZ reverse primer 5'-ATTTAGCGAAACCGCCAAGA-3'; genomic GAPDH forward primer 5'-CTCTGGCTCAGAGGGTTTGG-3' and genomic GAPDH reverse primer 5'-ACAGAAACCAGTGGGCTTTGA-3'. Standards for genomic GAPDH and nLacZ transgene were prepared from serially diluted amplicons purified using an E.Z.N.A® Gel Extraction Kit (Omega Bio-tek, Inc., Doraville, GA, USA). All real-time PCR reactions were performed by loading 150 ng of DNA per tube in a 30 µL total volume with SYBR®

Green Master Mix (Applied Biosystems, Inc., Foster City, CA, USA) in a Bio-Rad iCycler (2 min at 50ºC, 10 min at 95ºC, and then 40 cycles of 15 sec at 95°C and 1 min at 60°C). No template control reactions were used to determine the detection limits for each gene. Quantification of the relative number of integrated transgenes was based on the relative standard curve method and expressed as the relative nlacZ copy number normalized to the GAPDH endogenous reference gene with relative copy number in nontransduced control subtracted as background [31, 32]. Values for each point are the average of three independent transduction experiments done in triplicate.

Data analysis. Data are summarized as the mean ± the standard deviation for at least triplicate samples. Statistical analysis was performed with MINITAB® Release 12.23 software (Minitab, Inc., State College, PA, USA) using a one-way analysis of variance (ANOVA) for repeated measurements of the same variable. The Tukey multiple comparison test was used to conduct pairwise comparisons between means. Differences at $p < 0.05$ were considered statistically significant.

4.3 Results

Previously we found that retroviruses integrate significantly fewer genes into the chromosomal DNA of murine embryonic stem (mES) cells than NIH 3T3 mouse fibroblasts. We wanted to examine which steps in the transduction process were restricted in ES cell transduction. To identify the key rate-limiting steps of transduction of ES cells, we quantitatively compared the levels of retrovirus and lentivirus binding, integration, and expression in R1 mES cells to those observed in cells that are easy to transduce: NIH 3T3 murine fibroblasts.

To compare the efficiency of the initial binding steps of transduction in R1 mES and NIH 3T3 cells, we quantified the rate that fluorescently labeled retrovirus (*RFP-lacZ*) and lentivirus (*GFP-lacZ*) particles attach to and are adsorbed by R1 mES and NIH 3T3

cells. We defined as "reversibly-bound" those viruses that were initially associated with the cells but came off when washed with an isotonic buffer. We defined as "irreversibly-bound" those viruses that remained associated with the cells even after these washes. R1 mES and NIH 3T3 cells were incubated with 1 mL per well of either *RFP-lacZ* retrovirus or *GFP-lacZ* lentivirus and 8 μg per mL PB, and immediately centrifuged for 30 min at room temperature to deliver the viruses to the cells as a single cohort. Cells were processed to quantify the levels of virus binding immediately following centrifugation, or 1, 2, and 7 hours after the start of the incubation period.

We wondered if differences in the rate that retroviruses and lentiviruses spontaneously lose their activity (i.e., decay) might differentially affect how many active viruses would ultimately end up bound to the cells in our virus binding assays. We therefore estimated the fraction of viruses that lost their activity during the 30 minute virus binding step. In a previous study, we showed that the half-life of retroviruses is about 7.5 hours at 37°C [30]. To determine if the half-life of lentiviruses were significantly different, we measured the half-life of lentiviruses at 37°C and found that ecotropic pseudotyped lentiviruses had a half-life of 17 ± 1.8 hours and VSV-G pseudotyped lentiviruses had a half-life of 19 ± 0.2 hours (Figure 4.1). Based on these half-lives, we estimate that less than 2% of the lentiviruses and less than 5% of the retroviruses lose their activity during the virus binding step (which is mediated by centrifugation of the virus onto the cells for 30 minutes). We concluded that the number of active viruses that bound to the cells was not significantly affected by differences in the virus decay rates.

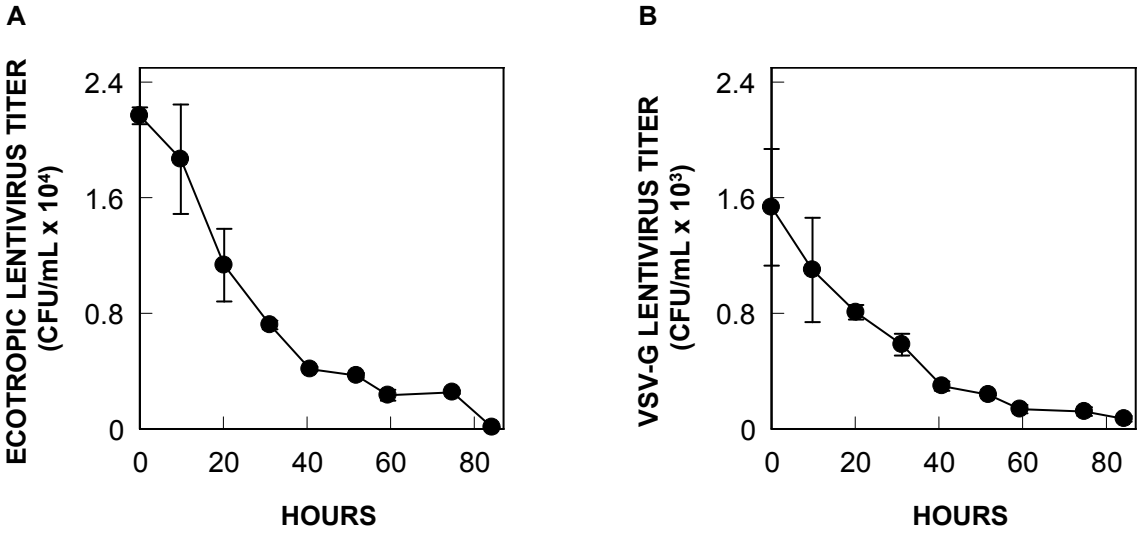

Figure 4.1. The half-lives of ecotropic and VSV-G pseudotyped lentivirus are similar. Stocks of lentivirus (*lacZ*) pseudotyped with either the ecotropic or VSV-G envelope protein were incubated at 37°C for a range of times up to 85 h. Samples were taken at approximately every 10 h, frozen, later thawed and brought to 8 µg/mL PB, and then used to transduce NIH 3T3 cells. Three days later, in the X-gal titer assay, the number of clusters of transduced cells were counted and multiplied by the dilution factor to determine the virus titer. From the decay profiles, the half-life of ecotropic (A) and VSV-G (B) *lacZ* lentivirus was determined. Each point shows the mean ± standard deviation of three replicates.

Following incubation of the viruses with the cells, the virus supernatant was collected and the cells treated with non-enzymatic dissociation buffer to remove reversibly-bound virus particles. Cells were collected from the wells and pelleted by centrifugation to separate them from the dissociation buffer. To determine the amount of irreversibly-bound virus, the pelleted cells were resuspended in lysis buffer. Next, the amount of lentivirus (p24) and retrovirus (p30) capsid proteins present in the virus supernatant, dissociation buffer supernatant, and cell lysates were quantified by ELISA. We found that similar numbers of retroviruses were delivered to both R1 mES and NIH 3T3 cells (Figure 4.2). At one hour post transduction, about 30% of the retrovirus particles in the virus stock were delivered to both R1 mES (Figure 4.2A) and NIH 3T3 (Figure 4.2B) cells and easily removed as reversibly-bound virus. However, we found that up to 4-fold less retrovirus was irreversibly-bound to R1 mES cells than to NIH 3T3 cells (Figure 4.2C). Similarly, at one hour post transduction, 30% or more of the lentivirus particles in the virus stock were delivered to R1 mES (Figure 4.3A) and NIH 3T3 (Figure 4.3B) cells and easily removed as reversibly-bound virus, while about 3-fold fewer lentiviruses irreversibly-bound to R1 mES cells than to NIH 3T3 cells (Figure 4.3C).

As an independent, parallel measure of virus adsorption, we used confocal immunofluorescence microscopy and image analysis software to quantitatively compare the number of cell-associated *RFP-lacZ* retrovirus and *GFP-lacZ* lentivirus particles (either bound or internalized) (Figure 4.4 A and B). R1 mES and NIH 3T3 cells, seeded previously in gelatin-coated glass-bottom plates, were transduced with 1 mL per well of either *RFP-lacZ* retrovirus or *GFP-lacZ* lentivirus and 8 μg per mL PB and immediately centrifuged for 30 min at room temperature to deliver the viruses to the cells as a single cohort. Cells were processed to quantify the levels of virus binding immediately following centrifugation, or 1 or 2 hours after the start of the incubation period. Similar to

the biochemical assays of virus binding, image analysis showed that about 4-fold fewer retroviruses and lentiviruses bound to R1 mES cells than to NIH 3T3 cells (Figure 4.4C and 4.4D).

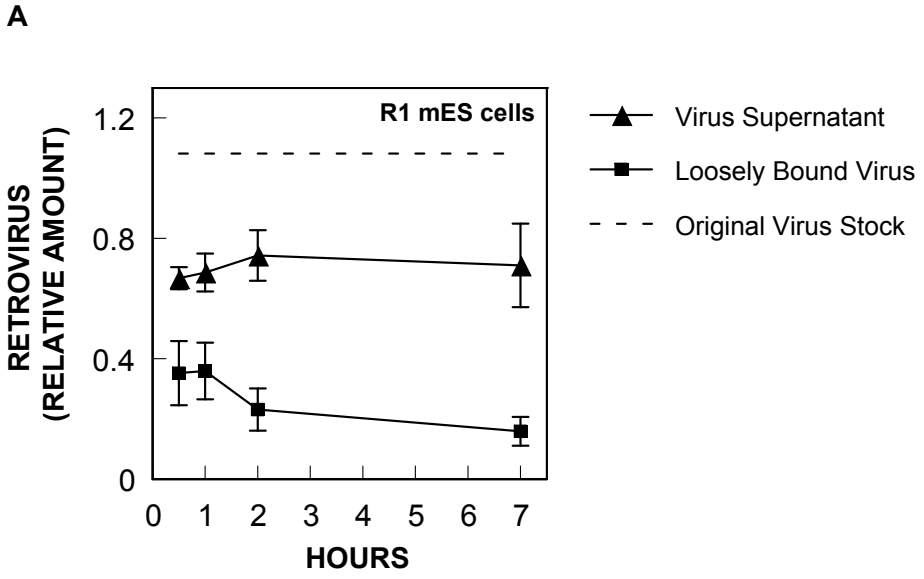

Figure 4.2. Fewer retroviruses bind to R1 mES cells than to NIH 3T3 cells as determined by virus capsid ELISA. *RFP-lacZ* retrovirus stocks were brought to 8 µg/mL PB and then added to R1 mES and NIH 3T3 cells seeded the previous day at 3.5 and 1.0 x 10^5 cells per well, respectively, in gelatin-coated 6-well plates. After addition of the retrovirus stocks to the cells, the tissue culture dishes were centrifuged (30 min, 1100 g, room temperature) and incubated for a range of times (0.5, 1, 2, and 7 h) at 37°C in a humidified tissue culture incubator. At the various times, the retrovirus supernatant was collected from the wells. Cells were washed once with PBS and dislodged from the tissue culture plates with non-enzymatic dissociation buffer. Cell suspensions were then centrifuged and the dissociation buffer supernatant was removed and collected. Cell pellets were resuspended in cell lysis buffer. The retrovirus supernatant, dissociation buffer supernatant, and cell lysate samples were analyzed for retrovirus concentration by p30 ELISA. Values for each point account for dilution factor and collection sample volume. The relative retrovirus in the original virus stock added to wells (- - - -) and in the retrovirus supernatant (▲) and dissociation buffer supernatant (■) are shown for R1 mES cells (A). The relative retrovirus in the original virus stock added to wells (- - - -) and in the retrovirus supernatant (Δ) and dissociation buffer supernatant (□) are shown for NIH 3T3 cells (B). To determine the relative amount of tightly-bound virus (C) in the cell lysates in R1 mES (●)and NIH 3T3 (○) cells at various times, p30 levels were normalized to the levels of p30 in the original virus stock added to wells and to the number of cells per well at the start of the transduction (relative retrovirus number per cell). Each point shows the mean ± standard deviation of three replicates.

B

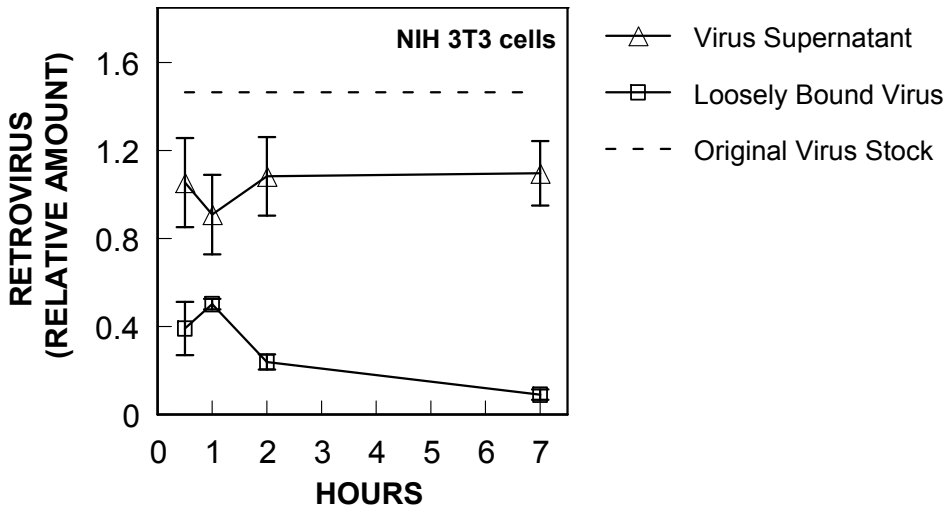

C

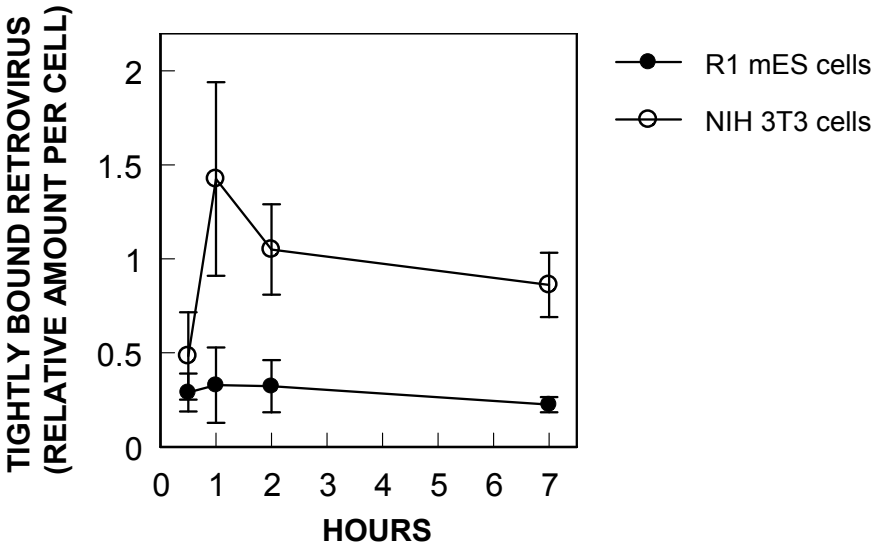

Figure 4.2 continued

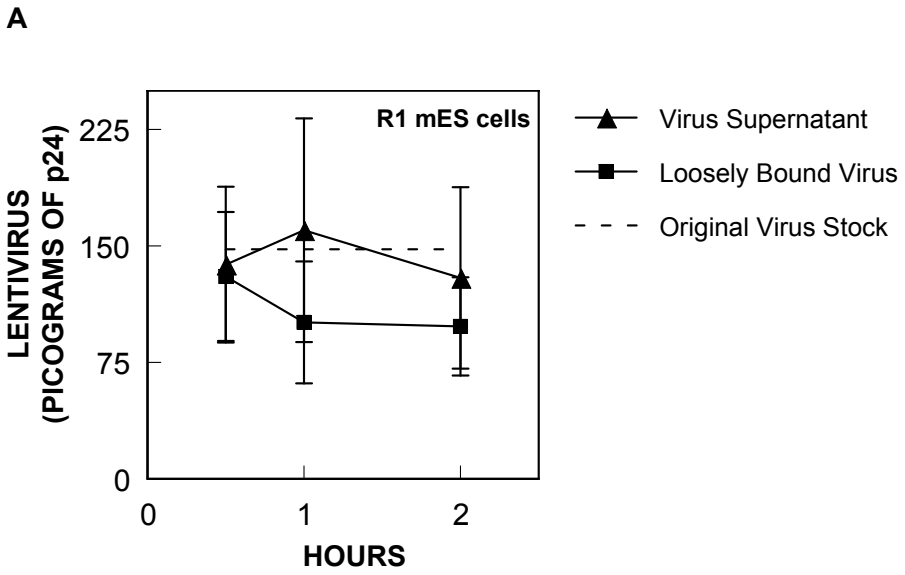

Figure 4.3. Fewer lentiviruses bind to R1 mES cells than to NIH 3T3 cells as determined by virus capsid ELISA. *GFP-lacZ* lentivirus stocks were brought to 8 µg/mL PB and then added to R1 mES and NIH 3T3 cells seeded the previous day at 3.5 and 1.0 x 10^5 cells per well, respectively, in gelatin-coated 6-well plates. After addition of the lentivirus stocks to the cells, the tissue culture dishes were centrifuged (30 min, 1100 g, room temperature) and incubated for a range of times (0.5, 1, and 2 h) at 37°C in a humidified tissue culture incubator. At the various times, the lentivirus supernatant was collected from the wells. Cells were washed once with PBS and dislodged from the tissue culture plates with non-enzymatic dissociation buffer. Cell suspensions were then centrifuged and the dissociation buffer supernatant was removed and collected. Cell pellets were resuspended in cell lysis buffer. The lentivirus supernatant, dissociation buffer supernatant, and cell lysate samples were analyzed for lentivirus concentration by p24 ELISA. Levels of p24 in the original virus stock added to wells (- - - -) and p24 levels in the retrovirus supernatant (▲) and dissociation buffer supernatant (■) are shown for R1 mES cells (A). Levels of p24 in the original virus stock added to wells (- - - -) and p24 levels in the retrovirus supernatant (∆) and dissociation buffer supernatant (□) are shown for NIH 3T3 cells (B). To determine the relative amount of tightly-bound virus (C) in the cell lysates in R1 mES (●) and NIH 3T3 (○) cells at various times, p24 levels were normalized to the number of cells per well at the start of the transduction (lentivirus number per cell). Each point shows the mean ± standard deviation of three independent experiments done in duplicate.

B

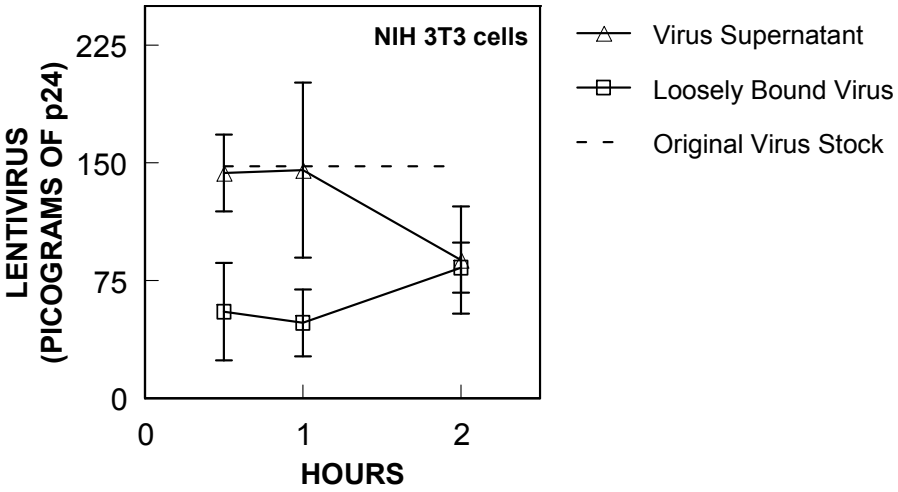

C

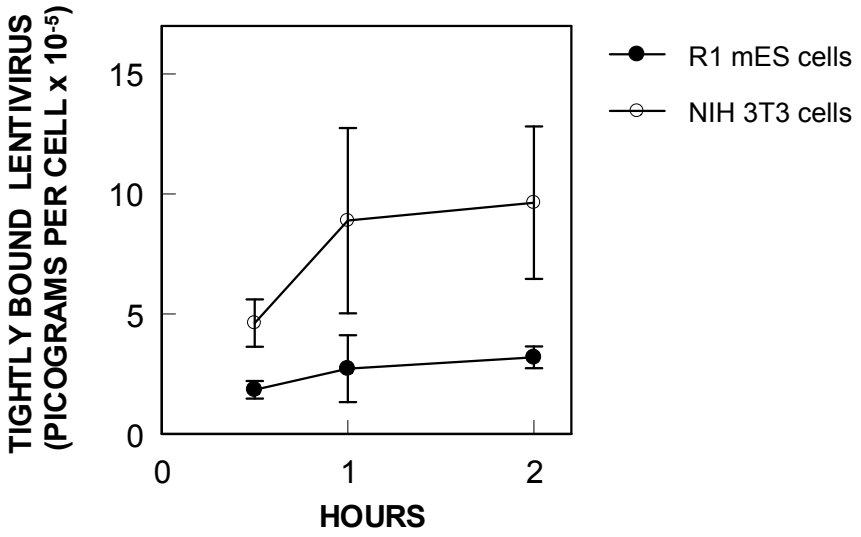

Figure 4.3 continued

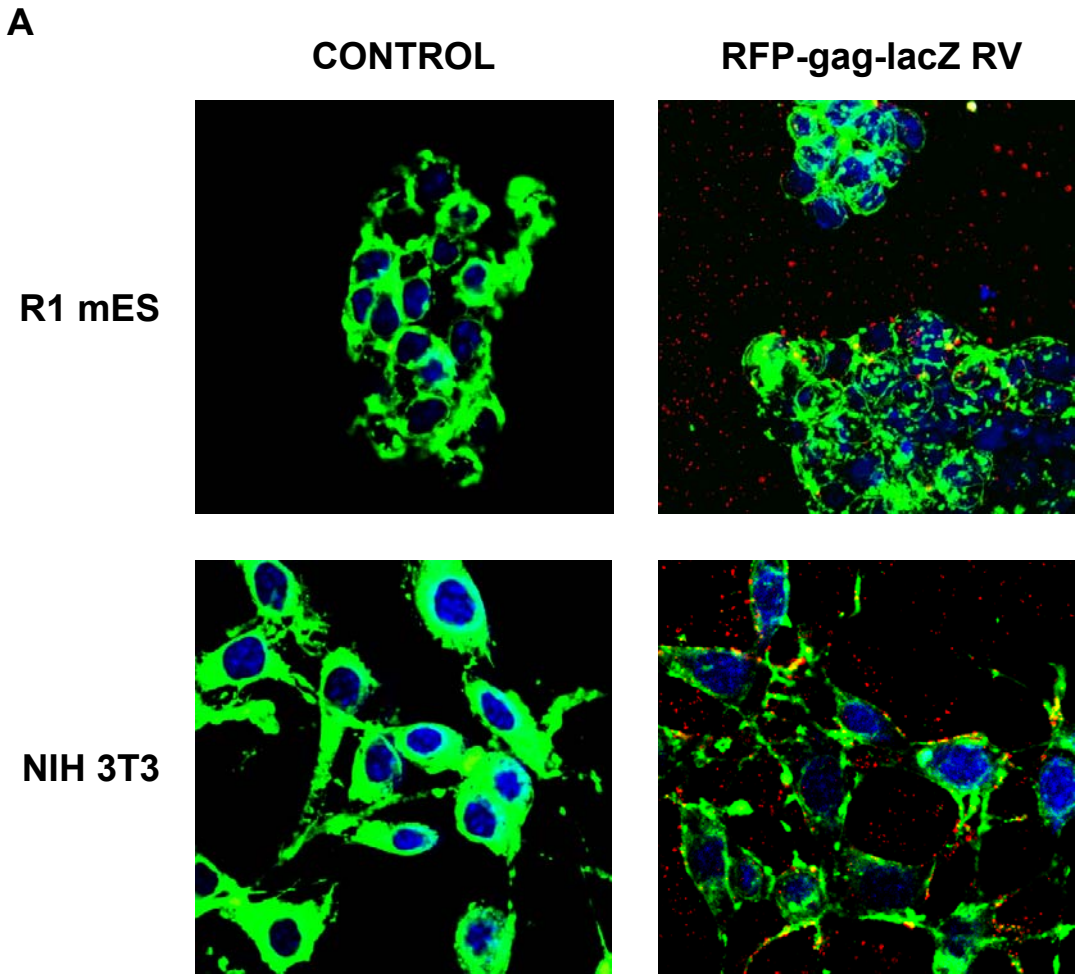

Figure 4.4. Fewer retroviruses and lentiviruses bind to R1 mES than to NIH 3T3 cells as determined by immunofluorescence microscopy. *RFP-lacZ* retrovirus and *GFP-lacZ* lentivirus stocks were brought to 8 μg/mL PB and then added to R1 mES and NIH 3T3 cells seeded the previous day at 3.5 x 10^5 and 7.0 x 10^4 cells per well, respectively, in glass-bottom, gelatin-coated 12-well plates. After addition of the retrovirus and lentivirus stocks to the cells, the glass-bottom tissue culture dishes were centrifuged (30 min, 1100 g, room temperature) and incubated at 37°C for a range of times (0.5, 1, and 2 h). At the various times, cells were removed from 37°C and chilled on ice for 30 min to block endocytosis. Concanavalin-stained cells were fixed and then stained with DAPI to visualize cell nuclei. Cells transduced with RFP-lacZ retrovirus (A) and GFP-lacZ lentivirus (B) were visualized by confocal microscopy. The extent to which the RFP-lacZ retrovirus and GFP-lacZ lentivirus were cell-associated (bound or internalized) with R1 mES (C) and NIH 3T3 (D) cells was quantified using image analysis software (ImageJ). Each point shows the mean ± standard deviation of three replicates.

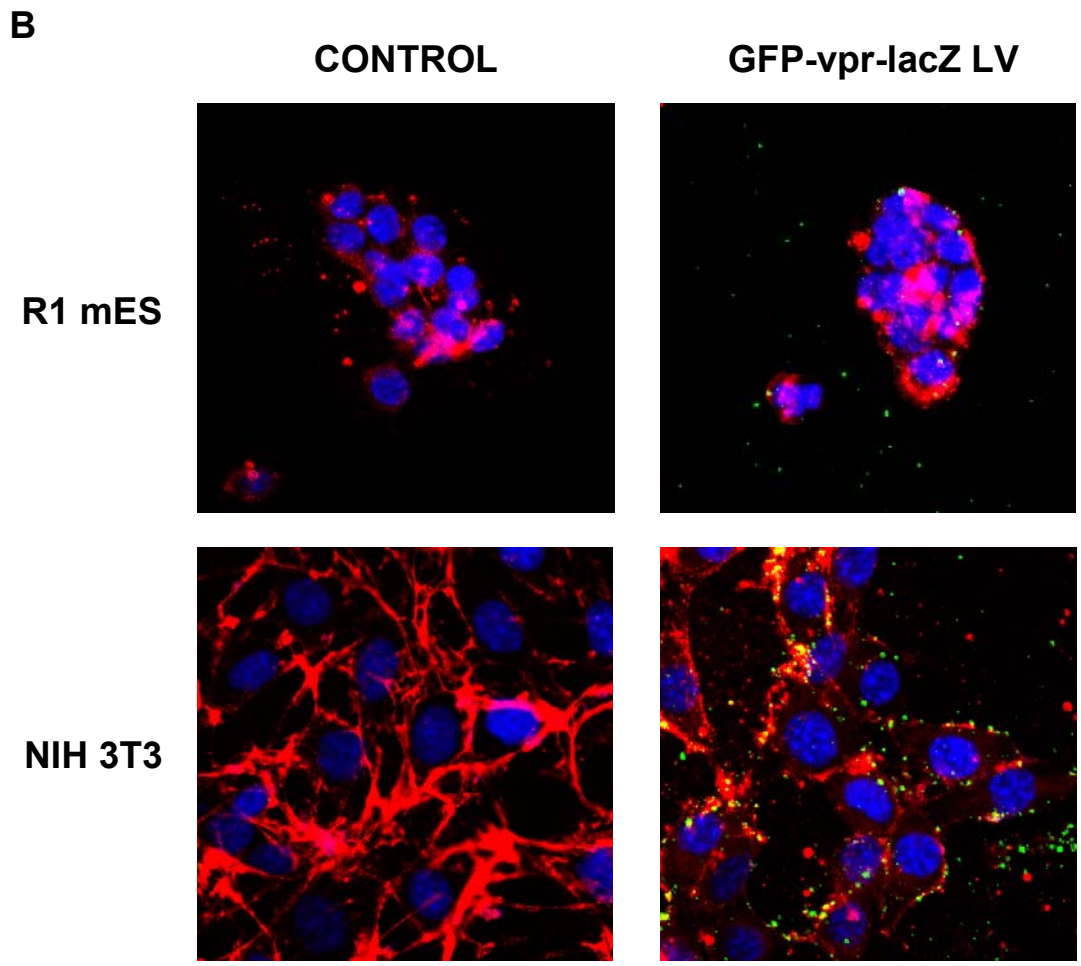

Figure 4.4 continued

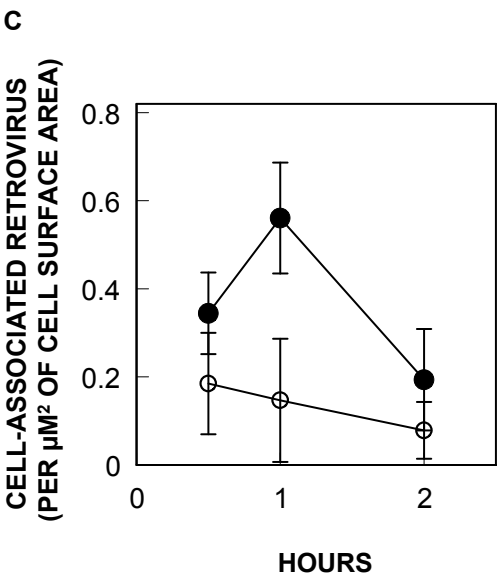

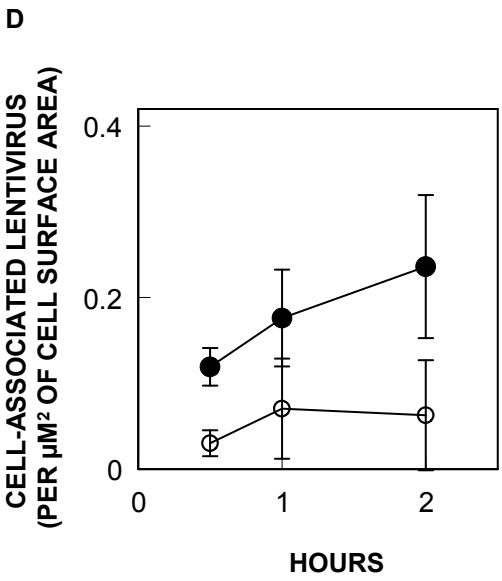

Figure 4.4 continued

To compare the efficiency with which post-binding steps of transduction were completed within R1 mES and NIH 3T3 cells, we quantified the number of retrovirus and lentivirus transgenes that successfully integrated into the chromosomal DNA of the cells. We transduced R1 mES and NIH 3T3 cells with *RFP-lacZ* retrovirus and *GFP-lacZ* lentivirus, and then five days later used real-time PCR to quantify the number of integrated *lacZ* transgenes as referenced to the number of endogenous *GAPDH* genes. We found that about ten-fold fewer lentivirus *lacZ* transgenes and about three-fold fewer retrovirus *lacZ* transgenes integrated into R1 mES cells than in NIH 3T3 cells (Table 4.1).

Next, we wanted to compare the extent to which retrovirus and lentivirus transgenes were expressed in mES cells versus in NIH 3T3 fibroblasts. To measure the efficiency of transgene expression per cell, we plated R1 mES and NIH 3T3 cells in 96-well plates, transduced them with *RFP-lacZ* retrovirus and *GFP-lacZ* lentivirus stocks in the presence of 8 μg/mL PB. Three days later we quantified the levels of β-galactosidase activity in extracts of the cells, and normalized these levels to the number of viable cells. We found that lentivirus and retrovirus transgene expression levels were 8 to 11-fold lower, respectively, in R1 mES cells than in NIH 3T3 cells (Table 4.1).

Taking together our virus binding, integration and transgene expression data, we estimated the efficiency with which retroviruses and lentiviruses completed the major steps in the transduction process in R1 mES cells relative to NIH 3T3 cells (Table 4.2). The relative efficiency of virus binding, virus integration and transgene expression in R1 mES cells, as compared to NIH 3T3 cells, was about 25%, 130%, and 27%, respectively, for retroviruses, and 33%, 30% and 130%, respectively, for lentiviruses.

Table 4.1. R1 mES cells integrate fewer viral transgenes and demonstrate lower transgene expression levels per cell than NIH 3T3 cells.

Virus	Cell Type	Relative Number of Integrated Transgenes [a]	Relative Transgene Expression Per Cell [b]
RFP-lacZ Retrovirus	R1	0.78 ± 0.19 *	122 ± 14 *
	NIH 3T3	2.0 ± 0.63	1400 ± 160
GFP-lacZ Lentivirus	R1	0.17 ± 0.02 †	4.2 ± 1.2 †
	NIH 3T3	1.8 ± 0.22	34.0 ± 0.53

[a] *RFP-lacZ* retrovirus and *GFP-lacZ* lentivirus stocks were brought to 8 µg/mL PB and then added to R1 mES and NIH 3T3 cells seeded the previous day at 1.5 x 105 and 7.0 x 104 cells per well, respectively, in gelatin-coated 12-well plates. After addition of the retrovirus and lentivirus stocks to the cells, the tissue culture dishes were centrifuged (30 min, 1100 g, room temperature), and then cultured at 37°C in a humidified tissue culture incubator. Five days later the chromosomal DNA of R1 mES cells and NIH 3T3 cells was isolated, and real-time PCR was used to quantify the number of integrated lacZ transgenes relative to the number of endogenous GAPDH genes. Each point shows the mean ± standard deviation of three independent experiments.

[b] *RFP-lacZ* retrovirus and *GFP-lacZ* lentivirus stocks were brought to 8 µg/mL PB and then added to R1 mES and NIH 3T3 cells seeded the previous day at 10,000 and 5,000 cells per well, respectively, in gelatin-coated 96-well plates. After addition of the retrovirus and lentivirus stocks to the cells, the tissue culture dishes were centrifuged (30 min, 1100 g, room temperature), and then cultured at 37°C in a humidified tissue culture incubator. Three days later, the retrovirus and lentivirus transgene expression levels and the number of cells per well were quantified using the FluoReporter® lacZ/Galactosidase Quantitation Kit assay and the alamarBlue® assay. Each value shows the mean ± standard deviation of three replicates.

* Statistically significant differences ($P \leq 0.05$) from NIH 3T3 cells transduced with *RFP-lacZ* retrovirus.

† Statistically significant differences ($P \leq 0.05$) from NIH 3T3 cells transduced with *GFP-lacZ* lentivirus.

Table 4.2. Fractional efficiencies with which retroviruses and lentiviruses complete major steps in the transduction process in R1 mES cells relative to NIH 3T3 cells.

Virus	Virus Binding (based on ELISA) *	Virus Integration †	Transgene Expression Per Cell †
RFP-lacZ retrovirus	0.25	1.3	0.27
GFP-lacZ lentivirus	0.33	0.30	1.3

* The efficiency of binding was defined as the ratio of the values for binding based on the ELISA assay in R1 mES cells to the values for binding in NIH 3T3 cells.

† The efficiencies of post binding steps were defined as the ratio of the values in R1 mES cells to values in NIH 3T3 cells multiplied by the reciprocal of the efficiency of the previous step in transduction.

4.4 Discussion

Retroviruses are an excellent tool for genetically modifying cells, but their use for transducing embryonic stem (ES) cells has met with limited success due to low transgene expression levels. Expression levels are low because ES cells employ several mechanisms to efficiently silence integrated retrovirus transgenes. We wondered if other steps of retrovirus transduction, in addition to gene expression, were restricted in ES cells. Using recombinant MLV-derived retrovirus and recombinant HIV-1-derived lentivirus vectors, we compared three major steps in the transduction of R1 mES and NIH 3T3 cells: 1) the number of active virus particles that adsorb to cells in a given time as quantified by ELISAs for virus capsid proteins and by confocal microscopy and image analysis of fluorescently labeled virus particles; 2) the number of integrated transgenes as quantified by real-time PCR; and 3) the corresponding level of gene expression as quantified by the level of enzyme activity in extracts of the transduced cells. We found that 3 to 4-fold fewer retroviruses and lentiviruses bound to R1 mES cells than to NIH 3T3 cells. Interestingly, retroviruses and lentiviruses differed in the efficiency with which they completed post-binding steps of transduction. We detected three-fold fewer integrated retrovirus transgenes, and 11-fold lower expression levels, in R1 mES cells than in NIH 3T3 cells, and 10-fold fewer integrated lentivirus transgenes, and 8-fold lower expression levels, in R1 mES cells than in NIH 3T3 cells. These results suggest that both retroviruses and lentiviruses bind less efficiently to mES cells than to NIH 3T3 cells. In addition, retrovirus transduction appears to be limited by low levels of transgene expression, whereas lentivirus transduction appears to be limited by inefficient post-binding steps of transduction.

Our observation that R1 mES cells bind 3 to 4-fold fewer viruses than NIH 3T3 cells may be due in part to differences in the sizes of the cells. NIH 3T3 cells have previously been reported to have an average radius of about 7 μM, whereas mES cells

appear to be slightly smaller on average, with radii ranging from 4 to 7 μM [33]. Andreadis et al showed that the number of active viruses delivered per cell (A) is a function of the average radius of the cells being transduced and can be estimated from the following relationship:

$$A = 4a_c DC_{vo} l$$

where a_c is the average radius of the target cells, D is the diffusion coefficient of the virus, C_{vo} is the initial concentration of active retrovirus at the start of the infection, and l is an integrated function of time, the diffusion coefficient, the half-life of the virus, and the radius of the target cells [33, 34]. This relationship indicates that differences in cell size can account for about a 2-fold difference in the number of active viruses delivered per cell, which suggests that factors other than differences in cell size may reduce the efficiency of virus binding to mES cells [33, 35].

Interestingly, our data suggests that retroviruses complete post-binding steps of transduction as efficiently in mES cells as in NIH 3T3 cells. This is because the extent to which retrovirus integration was reduced in mES cells (about 3-fold) was similar to the extent to which binding was reduced (about 4-fold), which suggests that once bound, a retrovirus has about the same probability of successfully integrating its genetic material in the chromosomal DNA of mES cells as it would if it were bound to an NIH 3T3 murine fibroblast. In contrast, out data suggests that lentiviruses do not complete post-binding steps of transduction as efficiently in mES as in NIH 3T3 cells. This is because 4-fold fewer lentiviruses bound to mES cells than to NIH 3T3 cells, but 10-fold fewer integrated transgenes were detected in mES cells than in NIH 3T3 cells. This suggests that a lentivirus, once bound to an mES cell, is nearly 3-fold less likely to successfully integrate its genetic material into the chromosomal DNA than if it had bound to an NIH 3T3 cell. It is interesting to consider why lentiviruses, when infecting mES cells, are less likely to

successfully complete the intracellular steps of transduction. Several host cell factors have been identified in other cell types that interfere with intracellular steps of retrovirus or lentivirus transduction. For example, TRIM5α binds to incoming viruses, disrupts their ability to uncoat and to undergo reverse transcription, and marks them for degradation [16]. Another factor, moesin, when overexpressed in host cells, downregulates the formation of stable microtubules which reduces the efficiency of reverse transcription and hinders the movement of the retrovirus pre-integration complexes through the cell [17]. It would be interesting to determine if these, or other currently unidentified mES cell factors, interfere with post-binding steps of lentivirus transduction, and if so, to examine the mechanism by which they do so.

Finally, our data suggests that lentivirus transgenes may be expressed more efficiently in mES cells than retrovirus transgenes. This is because the extent to which lentivirus transgene expression was reduced in mES cells (about 8-fold) was similar to the extent to which the number of integrated transgenes was reduced (about 10-fold), which suggests that once integrated, a lentivirus provirus has about the same probability of being expressed in mES cells as it does in NIH 3T3 fibroblasts. In contrast, the extent to which retrovirus transgene expression was reduced in mES cells (nearly 12-fold) was more significant than the extent to which the number of integrated transgenes was reduced (less than 3-fold), which suggests that once integrated, a retrovirus provirus is at about 4-fold less likely to be expressed in mES cells than in an NIH 3T3 fibroblast.

Taken together, our results suggest that different strategies should be employed to improve retrovirus and lentivirus transduction of mES cells. Retrovirus transduction would benefit most from the development of vectors that are resistant to the mechanisms by which mES cells shutdown gene expression. In contrast, lentivirus transduction would benefit most from the identification of the specific intracellular steps of transduction that are rate-limiting, an understanding of the mechanisms by which

these steps impede transduction, and the development of strategies to improve the efficiency with which these steps are completed.

4.5 Acknowledgements

We thank Todd McDevitt for the R1 mES cell line, Stephen Russell for the ecotropic Env construct, Scott Case for the VSV-G Env construct and the lentivirus packaging construct, Michael Conte for the LacZ retrovirus vector, Walther Mothes for the RFP-Gag construct and Thomas Hope for the GFP-Vpr construct. This work was supported by the Georgia Tech/Emory Center for the Engineering of Living Tissues (NSF Engineering Research Center: EEC-9731643).

4.6 References

[1] F.M. Watt, B.L. Hogan, Out of Eden: stem cells and their niches, Science 287 (2000) 1427-1430.

[2] A.G. Smith, Embryo-derived stem cells: of mice and men, Annu Rev Cell Dev Biol 17 (2001) 435-462.

[3] F. Yates, G.Q. Daley, Progress and prospects: gene transfer into embryonic stem cells, Gene Ther 13 (2006) 1431-1439.

[4] S.Y. Moon, Y.B. Park, D.S. Kim, S.K. Oh, D.W. Kim, Generation, culture, and differentiation of human embryonic stem cells for therapeutic applications, Mol Ther 13 (2006) 5-14.

[5] A.M. Wobus, K.R. Boheler, Embryonic stem cells: prospects for developmental biology and cell therapy, Physiol Rev 85 (2005) 635-678.

[6] C.S. Swindle, H.G. Kim, C.A. Klug, Mutation of CpGs in the murine stem cell virus retroviral vector long terminal repeat represses silencing in embryonic stem cells, J Biol Chem 279 (2004) 34-41.

[7] M. Schuldiner, J. Itskovitz-Eldor, N. Benvenisty, Selective ablation of human embryonic stem cells expressing a "suicide" gene, Stem Cells 21 (2003) 257-265.

[8] J. Ellis, Silencing and variegation of gammaretrovirus and lentivirus vectors, Hum Gene Ther 16 (2005) 1241-1246.

[9] D. Pannell, C.S. Osborne, S. Yao, T. Sukonnik, P. Pasceri, A. Karaiskakis, M. Okano, E. Li, H.D. Lipshitz, J. Ellis, Retrovirus vector silencing is de novo methylase independent and marked by a repressive histone code, Embo J 19 (2000) 5884-5894.

[10] S. Yao, T. Sukonnik, T. Kean, R.R. Bharadwaj, P. Pasceri, J. Ellis, Retrovirus silencing, variegation, extinction, and memory are controlled by a dynamic interplay of multiple epigenetic modifications, Mol Ther 10 (2004) 27-36.

[11] J. Ellis, S. Yao, Retrovirus silencing and vector design: relevance to normal and cancer stem cells?, Curr Gene Ther 5 (2005) 367-373.

[12] A. Pfeifer, M. Ikawa, Y. Dayn, I.M. Verma, Transgenesis by lentiviral vectors: lack of gene silencing in mammalian embryonic stem cells and preimplantation embryos, Proc Natl Acad Sci U S A 99 (2002) 2140-2145.

[13] J.M. Chilton, J.M. Le Doux, Complexation of retroviruses with polymers significantly increases the number of genes transferred to murine embryonic stem cells but does not raise transgene expression levels, Biotechnol Appl Biochem (2008).

[14] U. Chatterji, M.D. Bobardt, P. Gaskill, D. Sheeter, H. Fox, P.A. Gallay, Trim5alpha accelerates degradation of cytosolic capsid associated with productive HIV-1 entry, J Biol Chem 281 (2006) 37025-37033.

[15] H.L. Liu, Y.Q. Wang, C.H. Liao, Y.Q. Kuang, Y.T. Zheng, B. Su, Adaptive evolution of primate TRIM5alpha, a gene restricting HIV-1 infection, Gene 362 (2005) 109-116.

[16] S.P. Goff, Genetic control of retrovirus susceptibility in mammalian cells, Annu Rev Genet 38 (2004) 61-85.

[17] J. Haedicke, K. de Los Santos, S.P. Goff, M.H. Naghavi, The Ezrin-radixin-moesin family member ezrin regulates stable microtubule formation and retroviral infection, J Virol 82 (2008) 4665-4670.

[18] S. Best, P. Le Tissier, G. Towers, J.P. Stoye, Positional cloning of the mouse retrovirus restriction gene Fv1, Nature 382 (1996) 826-829.

[19] K.N. Bishop, M. Bock, G. Towers, J.P. Stoye, Identification of the regions of Fv1 necessary for murine leukemia virus restriction, J Virol 75 (2001) 5182-5188.

[20] H. Harlow, D. Lane, Antibodies: A laboratory manual., Cold Spring Harbor Laboratory Press, Cold Spring Harbor, 1998.

[21] S.S. Case, M.A. Price, C.T. Jordan, X.J. Yu, L. Wang, G. Bauer, D.L. Haas, D. Xu, R. Stripecke, L. Naldini, D.B. Kohn, G.M. Crooks, Stable transduction of quiescent CD34(+)CD38(-) human hematopoietic cells by HIV-1-based lentiviral vectors, Proc Natl Acad Sci U S A 96 (1999) 2988-2993.

[22] L. Naldini, U. Blomer, P. Gallay, D. Ory, R. Mulligan, F.H. Gage, I.M. Verma, D. Trono, In vivo gene delivery and stable transduction of nondividing cells by a lentiviral vector, Science 272 (1996) 263-267.

[23] F.L. Cosset, Y. Takeuchi, J.L. Battini, R.A. Weiss, M.K. Collins, High-titer packaging cells producing recombinant retroviruses resistant to human serum, J Virol 69 (1995) 7430-7436.

[24] N.M. Sherer, M.J. Lehmann, L.F. Jimenez-Soto, A. Ingmundson, S.M. Horner, G. Cicchetti, P.G. Allen, M. Pypaert, J.M. Cunningham, W. Mothes, Visualization of retroviral replication in living cells reveals budding into multivesicular bodies, Traffic 4 (2003) 785-801.

[25] D. McDonald, M.A. Vodicka, G. Lucero, T.M. Svitkina, G.G. Borisy, M. Emerman, T.J. Hope, Visualization of the intracellular behavior of HIV in living cells, J Cell Biol 159 (2002) 441-452.

[26] Retroviral Gene Transfer and Expression User Manual, Clontech Laboratories, Inc., Mountain View, 2006.

[27] B. Palsson, S. Andreadis, The physico-chemical factors that govern retrovirus-mediated gene transfer, Exp Hematol 25 (1997) 94-102.

[28] J.M. Le Doux, H.E. Davis, J.R. Morgan, M.L. Yarmush, Kinetics of retrovirus production and decay, Biotechnol Bioeng 63 (1999) 654-662.

[29] J. Price, D. Turner, C. Cepko, Lineage analysis in the vertebrate nervous system by retrovirus-mediated gene transfer, Proc Natl Acad Sci U S A 84 (1987) 156-160.

[30] N. Landazuri, J.M. Le Doux, Complexation of retroviruses with charged polymers enhances gene transfer by increasing the rate that viruses are delivered to cells, J Gene Med 6 (2004) 1304-1319.

[31] L. Sastry, T. Johnson, M.J. Hobson, B. Smucker, K. Cornetta, Titering lentiviral vectors: comparison of DNA, RNA and marker expression methods, Gene Ther 9 (2002) 1155-1162.

[32] Relative Quantitation Of Gene Expression: ABI PRISM 7700 Sequence Detection System: User Bulletin #2: Rev B Applied Biosystems, Inc., Foster City, 1997

[33] S. Andreadis, T. Lavery, H.E. Davis, J.M. Le Doux, M.L. Yarmush, J.R. Morgan, Toward a more accurate quantitation of the activity of recombinant retroviruses: alternatives to titer and multiplicity of infection, J Virol 74 (2000) 3431-3439.

[34] S.T. Andreadis, J.R. Morgan, Quantitative measurement of the concentration of active recombinant retrovirus, Methods Mol Med 69 (2002) 161-172.

[35] Q. Zhou, A. Jouneau, V. Brochard, P. Adenot, J.P. Renard, Developmental potential of mouse embryos reconstructed from metaphase embryonic stem cell nuclei, Biol Reprod 65 (2001) 412-419.

CHAPTER 5

DEPLETION OF HISTONE H1 IN MURINE EMBYRONIC STEM CELLS AND TREATMENT WITH CYCLOSPORIN A DURING TRANSDUCTION DOES NOT IMPROVE GENE TRANSFER

5.1 Introduction

Before the full potential of embryonic stem (ES) cells in regenerative medicine can be realized, techniques to genetically modify them must be improved. Retroviral gene transfer to ES cells is particularly susceptible to gene silencing of integrated transgenes. One of the most commonly proposed mechanisms for silencing of retroviral vectors in stems cells is histone modification [1]. Silenced retroviral transgenes are marked by a repressive histone code characterized by deacetylation of histones H3 and H4 and the recruitment of linker histone H1 [2, 3].

In particular, linker histone H1 plays a dynamic role in maintaining higher order chromatin structure, spacing nucleosomes on the chromatin fiber [4-6]. Linker histone H1 associates with the nucleosome at the DNA entry/exit points [4] and facilitates the folding of nucleosomes into compact structures [7-10]. H1 is thought to prevent unwinding of the DNA and directly results in condensed or “silent” chromatin, usually acting as a transcriptional repressor in gene expression regulation [11]. Previously, Yao et al found that silent retrovirus chromatin following infection was established with an 8.4-fold hypoacetylation of histone H3 and 3.8-fold increase in linker histone H1 [1].

We therefore hypothesized that reduction in expression of histone 1 may alleviate silencing of retrovirus transgenes. To study the role of H1 in retroviral gene transfer, we transduced histone H1c, H1d, H1e triple null mouse embryonic stem cells with three different recombinant vectors – murine embryonic stem cell retrovirus (MSCV), and SIV and HIV-1 derived lentiviruses [12, 13].

5.2 Materials And Methods

Chemicals. Gluteraldehyde, 1,5-dimethyl-1,5-diazaundecamethylene polymethobromide (Polybrene, PB), and gelatin from porcine skin (Type A) were from Sigma Chemical Co. (St. Louis, MO, USA)

Plasmids. The expression plasmids encoding the were from Trent Spencer. The expression plasmid encoding the VSV-G (pMD.G) [14, 15] envelope protein was from Scott Case. The murine stem cell virus retroviral vector (pMSCV-IRES-eGFP) was from Catherine Verfaillie [16, 17]. The lentiviral packaging construct (pCMVΔR8.91) was from Scott Case [14]. The lacZ lentiviral vector (pTY-EFeGFP) was purchased from NIH AIDS Research and Reference Reagent Program (Bethesda, MD, USA). The SIV transfer vector (pCL20cSLFR), the SIV packaging construct (pCAG-SIVgprre), the SIV rev/tat plasmid (pCAG4-RTR-SIV), and a VSV-G envelope protein construct (pCAGGS-VSVG) were all from Trent Spencer.

Cell culture. NIH 3T3 mouse fibroblasts, were cultured in Dulbecco's modified Eagle's medium (DMEM; Mediatech, Inc., Herndon, VA, USA) with 10% bovine calf serum (BCS; Hyclone Labs, Inc., Logan, UT, USA), and 100 U of penicillin and 100 µg of streptomycin (Hyclone Labs, Inc., Logan, UT, USA) per mL. The packaging cell line GP2-293 was cultured on collagen-coated plates (BD Biosciences Discovery Labware, Bedford, MA, USA) in DMEM (Mediatech, Inc., Herndon, VA, USA) with 10% fetal bovine serum (FBS; Hyclone Labs, Inc., Logan, UT, USA) and 100 U of penicillin and 100 µg of streptomycin per mL. The packaging cell line 293T was cultured in DMEM (Mediatech, Inc., Herndon, VA, USA) with 10% fetal bovine serum (FBS; Hyclone Labs, Inc., Logan, UT, USA) and 100 U of penicillin and 100 µg of streptomycin per mL. Undifferentiated D3 murine embryonic stem (mES) cells, obtained from ATCC, and undifferentiated F4 (wild-type) and F6 (H1c/H1d/H1e null) mES cells, a kind gift from Yuhong Fan (Georgia Tech), were cultured on 0.1% porcine gelatin-coated tissue culture flasks and plated in

ES Complete Medium (ES-DMEM; ATCC, Manassas, VA, USA) supplemented with 4mM L-glutamine (Invitrogen Corp., Carlsbad, CA, USA), 150 M β-mercaptoethanol (Sigma Chemical Co., St. Louis, MO, USA), 10% heat-inactivated fetal (ES Cell-Qualified FBS; Invitrogen Corp., Carlsbad, CA, USA), 1% MEM non-essential amino acids (Invitrogen Corp., Carlsbad, CA, USA), 100 U of penicillin and 100 µg of streptomycin (Invitrogen Corp., Carlsbad, CA, USA) per mL, and 10^3 U of leukemia inhibitory factor (LIF; Chemicon International Inc., Ternecula, CA, USA) per mL.

Production of recombinant retroviruses. To generate stocks of MSCV-eGFP retrovirus, GP2-293 cells, a HEK 293-based packaging cell line that stably expresses the retroviral *gag* and *pol* genes (Clontech Laboratories, Inc., Mountain View, CA, USA) [18], were plated in 0.01% poly-L-lysine-coated T175 flasks ($12.5x10^6$ cells) in DMEM that contained heat inactivated FBS (10%) but no antibiotics. The next day, Lipofectamine™ 2000 (Invitrogen Corp., Carlsbad, CA, USA) was used according to the manufacturer's recommendations to cotransfect the cells with 36 µg each of 2 plasmids: the VSV-G envelope glycoprotein expression plasmid (pMD.G) and the retrovirus vector pMSCV-IRES-eGFP. Six hours after transfection, the medium was replaced with fresh 30 mL DMEM/FBS with antibiotics and again at 36 hours after transfection. Virus-laden tissue culture medium was harvested every 12 hours at 48, 60, 72, and 84 hours post-transfection, filter-sterilized (0.45 µm), combined, aliquotted and then frozen (-80ºC) for later use. To generate stocks of HIV-1-eGFP lentivirus, we followed the same procedure to cotransfect 293T cells, except with 24 µg each of 3 plasmids: the VSV-G envelope glycoprotein expression plasmid (pMD.G), the lentivirus packaging construct pCMVΔR8.91 and the lentivirus vector pTY-EFeGFP. To generate stocks of SIV-eGFP lentivirus, we followed the same procedure to cotransfect 293T cells, except with 4 plasmids: 30 µg of the SIV transfer vector (pCL20cSLFR), 18 µg of the SIV packaging

construct (pCAG-SIVgprre), 6 µg of the the SIV rev/tat plasmid (pCAG4-RTR-SIV), and 6 µg of the VSV-G envelope glycoprotein expression plasmid (pCAGGS-VSVG).

Diluted titer assay. To determine virus titer, ten-fold serial dilutions of MSCV-eGFP virus stock (from 48 hr harvests) were made in ES Complete Medium and Polybrene (8µg per mL). Serially diluted virus (1 mL per dish) was used to transduce D3 and R1 mES and NIH 3T3 cells that had been seeded at 3.5 x 10^5 and 1.5 x 10^5 cells per dish, respectively, in 35 mm gridded (2 mm) dishes (Nalge Nunc International, Rochester, NY, USA). The viral supernatants were removed 24 hours later and replaced with fresh medium. Three days post transduction, the number of clusters of eGFP+ mES and NIH 3T3 cells (typically in clusters of 2, 4, 8, or 16 green cells) were counted with the aid of an inverted epifluorescence microscope (IX-50; Olympus America, Inc., Melville, NY, USA), and multiplied by the dilution factor to determine the titer (i.e., the number of eGFP+ colony forming units (CFU) per mL). Results are representative of three independent experiments.

Transduction with viral vectors. To evaluate gene transfer, D3, F4, and F6 mES and NIH 3T3 cells were plated at 3.5 x 10^5 and 1.5 x 10^5 cells per well, respectively, in gelatinized 6-well tissue culture plates. The next day, 8 µg per mL of cationic polymer Polybrene (PB) was added to VSV-G MSCV-eGFP, VSV-G SIV-eGFP, and VSV-G HIV-1-eGFP virus stocks and mixed by vortexing. Cells were transduced with 1 mL of virus per well, and plates were centrifuged for 30 min at 1,100 g at room temperature. The viral supernatants were removed 24 hours later and replaced with fresh medium. Three days later the level of gene transfer was evaluated by fluorescence microscopy, flow cytometry, and real-time PCR.

Fluorescence microscopy. Three days after transduction, epifluorescent and phase contrast images (10X) of D3 mES cells were taken with an inverted

epifluorescence microscope (IX-50; Olympus America, Inc., Melville, NY, USA). Images represent three independent experiments.

Flow cytometry. The percentage of eGFP+ cells in transduced D3 and R1 mES cells was determined 3 days post transduction via flow cytometry using a BD LSR analyzer (BD Biosciences, San Jose, CA, USA). Nontransduced control and transduced cells were trypsinized, pelleted, washed, and resuspended in 1X PBS plus 10% FBS to achieve a single-cell suspension. Thirty thousand events were collected per sample. Nontransduced cells served as negative controls and were used to monitor autofluorescence and set fluorescence thresholds. Viable cells were gated using forward and side scatter properties. Results are representative of three independent experiments.

Determination of relative transgene copy number by real-time PCR. To determine the number of integrated eGFP transgenes per cell, the genomic DNA of transduced D3 mES cells was extracted 5 days post transduction using the DNeasy® Tissue Kit (Qiagen Inc., Valencia, CA, USA), with RNase (Qiagen Inc., Valencia, CA, USA) treatment of DNA performed prior to lysis. The sequences of the primers (Integrated DNA Technologies, Inc., Coralville, IA, USA) used to amplify the DNA were as follows: eGFP forward primer 5'-AGCAAAGACCCCAACGAGAA-3' and eGFP reverse primer 5'-GGCGGCGGTCACGAA-3'; genomic GAPDH forward primer 5'-CTCTGGCTCAGAGGGTTTGG-3' and genomic GAPDH reverse primer 5'-ACAGAAACCAGTGGGCTTTGA-3'. Standards for genomic GAPDH and eGFP transgene were prepared from serially diluted amplicons purified using an E.Z.N.A® Gel Extraction Kit (Omega Bio-tek, Inc., Doraville, GA, USA). All real-time PCR reactions were performed by loading 150 ng of DNA per tube in a 30 µL total volume with SYBR® Green Master Mix (Applied Biosystems, Inc., Foster City, CA, USA) in an ABI PRISM™ 7700 Sequence Detector (2 min at 50ºC, 10 min at 95ºC, and then 40 cycles of 15 sec at

95°C and 1 min at 60°C). No template control reactions were used to determine the detection limits for each gene. Quantification of the relative number of integrated transgenes was based on the relative standard curve method and expressed as the relative eGFP copy number normalized to the GAPDH endogenous reference gene [19, 20]. Results are the average of three independent experiments.

5.3 Results

Given the relative ineffectiveness of retroviral gene transfer to embryonic stem (ES) cells due to silencing, we wondered if silencing could be ameliorated in mES cells triple null for linker histone H1 and how retroviral gene transfer would then compare to two other commonly used lentiviral vectors.

We first wanted to characterize our virus stocks by measuring their titer on murine NIH 3T3 fibroblasts. We found that our MSCV-eGFP retrovirus stocks had the highest titer, about 4-fold higher than SIV-eGFP lentivirus and 100-fold higher than HIV-eGFP lentivirus stocks (Table 5.1).

We next evaluated how many transgenes our virus stocks delivered to undifferentiated ES cells. We transduced D3 mES cells with our three different virus stocks with 8 μg/mL of Polybrene (PB) added and 5 days later used real-time PCR to quantify the number of eGFP transgenes. We found that the relative number of genes transferred to D3 mES cells by each virus corresponded well with the titer found on NIH 3T3 cells (Table 5.1). However, the intensity of fluorescence within individual cells (Figure 5.1) was not indicative of the number of transgenes integrated. MSCV-eGFP retrovirus had the highest titer and delivered more transgenes to D3 mES cells. However, D3 mES cells transduced with MSCV-eGFP demonstrated a lower intensity of fluorescence in individual cells than D3 mES cells transduced with either HIV-1-eGFP

and SIV-eGFP lentiviruses, suggesting a degree of silencing of the integrated retroviral transgenes using the MSCV-eGFP retroviral vector.

Table 5.1 Titers of virus stocks and transgenes delivered

Virus Stock	Colony-forming units per mL (*CFU/mL*) in NIH 3T3 cells[a]	Relative Integrated eGFP Transgenes in D3 mES cells ($\times 10^{-1}$)[b]
MSCV-eGFP	4.1 ± 0.01 ($\times 10^5$)	6.2 ± 0.5
SIV-eGFP	9.2 ± 0.19 ($\times 10^4$)	3.1 ± 0.48
HIV-1-eGFP	4.1 ± 0.16 ($\times 10^3$)	0.057 ± 0.0078

[a] NIH 3T3 cells, plated (70,000 cells/well) the previous day in 12-well tissue culture plates, were transduced with stocks of VSV-G pseudotyped MSCV-eGFP retrovirus, SIV-eGFP lentivirus, or HIV-1-eGFP lentivirus that had been serially diluted in fresh medium and brought to 8 μg/mL Polybrene (PB). Three days later, the number of clusters of transduced cells (eGFP+) was counted by epifluorescence microscopy and multiplied by the dilution factor to determine the virus titer. Each value is the mean ± standard deviation of three replicates.

b Virus stocks with 8 μg/mL Polybrene (PB) added were used to transduce gelatinized 6-well tissue culture plates that had been seeded the previous day with D3 mES cells (350,000 per well) . Cells were centrifuged (1,100 g, 30 min, 25°C), and then cultured at 37°C in a humidified tissue culture incubator. Five days later the chromosomal DNA of D3 (●), R1 (○), and NIH 3T3 cells (▲) was isolated, and real-time PCR was used to quantify the number of integrated eGFP transgenes relative to the number of endogenous GAPDH genes. Each point represents the mean ± standard deviation of three independent experiments.

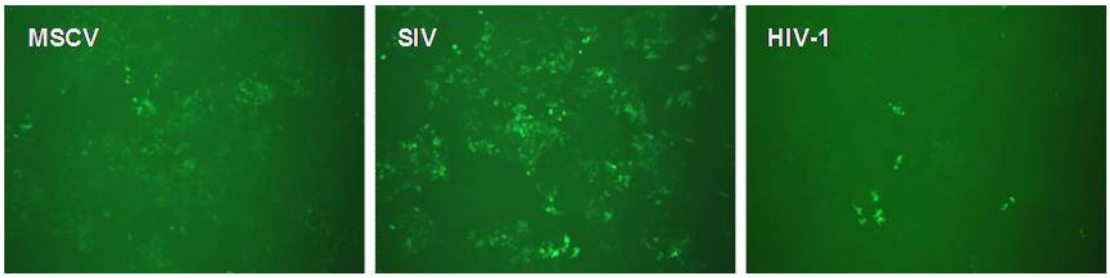

Figure 5.1. Transduction of D3 mES cells with SIV-eGFP lentivirus and HIV-1-eGFP lentivirus shows higher transgene expression per individual cell than with MSCV-eGFP retrovirus. Retrovirus and lentivirus stocks, with 8 μg/mL PB added, were used to transduce D3 mES cells seeded the previous day (350,000 cells per well) in gelatinized 6-well tissue culture plates. Cells were centrifuged (1,100 g, 30 min, 25°C) and then cultured at 37°C in a humidified tissue culture incubator. Three days later the cells were visualized by epifluorescence microscopy.

To determine the effects of H1 in viral gene transfer, we next transduced F6 mES cells null for three H1 genes – H1c, H1d,H1e – which have 50% of the normal level of H1, along with wild-type F4 mES cells of the same cell line. Three days following transduction, we evaluated the number of eGFP+ cells by flow cytometry. Interestingly, we found that triple null F6 mES cells did not improve viral gene transfer and had about a 2-fold reduction in the number of eGFP+ cells for all three viruses in comparison to wild-type F4 mES cells.

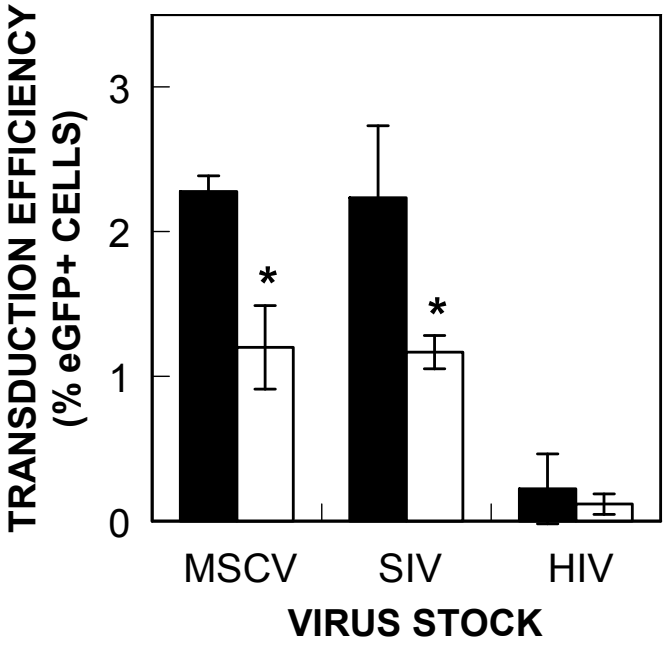

Figure 5.2. Triple null F6 mES cells have 2-fold fewer eGFP+ cells than wild-type F4 mES cells when transduced with all three virus stocks. Retrovirus and lentivirus stocks, with 8 μg/mL PB added, were used to transduce F4 (black bars) and F6 (white bars) mES cells seeded the previous day (350,000 cells per well) in gelatinized 6-well tissue culture plates. Cells were centrifuged (1,100 g, 30 min, 25°C) and then cultured at 37°C in a humidified tissue culture incubator. Three days later, the number of eGFP+ cells was determined by flow cytometry. Values represent the mean ± standard deviation of triplicate measurements. Statistically significant differences ($P \leq 0.05$) from transduction efficiency in wild-type F4 mES cells are denoted with an asterisk.

5.4 Discussion

Most strategies to reduce silencing of retroviral transgenes involve improving retroviral vector design. In an alternative strategy, we decided to determine if gene transfer to murine embryonic stem (mES) cells could be improved by depletion of the linker histone H1, which has been implicated in retrovirus silencing. We compared three different commonly used viral vectors – MSCV, SIV, and HIV-1 – in mES cells. The number of virus integrated transgenes correlated well with titers for our three different

virus stocks. We transduced triple null F6 mES cells and wild-type F4 mES cells with the three different viruses and found that transduced triple null F6 mES cells showed a 2-fold reduction in the number of eGFP+ cells for all three viruses in comparison to F4 wild-type mES cells.

The observation that triple null F6 mES cells had about a 2-fold reduction in the number of eGFP+ cells following transduction with all three viruses in comparison to wild-type F4 mES cells may offer interesting implications for understanding virus integration patterns. Retroviruses were originally thought to integrate randomly, but recent studies have challenged this notion. Studies have now shown that murine leukemia virus (MLV)-derived retroviral vectors prefer to integrate at transcription start sites, and lentiviral vectors derived from simian immunodeficiency virus (SIV) and human immunodeficiency virus type 1 (HIV-1) target integration within transcription units and gene-dense regions of the genome [21]. More specifically, Beard et al found that MLV-derived and HIV-derived vectors integrated near genes involved in growth and survival [22].

Fan et al, who derived the triple null mES cells, found that depletion of H1 in the triple null mES cells lead to highly specific changes in gene expression in comparison to wild-type mES cells. Thirty-eight genes were upregulated and 10 genes were downregulated 2-fold or more ($p \leq 0.05$) in triple null mES cells in comparison to wild-type mES cells [13]. The genes that were downregulated include: IGF-II, insulin receptor substrate-2 (Irs2), H2B histone family member S (H2bfs), cytoplasmic beta-actin, zinc finger protein regulator of apoptosis and cell cycle arrest (Zac1), proliferin, neural precursor cell expressed developmentally downregulated Nedd9 (Nedd9), Vanin-1, BCL-6, and desmocollin type 2 (DSC2) [13]. Several of these genes are involved in controlling cell growth and survival. Taken together with the 2-fold reduction in the number of eGFP+ cells in triple null F6 mES cells that we observed, it is possible that

our viral vectors targeted these down-regulated genes for integration. Viral vectors targeting these genes for integration may not have been effectively expressed, leading to a drop in the number of eGFP+ cells.

If so, we have identified several candidate genes that are readily targeted by retroviral and lentiviral vectors for integration in undifferentiated mES cells. Further work analyzing the genomic motifs or cellular proteins associated with these and similar genes is then warranted in order to design viral vectors capable of directed integration for specific clinical applications.

5.5 Acknowledgements

We thank Yuhong Fan for the F4 wild-type and F6 mES cell lines and assistance, Scott Case for the VSV-G Env construct, Trent Spencer for the four SIV constructs and Catherine Verfaillie for the MSCV retroviral vector. This work was supported by the Georgia Tech/Emory Center for the Engineering of Living Tissues (NSF Engineering Research Center: EEC-9731643).

5.6 References

[1] S. Yao, T. Sukonnik, T. Kean, R.R. Bharadwaj, P. Pasceri, J. Ellis, Retrovirus silencing, variegation, extinction, and memory are controlled by a dynamic interplay of multiple epigenetic modifications, Mol Ther 10 (2004) 27-36.

[2] D. Pannell, C.S. Osborne, S. Yao, T. Sukonnik, P. Pasceri, A. Karaiskakis, M. Okano, E. Li, H.D. Lipshitz, J. Ellis, Retrovirus vector silencing is de novo methylase independent and marked by a repressive histone code, Embo J 19 (2000) 5884-5894.

[3] I. Lemasson, N.J. Polakowski, P.J. Laybourn, J.K. Nyborg, Transcription factor binding and histone modifications on the integrated proviral promoter in human T-cell leukemia virus-I-infected T-cells, J Biol Chem 277 (2002) 49459-49465.

[4] A. Izzo, K. Kamieniarz, R. Schneider, The histone H1 family: specific members, specific functions?, Biol Chem (2008).

[5] R. Schneider, R. Grosschedl, Dynamics and interplay of nuclear architecture, genome organization, and gene expression, Genes Dev 21 (2007) 3027-3043.

[6] E. Meshorer, D. Yellajoshula, E. George, P.J. Scambler, D.T. Brown, T. Misteli, Hyperdynamic plasticity of chromatin proteins in pluripotent embryonic stem cells, Dev Cell 10 (2006) 105-116.

[7] P.T. Georgel, J.C. Hansen, Linker histone function in chromatin: dual mechanisms of action, Biochem Cell Biol 79 (2001) 313-316.

[8] V. Ramakrishnan, The histone fold: evolutionary questions, Proc Natl Acad Sci U S A 92 (1995) 11328-11330.

[9] V. Ramakrishnan, Histone H1 and chromatin higher-order structure, Crit Rev Eukaryot Gene Expr 7 (1997) 215-230.

[10] V. Ramakrishnan, Histone structure and the organization of the nucleosome, Annu Rev Biophys Biomol Struct 26 (1997) 83-112.

[11] P.J. Laybourn, J.T. Kadonaga, Role of nucleosomal cores and histone H1 in regulation of transcription by RNA polymerase II, Science 254 (1991) 238-245.

[12] Y. Fan, T. Nikitina, E.M. Morin-Kensicki, J. Zhao, T.R. Magnuson, C.L. Woodcock, A.I. Skoultchi, H1 linker histones are essential for mouse development and affect nucleosome spacing in vivo, Mol Cell Biol 23 (2003) 4559-4572.

[13] Y. Fan, T. Nikitina, J. Zhao, T.J. Fleury, R. Bhattacharyya, E.E. Bouhassira, A. Stein, C.L. Woodcock, A.I. Skoultchi, Histone H1 depletion in mammals alters global chromatin structure but causes specific changes in gene regulation, Cell 123 (2005) 1199-1212.

[14] S.S. Case, M.A. Price, C.T. Jordan, X.J. Yu, L. Wang, G. Bauer, D.L. Haas, D. Xu, R. Stripecke, L. Naldini, D.B. Kohn, G.M. Crooks, Stable transduction of quiescent

CD34(+)CD38(-) human hematopoietic cells by HIV-1-based lentiviral vectors, Proc Natl Acad Sci U S A 96 (1999) 2988-2993.

[15] L. Naldini, U. Blomer, P. Gallay, D. Ory, R. Mulligan, F.H. Gage, I.M. Verma, D. Trono, In vivo gene delivery and stable transduction of nondividing cells by a lentiviral vector, Science 272 (1996) 263-267.

[16] R.C. Zhao, Y. Jiang, C.M. Verfaillie, A model of human p210(bcr/ABL)-mediated chronic myelogenous leukemia by transduction of primary normal human CD34(+) cells with a BCR/ABL-containing retroviral vector, Blood 97 (2001) 2406-2412.

[17] J.C. Pui, D. Allman, L. Xu, S. DeRocco, F.G. Karnell, S. Bakkour, J.Y. Lee, T. Kadesch, R.R. Hardy, J.C. Aster, W.S. Pear, Notch1 expression in early lymphopoiesis influences B versus T lineage determination, Immunity 11 (1999) 299-308.

[18] Retroviral Gene Transfer and Expression User Manual, Clontech Laboratories, Inc., Mountain View, 2006.

[19] L. Sastry, T. Johnson, M.J. Hobson, B. Smucker, K. Cornetta, Titering lentiviral vectors: comparison of DNA, RNA and marker expression methods, Gene Ther 9 (2002) 1155-1162.

[20] Relative Quantitation Of Gene Expression: ABI PRISM 7700 Sequence Detection System: User Bulletin #2: Rev B Applied Biosystems, Inc., Foster City, 1997

[21] P. Hematti, B.K. Hong, C. Ferguson, R. Adler, H. Hanawa, S. Sellers, I.E. Holt, C.E. Eckfeldt, Y. Sharma, M. Schmidt, C. von Kalle, D.A. Persons, E.M. Billings, C.M. Verfaillie, A.W. Nienhuis, T.G. Wolfsberg, C.E. Dunbar, B. Calmels, Distinct genomic integration of MLV and SIV vectors in primate hematopoietic stem and progenitor cells, PLoS Biol 2 (2004) e423.

[22] B.C. Beard, D. Dickerson, K. Beebe, C. Gooch, J. Fletcher, T. Okbinoglu, D.G. Miller, M.A. Jacobs, R. Kaul, H.P. Kiem, G.D. Trobridge, Comparison of HIV-derived

lentiviral and MLV-based gammaretroviral vector integration sites in primate repopulating cells, Mol Ther 15 (2007) 1356-1365.

CHAPTER 6

CONCLUSIONS AND FUTURE DIRECTIONS

6.1 Summary of results

In Chapter 2 we constructed two MSCV-derived retroviral vectors encoding for proendocrine transcription factors Ngn3 and PDX-1. We genetically modified mES cells with our Ngn3 retrovirus to ectopically express Ngn3, and we found its overexpression was followed by a 2-fold upregulation at 5 days post transduction of NeuroD1/Beta2, Pax4, Dll-1, and PDX-1, other important proendocrine transcription factors whose expression is regulated by or downstream of Ngn3. These results suggest that pluripotent mES cells may be competent to respond to Ngn3 and support our hypothesis that ectopic expression of these factors can be used to induce mES cells to adopt an endocrine fate. However, following long-term culture and embryoid body differentiation, expression of most proendocrine transcription factors decreased. In addition, our retrovirus transduction methods were inefficient for gene transfer to mES cells, demonstrated by low transgene expression levels of both Ngn3 and the eGFP reporter gene in EFC1 mES cells in comparison to NIH 3T3 fibroblasts, an easy to transduce cell type.

In Chapter 3 we investigated whether delivering more transgenes would improve retroviral gene transfer to murine embryonic stem (mES) cells. We formed polymer complexes with MSCV-derived ecotropic retroviruses, concentrated them up to 40-fold, and transduced two different murine embryonic stem cell lines, and a mouse fibroblast cell line as a control. The number of integrated transgenes increased more than 50-fold in the embryonic stem cell lines, yet, surprisingly, transgene expression did not increase. Interestingly, the embryonic stem cells had significantly fewer integrated

transgenes than the mouse fibroblasts, even though transduction conditions were identical, which suggests that embryonic stem cells may restrict a post-binding step of retrovirus transduction.

In Chapter 4 we investigated which steps of the virus lifecycle restrict efficient transduction of ES cells as compared to a cell type that is much more easily transduced (i.e., NIH 3T3 murine fibroblasts). Using recombinant MMuLV-derived retrovirus and recombinant HIV-1-derived lentivirus, we compared three major steps in the transduction of R1 mES and NIH 3T3 cells: 1) the number of active virus particles that absorb to cells in a given absorption time using ELISA assays and confocal microscopy and image analysis; 2) the number of integrated transgenes using real-time PCR; and 3) the corresponding level of gene expression. We found that retroviruses and lentiviruses similarly bind 3 or 4-fold less efficiently to R1 mES cells than to NIH 3T3 cells. R1 mES cells integrated 3-fold fewer retrovirus transgenes than NIH 3T3 cells and showed 11-fold lower retrovirus transgene expression levels. In comparison, R1 mES cells integrated 10-fold fewer lentivirus transgenes than NIH 3T3 cells and showed 8-fold lower lentivirus transgene expression levels. Although silencing remains the biggest obstacle to retroviral gene transfer, these results indicate virus binding and integration in the transduction process are also limiting in ES cells.

In Chapter 5 we investigated whether depletion of histone 1 would alleviate silencing of retrovirus transgenes and improve gene transfer. To study the role of H1 in retroviral gene transfer, we transduced histone H1c, H1d, H1e triple null mouse embryonic stem cells with three different recombinant vectors – murine embryonic stem cell retrovirus (MSCV), and SIV and HIV-1 derived lentiviruses. We found that transduction of mES cells depleted of histone H1 did not improve viral gene transfer, and triple null mES cells had about a 2-fold reduction in the number of eGFP+ cells for all three viruses in comparison to wild-type mES cells.

6.2 Conclusions

In conclusion, we determined:

1. The number of integrated transgenes delivered to murine embryonic stem (mES) cells can be increased with virus concentration, but transgene expression does not increase; mES cells integrate fewer transgenes than easily transduced NIH 3T3 cells.
2. Binding and integration of both retroviruses and lentiviruses is restricted in mES cells.
3. Depletion on linker histone H1 in mES cells does not improve gene transfer.

6.3 Future Considerations

The following are suggestions for future research:

1. Although we could increase the number of transgenes delivered to mES cells, expression of integrated transgenes remained low. Future work should continue to focus on improving retroviral vector design to decrease retrovirus susceptibility to silencing.
2. Complexation of virus with polymers proved an effective way to concentrate retrovirus and increase the number of transgenes delivered to mES cells. Complexation with polymers should also be applied to lentiviruses to study the relationship between virus dosage and transgene expression to standardize gene transfer protocols for ES cells using lentiviruses.
3. We found that mES cells expressed similar levels of mRNA for the ecotropic and amphotropic retrovirus receptors as NIH 3T3 cells. Future work should evaluate the number of functional receptors at the cell surface of mES cells and whether gene transfer can be improved by upregulating receptor expression.

4. We found that mES cells integrated 10-fold fewer lentiviral transgenes than NIH 3T3 cells. Future work should determine if host cell factors restricting the lentivirus life cycle are more highly expressed in undifferentiated ES cells.
5. We found that gene transfer to ES cells was not improved through depletion of linker histone H1 in mES cells. Further work should investigate the effects of alternative modifications to chromatin structure on gene transfer to develop more effective ways to reduce retrovirus silencing.

APPENDIX A

EXPERIMENTAL PROTOCOLS

A.1 Confocal Microscopy Image Analysis to Determine Number of Cell-Associated Virus Particles

In LSM Image Browser:

1. Converst z-stack series of confocal microscopy images to 3-D projection to combine all image slices

    a. Open z-stack series taken using Zeiss LSM 510 confocal microscope

    b. Conduct Projection of image

        i. Use Projection button

        ii. Settings:

            1. Projection: set turning axis, number of projections, difference angle as desired

            2. Transparency: Maximum

        iii. Hit Apply

    c. Save new "Total Projection image" – these projection images are created to measure total virus particles in confocal microscopy z-stack series

2. Create projection images of just cell regions

    a. Select cell regions on new "Projection image" – these projection images are created to measure only cell-associated virus particles in confocal microscopy z-stack series

    b. Use Overlay button

        i. In Overlay options use Closed Free Shape button to select cell regions with cell-associated virus particles (must used Closed region button, not Open region); typically 1-3 regions needed per cell

ii. Once regions selected, highlight regions, move highlighted boxes to make adjustments

iii. Once all cell regions selected, make sure all regions are not highlighted

c. Extract regions into new window

i. Use Extract Regions button

d. Save new "Cell Region Projection image"

3. Conduct this protocol on Control images (no virus) as well as Virus images

In ImageJ:

4. ImageJ can open projection images created in the LSM Image Browser

5. Determine background levels for each color channel

a. Use Control Projection images created above

b. Image – Adjust – Brightness/Contrast

6. Determine Number of Cell-Associated Virus Particles

a. Open "Cell Region Projection image" created above in LSM Image Browser; make sure image separated into 3 color channel images

b. Select appropriate color channel with just virus particles

i. Red Channel: RFP-gag retrovirus

ii. Green Channel GFP-vpr lentivirus

c. Adjust Brightness/Contrast to eliminate background

i. Hit "Yes" to Apply to all slices when prompted

d. Make sure to return to first slice showing virus particles

e. Run Count Virus Particles Macro (created by Jamie Chilton)

i. Hit "Yes" to Apply to all slices when prompted

f. Organize/label data reports generated by Macro in Excel

    i. Reports record particle number, particle size, average particle size, total particle count

g. Save new image of counted virus particles generated by Macro as jpeg image

h. Use new jpeg image and data reports to check virus count

    i. Check each new image/data reports to determine if two or more touching virus particles were counted as one large particle

        1. Divide large particles by average single virus particle size, adjust reports as needed

i. Determine Total Number of Virus Particles present in image

    i. Conduct same protocol as above for Cell-associated virus particles, except follow protocol on "Total Projection images" created above

j. Determine Surface Area of Cells

    i. Open "Cell Region Projection image" created above in LSM Image Browser; make sure image separated into 3 color channel images

k. Select appropriate color channel with just cells

    i. Red Channel: Cell surface labeled with Concanavalin A_{594} to appear red

    ii. Green Channel: Cell surface labeled with Concanavalin A_{488} to appear green

l. Copy and Paste appropriate color channel into new image window as black and white image

    i. When prompted with dialog box, make sure image size and file type the same as original LSM image

    ii. Must create new image otherwise Macro will not interpret color image

m. Manually adjust Brightness/Contrast and use Flood Fill Tool and Paintbrush Tool as needed to fill in cell bodies

n. Convert image to Binary black and white image

i. Process – Binary – Threshold

ii. May need to undo and make more adjustments if cell bodies are not accurately interpreted as area regions

iii. In some cases may be easier to adjust non cellular regions as areas and minus them from total area of image to get cell body area

o. Calculate surface area of cell bodies

i. Analyze – Analyze Particles (on ImageJ menu bar)

p. Organize/label data reports generated by Macro in Excel

i. Reports record individual region number, individual region area, average region area, total area of regions, area of region as fraction of total area (units are in pixels)

q. Save new image of counted cell body surface areas generated by Macro as jpeg image

r. Once in Excel convert pixel^2 to μm^2 and calculate number of cell-associated virus particles per μm^2

7. Determine number of Cell Nuclei

a. Open "Cell Region Projection image" created above in LSM Image Browser; make sure image separated into 3 color channel images

b. Select Blue color channel with just cell nuclei

c. Adjust Brightness/Contrast to eliminate background

i. Hit "Yes" to Apply to all slices when prompted

d. Make sure to return to first slice showing cell nuclei or Macro won't run

e. Run Blue Nuclei Macro (created by Jamie Chilton)

f. Organize/label data reports generated by Macro with nuclei counts in Excel

APPENDIX B

ADDITIONAL DATA

B.1 Determination of the starting concentration of active virus (C_{v0}) in virus stocks and active virus particles delivered per cell (A).

In a diluted titer assay, two-fold serial dilutions of VSV-G *lacZ* retrovirus and VSV-G *lacZ* lentivirus stocks were made in DMEM/BCS and Polybrene (8μg per mL). Serially diluted virus (1 mL per well) was used to transduce NIH 3T3 cells that had been seeded at 2 x 10^4 cells per well in 6-well plates the previous day. The viral supernatants were removed 5 hours later and replaced with fresh medium. Three days post transduction, the cells were fixed and stained for β-galactosidase activity with X-Gal [1]. The number of colonies of *lacZ*+ NIH 3T3 cells were counted with the aid of a dissecting microscope, and multiplied by the dilution factor to determine CFU. In parallel triplicate wells, the number of cells at the start of transduction was counted.

The initial concentration of active retrovirus and lentivirus (C_{vo}) was estimated from the following relationship:

$$C_{vo} = \frac{CFU}{\eta 4 a_c D N_{co} I} \qquad [2]$$

where *CFU* is the number of colony-forming units (determined from the diluted titer assay described above), a_c is the average radius of NIH 3T3 cells (7 μm), D is the diffusion coefficient of the virus (6.264 x 10^{-5} cm^2/h), N_{co} is the total number of cells at the start of transduction, and I is an integrated function of time, the diffusion coefficient, the half-life of the virus, and the radius of the target cells [2, 3]. The integral I was evaluated and is described by the following equation:

$$I = \int_0^t h(a_c, t) e^{-k_{dv} t} dt$$

where the function $h(a_c,t)$ was derived by Shoup and Szabo, describing at time t, the flux of particles on each cell over the steady-state particle flux [4].

The number of active retrovirus and lentivirus particles delivered per cell (A) was then estimated from the following relationship:

$$A = \eta 4 a_c D C_{vo} I \qquad [2]$$

Results are the average of three independent experiments.

.

Table B.1 Numerical values of the integral *I* for aVSV-G-pseudotyped lentivirus with a half-life of 19 hours.[a]

t (h)	$I = \int_0^t h(a_c,t)e^{-k_{dv}t}dt$										
	a_c = 3μm	a_c = 4μm	a_c = 5μm	a_c = 7μm	a_c = 9μm	a_c = 11μm	a_c = 13μm	a_c = 15μm	a_c = 17μm	a_c = 19 μm	a_c = 21 μm
0.5	0.515	0.521	0.528	0.541	0.554	0.568	0.581	0.595	0.609	0.622	0.636
1.0	1.009	1.018	1.027	1.046	1.064	1.083	1.102	1.121	1.14	1.159	1.178
1.5	1.493	1.504	1.515	1.537	1.56	1.582	1.605	1.628	1.651	1.674	1.697
2.0	1.967	1.979	1.992	2.018	2.043	2.069	2.095	2.121	2.147	2.174	2.2
2.5	2.431	2.446	2.46	2.488	2.517	2.545	2.574	2.603	2.632	2.661	2.69
3.0	2.887	2.903	2.918	2.949	2.98	3.011	3.043	3.074	3.105	3.137	3.169
3.5	3.335	3.351	3.368	3.401	3.434	3.468	3.501	3.535	3.569	3.602	3.636
4.0	3.774	3.792	3.809	3.844	3.88	3.915	3.951	3.986	4.022	4.058	4.094
4.5	4.205	4.223	4.242	4.279	4.316	4.354	4.391	4.429	4.466	4.504	4.542
5.0	4.628	4.647	4.667	4.706	4.745	4.784	4.823	4.862	4.902	4.941	4.981
5.5	5.043	5.064	5.084	5.124	5.165	5.206	5.247	5.288	5.329	5.37	5.411
6.0	5.451	5.472	5.493	5.535	5.577	5.62	5.662	5.705	5.747	5.79	5.833
6.5	5.851	5.873	5.895	5.938	5.982	6.026	6.069	6.113	6.158	6.202	6.246
7.0	6.244	6.267	6.289	6.334	6.379	6.424	6.469	6.515	6.56	6.606	6.652
7.5	6.63	6.653	6.676	6.722	6.768	6.815	6.861	6.908	6.955	7.002	7.049
8.0	7.009	7.032	7.056	7.103	7.151	7.199	7.246	7.294	7.342	7.39	7.439

[a]Values of *I* are shown for various times of exposure of cells to VSV-G-pseudotyped lentivirus and various sizes (radius, a_c) of target cells. These values are used to calculate the initial concentration of active retrovirus at the start of infection (C_{vo}) and the number of active viruses delivered per cell (A).

Table B.2 *RFP-lacZ* retrovirus stocks deliver a higher number of active viruses per cell to NIH 3T3 fibroblasts. [a]

Virus Stock	Colony-forming units (*CFU*)	Initial concentration of active retrovirus at start of infection (C_{vo})	Number of active viruses delivered per cell (*A*)
RFP-lacZ Retrovirus Stock 1	4.57 ± 0.57 (x 10^5)	7.76 ± 2.31 (x 10^6)	5.54 ± 1.65
RFP-lacZ Retrovirus Stock 2	1.20 ± 0.61 (x 10^5)	2.66 ± 0.40 (x 10^6)	1.90 ± 0.28
GFP-lacZ Lentivirus Stock 1	3.92 ± 1.04 (x 10^3)	9.03 ± 2.97 (x 10^4)	7.34 ± 2.41 (x 10^{-2})

[a]Values of C_{vo} and *A* were calculated based on 5 hours of exposure of NIH 3T3 cells to the virus stocks; stocks are VSV-G pseudotyped virus.